ON THE 3-D RECONSTRUCTION OF PALEOZOIC AND MESOZOIC PALEOBOTANICAL PROBLEMATICA

By

ANDREW RONALD REES

A thesis submitted to the University of Birmingham for the degree of DOCTOR OF PHILOSOPHY

Earth Sciences
School of Geography, Earth and Environmental Sciences
College of Life Sciences
University of Birmingham
September 2012

ABSTRACT

Detailed descriptions of 3-D anatomically preserved specimens in paleobotany have been undertaken for over 100 years. Some of the most comprehensively characterised of these specimens are reproductive structures, especially cones and ovules. Throughout this time many of the ways of gaining information such specimens has remained static. In recent years new computer software and techniques have been developed that allow detailed 3-D computer reconstructions to be undertaken that allow holistic observations of the context of the whole organ.

Detailed 3-D reconstructions have been undertaken of several genera of Palaeozoic and Mesozoic paleobotanical reproductive organs. These complex structures have undergone traditional preparation, such as serial sectioning, preparation specifically for reconstruction such as serial grinding and non-destructive scanning micro X-ray tomography. Reconstructions were then produced in bespoke software, Serial Paleontological Image Editing and Rendering System (SPIERS).

The reconstructions produced provide a new understanding to the structure and functions of tissues within paleobotanical reproductive specimens. For the first time, specimens of extinct and extant genera have been compared using new reconstruction techniques in order to aid in the future understanding of their evolution and development, and to aid visualisation of complex structures for which illustrations in 2-D form are inadequate.

Acknowledgements

Breaking with tradition, I would like to firstly acknowledge my former employers, not for the usual reasons of providing financial support, or encouragement to further study, but for their close minded attitude and total opposition to free thinking. This provided me with huge motivation to come back to academia.

The first person I told of my intentions to return to study was my grandmother; she provided endless encouragement and was a constant source of inspiration. I owe her a debt that I can never repay. Thank you, you are sorely missed.

These people made my PhD happen in one form or another.

To Jason, from your initial positive response to my suggestion of further study and great ideas for a project, to the very late hours i subjected you to before submission of my thesis, I want to thank you for your constant support through some troubling times. There may have been times where we might have wanted to Kill each other, luckily that did not happen.

To my parents, your unquestioning support in all senses has allowed me to achieve this. I have not given you the easiest of times, but I hope you will agree it is all worth it. Thank you very much.

I have had endless academic support from people within and outside the University of Birmingham. I would like to say thanks too; Aruna and Gretchel for providing fantastic support within the department, Carl and Tim for much amusement on fieldwork, James for always smiling despite having to examine my thesis, Mark Sutton from Imperial College for being my second supervisor and providing the software needed to make my project happen, Richard Bateman and Paula Rudall from Kew Gardens for their support and answering some fairly silly botanical questions, Paul Kenrick from the Natural History Museum for giving me great access to collections and equipment, Margaret. Collinson from Royal Holloway for acting as a mentor and for giving great independent advice, Chris Cleal for teaching me a huge amount about carboniferous paleobotany and for buying me beer. Gar Rothwell for great advice and for flying for 20 hours to do field work and spraining his ankle within the 10 minutes of collecting, Everyone at the *Naturhistoriska riksmuseet* in Stockholm, you all made me feel very welcome and improved me as a researcher and lastly Barry Thomas, you provided me with many pints of beer, many stories and was a great and fair external examiner.

I would like to thank all of my friends, old and new:

Leyla for a lot of help and support and use of her spare room to stay over in Birmingham, Ken and Yvonne for great help when writing up, Lil for being a hippy and sharing specimens with me, Sarah for making me realising I was not the only grumpy person in the department, Ben for constant amusement, Nick for threatening to burn out my eyes with a red hot poker, Helen for always falling for the same tricks, Rob and Russ for their cider guidance, Neil for the weird adventures, Storey for his love affair with squared paper and constant shock of prawns in curry, Plamen for bringing back the Hitler haircut, Belcher for being Belcher, Tim for his early assistance with the models and gaming advice and Bryony for the calming lunches and cups of coffee

This thesis is dedicated to the memory of
Violet Edith Tudor

“There is grandeur in this view of life, with its several powers, having been originally breathed into a few forms or into one; and that, whilst this planet has gone cycling on according to the fixed law of gravity, from so simple a beginning endless forms most beautiful and most wonderful have been, and are being, evolved.”

Charles Darwin, 1859

TABLE OF CONTENTS

TABLE OF FIGURES

TABLE OF TABLES

CHAPTER 1

INTRODUCTION TO 3-D RECONSTRUCTIONS IN PALAEOBOTANY

Throughout the history of research in palaeobiology, images have been used to show and represent structures within a fossil and indeed the fossil as a whole. In the late 18th and early 19th century hand drawn images would be hand tinted to represent the specimens. With the introduction of photography in the late 19th and early 20th century the actual image of a specimen being studied could be shown and easily distributed, it then became possible to take photographs of the images seen with a microscope allowing a whole range of magnifications to be shown. A huge leap was made in the 1960's when the first scanning electron microscopes were commercially available. It would now be possible to image at very high levels of magnification, resolution and depth of field, indeed the surface

texture of a pollen grain could now clearly be seen.

The 21st century has led to a huge expansion in the ability to image objects. Digital photography is now standard practice, with images being easily modified and analysed by efficient and custom made computer software. CT scanning using X-rays, which had been developed over previous decades, has now become affordable to many researchers and desktop size CT scanners are now common in many university departments.

As a result of the advancement of digital photography, CT scanning and an ever constant increase in computing power. It is now possible and indeed accessible to produce high resolution three-dimensional (3-D) computer reconstructions of most types of fossil material.

For a significant amount of fossil plant material which has 3-D preservation, it is quite often the case that analysis does not change whether the fossil has two-dimensional (2-D) or 3-D preservation. Researchers lacking experience with anatomical preservation may describe three dimensional plants in the same way that they describe compression/impression specimens, or specimens that show 3-D preservation may be cut in to a series of 2-D sections. With the abundance of 3-D anatomically preserved fossil plant specimens, new techniques are required to take full advantage of the preservation that show the relationships between structures in a 3-D form, and to assist in the understanding and identification of paleobotanical specimens.

The ability to see a complex structure in a 3-D form has led to many attempts to create reconstructions from fossil plant specimens. Sollas & Sollas (1913) made reconstructions from plastic sheets and wax. Sollas & Sollas (1913) went on to produce a number of highly accurate, mathematically constructed 3-D drawings which were made to produce 3-

D reconstructions, however some of these were skewed as a result of lack of precision in alignment of successive sections. Baker (1973) used a different mathematical method which removed the distortion and gives a more accurate reconstruction; the drawings Baker produced were made from acetate peels and transferred on to paper.

Recent increases in computing performance have allowed 3-D reconstructions to be made using individual facets of existing computing packages in combination with new software programmes, as undertaken by Sutton *et al..* (2001a, 2004). Bespoke software has been written in recent years to allow a software package to create the whole reconstruction form a set of serial images. SPIERS (Serial Paleontological Image Editing and Rendering System) has been specifically designed for this purpose and has been used routinely through this project (Sutton *et al*., 2005, 2006).

With the abundance of high quality 3-D anatomically preserved palaeobotanical material and availability of advanced imaging equipment, have led to an increasing desire to digitise imagery and the analysis of specimens throughout sciences. Within palaeobotany this has been particularly advantageous as many species are based on a handful of species or a single, unique specimen, and to have a digital record of such specimens which can then be shared for evaluation is useful, especially in instances where observing and studying specimens require museum visits and/or specimen loan.

Demonstrated here are methodologies and examples of how 3-D reconstructions can be produced in paleobotany and the information that can be gathered from the reconstructions at this stage summarised. Choosing the appropriate method of preparation and reconstruction are vital, and as this is a rapidly developing area within palaeobotany, standard methodologies and approaches were not available at the start of the project and have been developed as part of the project.

At the beginning of this project, high speed computer workstations were commonly only used on software platforms which are not considered user friendly, such as Linux. The software used within this thesis is designed to be freely available and as easy to use as possible on mainstream software platforms. As a result of the continued decrease in the cost per unit of computer processing and increased refinement of software, the models produced at the end (temporally) of this thesis are of much greater resolution and complexity than those at the start. Many of the models produced at the beginning of the project were improved towards the end as the ability was there to do so. Also within the time frame of this project, two commercially available high resolution CT scanners came online in the UK for use. This allowed specimens to be scanned with x5 greater resolution and also to be scanned within reasonable dense surrounding matrix. A method that was not an option at the beginning of the project. The SPIERS software used for the majority of these reconstructions has been updated numerous times during this project, each time adding new and beneficial features, also from time to time compatibility issues.

3-D computer reconstructions can be produced to show detailed anatomical information and to show how reconstructions are a valuable tool to be used in conjunction with traditional methods to access, analyse and evaluate palaeobotanical specimens. In order to fully understand the structure of a fossil specimen, it has been required to subject living botanical material to the same type of 3-D reconstruction processes. Aspects of traditional taxonomy do not produce sufficient data to be able to accurately compare extinct and extant specimens. This thesis also shows how 3-D techniques can also be used to aid traditional taxonomy, with one CT scan allowing highly detailed and traditional 2-D sections and complex reconstructions to be made, all without damaging the specimen.

Discussed in detail are the approaches which need to be undertaken to produce a 3-D

reconstruction, how different specimens within different matrix need to be treated, and what governs the overall quality and data which can be acquired. Some approaches, such as laser scanning are shown but dismissed as the resolution is not currently adequate for the specimens within this thesis. The software and how it is used is also discussed, however this will quickly be superseded, however the principles of how the reconstructions are made are key to this thesis and are likely to form the foundations of all 3-D computer reconstructions and visualisations.

CHAPTER 2

MATERIAL PREPARATION AND RECONSTRUCTION METHODS

2.1 Introduction

It may at first seem over indulgent to have an entire chapter dedicated to methods of cutting, grinding or scanning specimens and then extracting the data from them using software. However, in paleobotany, this work is in its relative infancy and the potential for destroying important paleobotanical specimens and not being able to produce a scientifically valid reconstruction is high. In engineering a common phase used is ‘measure twice, cut once’, the same term is equally important, if not more so, when dealing with exceptionally well preserved 3-D fossils. Methods for specimen preparation specifically for creating a 3-D computer reconstruction are very simple, namely to produce tomographic planes (Figure 2.1). This can be achieved in two distinct ways either by a scanning technique such as micro X-ray CT or by physical cutting or grinding methods. The latter has been termed ‘Physical Optical Tomography’ (POT) by Sutton *et al*., (2008). The benefits of these specified methods will be discussed in detail.

Figure 2.1. Hypothetical diagram showing a series of tomographic planes through an idealised palaeobotanical specimen. Adjacent marks parallel to the specimen but perpendicular the plane of tomographic section.

In this project a variety of specimen preparation techniques have been used, including serial wafering (Hass & Rowe, 1999), serial grinding (Sutton, 2004a, 2006), and serial peeling (Galtier & Phillips, 1999) as well as approaches that used combinations of these techniques, these physical preparation techniques, along with digital image capture form POT. Once these physical planes have been produced they are then digitally photographed and interpreted in the SPIERSedit programme. Figure 2.2 shows how this interpretation looks to produce digital sections. In addition, the preparation methods of previously prepared materials will also be discussed. Such specimens are routinely deposited in museum collections and are of vital importance to paleobotany. However, they tend to be less than ideal for physical optical tomographic approaches, but their scientific importance cannot be overlooked and work-arounds need to be achieved. In many ways this is the natural progression of very early work undertaken in anatomical reconstructions by using physical model (Sollas & Sollas, 1913). Now appropriate computing resources are available, it is inevitable that 3D anatomical computer

reconstructions will become more common place in palaeobiology.

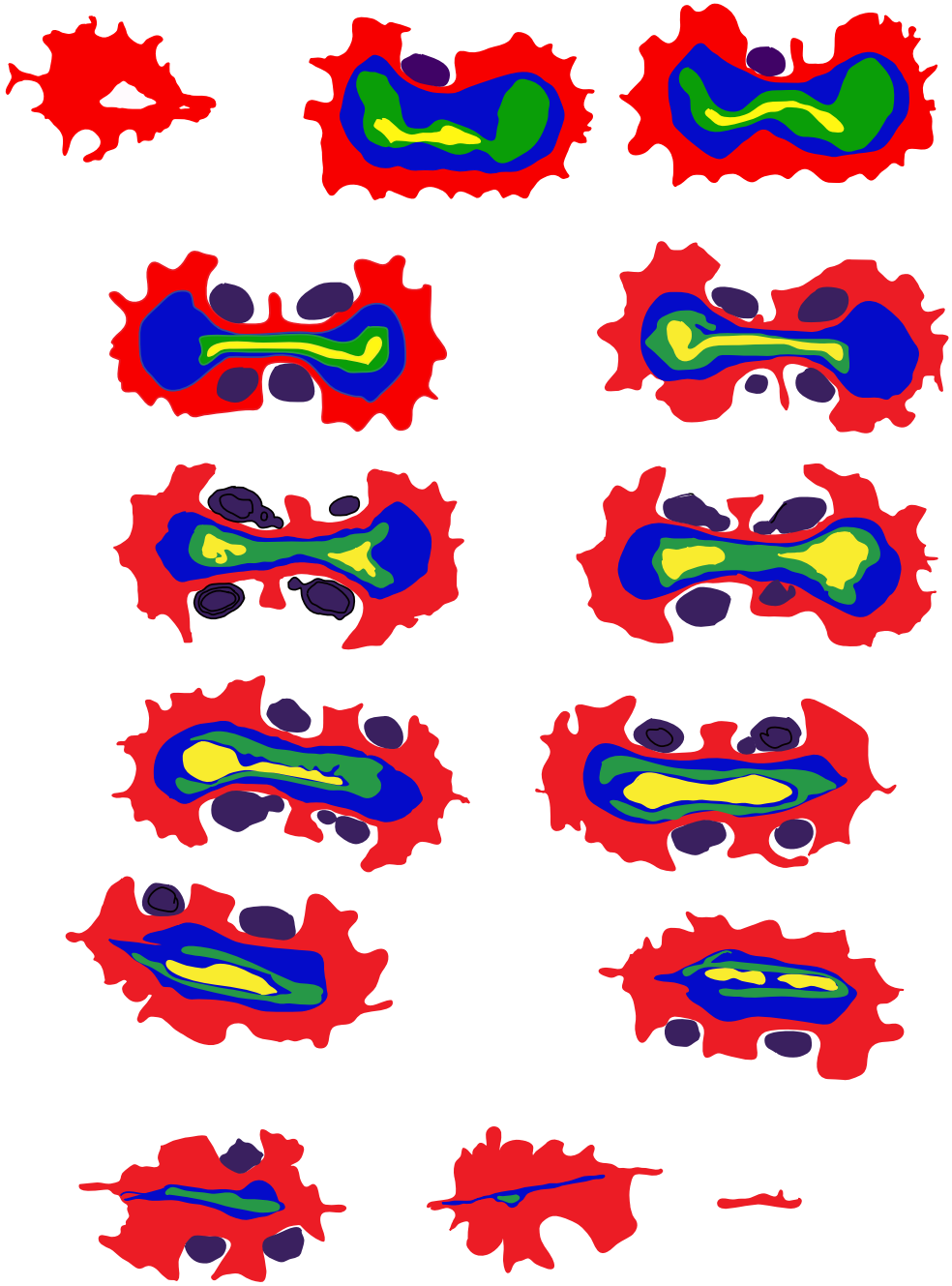

Figure 2.2 Interpreted tomographs of the ovule *Cardiocarpus dabizae* in transverse section from specimens as documented by Hilton et al. (2001) Green = megaspore, light blue – nucellus, Red = integument, purple = external glands in the integument.

2.2 Preparation methods

With preparation of new specimens, three distinct phases normally need to be undertaken. The first phase is to remove as much of the matrix surrounding the fossil as possible in order to reduce the amount of material to be cut or ground away; this process reduces the time required to cut or grind the specimen and is merely for efficiency purposes. This is also of great importance in X-ray micro CT scanning as removing more of the surrounding matrix enhances X-ray penetration to the fossil. In some specific specimens stabilisation will need to be undertaken; materials such as coal balls tend to be friable and even well consolidated material such as siderite can undergo brittle failure when forces are applied during cutting or grinding. Resin impregnation is best achieved under vacuum; this allows cutting and grinding to occur with the minimal amount of unplanned loss.

The second phase is to create alignment marks within the specimen or surrounding matrix. In order to accurately produce 3D reconstructions these are vital as they provide fixed datum points, these will be discuss later in the chapter. The final phase is the cutting or grinding method which will provide the surfaces from which digital images, can be taken for the reconstruction to be made.

2.2.1 Re-assembling the fossil

It is inevitable in some cases, that when specimens were collected the matrix was split to reveal the fossil. In these cases it is essential to repair the damage done and to fit the part

and counter-part back together before further preparation is undertaken. To avoid damage the part and counter-part should not be placed together until the specimen is ready to be re-constructed as specimens may be damaged by contact. It is essential to check the condition of the fossil material and the surrounding matrix before further preparation occurs and to treat forms of structural weakness with a resin infill before sections are cut. Optically clear adhesive is to be used. When undertaking a reconstruction on a specimen that has been repaired in such a way it is important to realise a small amount of the specimen will be lost and interpretation will be required.

2.2.2 Serial Wafering

In its most basic terms this method involves serially cutting a specimen along the same plane, with known thicknesses and spacing. Mounting the wafer on a microscope slide will help to stabilise the specimen and improve the optical quality for photography.

Two different saws have been used in this project. These are the Buehler Isomet low speed saw, and the Buehler Isomet 5000, automated high speed saw.

Buehler Isomet low speed saw is used with a 0.3 mm diamond edged wafering blade. This saw and blade combination allows for highly accurate cuts to be made with a minimal amount of surface scratches and cut marks. The specimen can be accurately positioned to give precise cut thicknesses and with a known amount of loss between successive cuts. This method is preferred where the specimen is in danger of breaking, the slow nature of this method for accurate adjustments to the cutting speed to be made in relation to the strength of the matrix of the specimen, whether it is reasonable soft or very brittle. The two controls on the speed of cutting are the weight added to the specimen and the

cutting speed. Adding weight to the specimen increased the force applied to the cutting surface; weaker lithologies can break apart if too much mass weight is added. For the fastest cutting time the maximum weight and greatest speed should be selected. Caution should be used as ‘forcing’ the rate of cutting with added weight and speed can lead to a detrimental surface finish, under these circumstance addition polishing is require, thus increasing tomographic spacing and reducing reconstruction resolution.

To begin the cutting process the blade must be partially submerged with water along with the addition of an appropriate lubrication medium. This serves two purposes, firstly it acts to clean the blade as it is cutting, and secondly it helps lubricate the blade to ensure that the cut is smooth. The specimens need to be firmly attached to the saw mount, this has to be done in such a way as to ensure the face which is to be cut, usually perpendicular to the long axis of the specimen, is parallel to the saw blade. If this is not set correctly oblique cuts will be made which makes reconstruction more difficult. Securing the specimen is of vital importance as movement during the cutting process causes gouge marks on the specimen and often causes damage to the saw blade.

On the low speed saw, cutting speeds are divided into a scale between 1 and 10, to start it is best to begin with a slow speed around 4. When the blade has cut a few millimetres into the material the speed can be slowly increased and weight added to the top of the sample in order to increase the rate of cutting. When the cutting is nearly complete it is advisable to reduce the cutting speed and reduce the amount of weight to prevent the specimen fracturing along the approximate line of the cut. The average cutting time for a 20mm x 40mm wafer is forty five minutes for siderite, however, this time can dramatically increase with harder materials and can take 2-3 days for indurated chert (L. G. Stevens, pers. com. 2007).

Buehler Isomet 5000 saw usage, although automated, relies on the same general principles as the low speed saw. The thickness of each wafer, saw speed, rate of cut and the number of cuts to be made are programmed into the saw and, subsequently becoming an automated process. The cut times are greatly reduced with the time per complete cut for siderite is approximately 8-10 minutes. This saw provides a good surface finish, however, the cuts can be made quicker although this will compromise the quality of the cut surface. A balance must always be maintained between feed rate and saw speed to achieve good surface finish and speed. The Isomet 5000 saw should be used where there is confidence in the stability of the specimen as corrections to the cutting speed should not be made once started.

Although the serial wafering method is difficult and time consuming, it has substantial benefits over traditional thin section techniques as it has lower ratio of specimen wastage and enables more tomographic planes revealed from a single specimen. The method used in this project is as described by Hass & Rowe (1999) but as modified by Hilton *et al*. (2003) for use on volcanicalistic tuffs in which clay minerals are present, using oil to lubricate specimens rather than water. In the presence of water clay minerals expand often leading to be breakup of the specimen.

Once cut individual wafers are to be washed and numbered using a pencil; pencil is advisable as solvents used later in the preparation process including mounting wafers remove ink. Wafers are then left to dry in a desiccation cupboard where the wafers are kept as clean as possible. Gentle polishing maybe required if cutting marks have remained, using fine (600-1000 µm) silicon carbide grit. Once prepared individual wafers are mounted on microscope slides(see below) before observations are made.

2.2.3 Acetate peel method

Acetate peeling is a method for making a permanent record of anatomically preserved plant tissue preserved in carbonates and silicates. The method is extensively described by Galiter & Philips (1999) and is summarised here, and in the current project is used extensively for specimens preserved in carbonate as either calcite or siderite.

Cut surfaces are etched in 5% hydrochloric acid (HCL) for approximately 30 seconds. The length of time which materials are etched depends on the amount of dissolvable material, usually carbonate, is present. Siderite commonly has a large proportion of carbonate cement and etches quickly and effectively. It is important to regularly change the acid being used for etching. The pH will begin to rise and become less effective. The etching process removes any acid dissolvable material. Plant tissues are unaffected by HCL and only the carbonate cement is dissolved. Subsequent removal of the cement and matrix creates a (relatively) high relief surface in which the acetate can bond to the plant tissue, allowing transfer onto the acetate.

After etching the specimen then has to be neutralised in water and thoroughly dried, using a combination of hot air and acetone. It is important not to touch the etched surface of the specimen as surface relief can be destroyed and grease from skin contact can affect the bonding between the acetate and specimen.

To place the acetate on to the surface to be peeled, the surface of the specimen should be flooded with acetone (the grade of acetone is relatively unimportant, HPLC grade and above is recommended). Once the surface is covered in acetone, the cellulose acetate sheet can be applied. The acetate should be rolled onto the surface of the specimen to

allow any trapped air bubbles to be expelled, this also minimises the risk of distorting the peel as the placement of the acetate is done by a constant steady movement. Any movement of the acetate once it has been applied to the surface should now be avoided, as the acetate is likely to rip. It is common to have small ripples forming under the surface of the acetate, this is usually due to a larger amount of acetone being present and usually this will not affect the quality of the peel.

The acetate needs to be left to dry for approximately 10 minutes, the surface will turn from being translucent to transparent and the acetate should be able to be removed easily without any excessive force. The edges should be immediately trimmed and the peel placed under a sheet of clean glass, preventing the edges from curling and to keep individual peels flat.

The peel method has advantages over other methods such as thin sectioning as it only takes between 3-10 minutes to produce a peel, and the equipment needed and costs are also kept to a minimum. It also has the advantage of being able to record more tomographic planes of the fossil than either thin sectioning or wafering and provides a permanent record of the fossil.

2.2.4 Serial grinding

Serial grinding is the method which will be used to create the highest resolution POT datasets for the 3D reconstruction work. Silicon carbide grinding material of mesh size 180 µm is used as this provide a coarse enough material to be effective at grinding but does not leave noticeable marks in siderite. Under low power microscope analysis marks are not noticeable in the plant tissues, using higher power does reveal scratch marks

however, this is beyond the magnification required for 3D reconstruction.

A fine layer of silicon carbide is placed on a glass plate and a small amount of water (c. 20 ml) is added. Grinding should be carried out using a circular motion and ensuring that the movement covers the whole of the glass plate. A constant pressure and angle needs to be maintained to ensure that an equal amount of material is removed from each successive grind and that it is equal over the surface of the specimen. The time for each grind depends on how much material is required to be removed and the hardness of the material. For 3D reconstruction high resolution data is required along with the relatively soft siderite gives grind time of 30 seconds. The amount of grinding undertaken represents a trade-off between speed of reconstruction and spacing of slices, with more grinding increasing the spacing between successive slices.

2.2.5 Combined approaches

It is important to keep a permanent record of the material. To do this an acetate peel is taken after 5 serial grinds, but this can be varied depending on the importance of the materials being investigated; less important can have greater spacing between successive peels, and rarer or unique materials can have a reduced spacing between peels.

Specialist hand grinders are available, in which the specimen is mounted and a set amount of material can be removed. This ensures that no changes in the grinding angle occur and each tomographic plane is the same distance. A limit of 40 mm is placed on the total thickness of the specimen and a total diameter of 5 cm of the mountable area, restricts the size of specimen which can be used in this grinder.

2.2.6 Mounting

Mounting refers to placing either a wafered section or an individual acetate peel onto a glass slide to enable microscope observations, and requires the use of Eukitt mounting medium and mixed isomer Xylene (CAS number 1330-20-7). These chemicals do pose a potential risk to human health and precautions need to be taken when being used (refer to the MSDS for Xylene for further information) including use of gloves to avoid skin contact, and use of a volatile organics grade fume cupboard.

Individual wafers normally require further preparation before they can be mounted. To stop any air bubbles being released into the eukitt mounting medium, a dilute version of Eukitt is used. Eukitt it diluted using Xylene to reduce its viscosity by approximately 50%, allowing it to be absorbed into the pore spaces of the rock material in place of air. The process involves submerging the wafers in the dilute Eukitt and being placed in a bell jar in which a vacuum can be created, the vacuum maintained for approximately 3 minutes. This excludes air from the wafer and allows the slide to be mounted without air bubbles. After a few minutes the vacuum can be broken although wafers need to remain submerged prior to mounting to ensure no air re-enters pore space.

To mount the wafer the slide and cover slip must be larger than the wafer itself. On a clean slide a ‘T’ shape should be made from Eukitt which is slightly smaller than the size of the wafer itself. This should be made in the centre of the slide to locate the specimen in the viewable part of the slide.

The wafer should then be placed gently on top of the Eukitt and allowed to settle for a minute. The wafer should be lowered gradually, placing one end down first and then

lowering the raised side slowly to exclude air from the preparation. A small amount of Eukitt should then be placed on top of the wafer; an appropriate size cover slip should be placed on top of the wafer, again putting one end down first and gently lowering the raised side to allow for the expulsion of air from the preparation.

If peels require mounting, the process is similar to that of wafer mounting. However, difference comes through peels first requiring softening by submerging in Xylene for 48 hours prior to mounting. This allows them to be mounted flat on the slide.

Once prepared mounted slides should now be place in to a desiccation cupboard, which is on a flat level surface, the Eukitt will take approximately two weeks to fully set, although after several hours they will be dry enough to be gently handled and photographed if required. The method which has been used is a modified version of Hass & Rowe (1999). Eukitt is used in place of Lakeside cement as it does not require a hotplate to set. Eukitt still provides a clear optical medium when set and has a neutral refractive index such that it does not discolour the preparation (as opposed to Canada Balsam).

2.3 Software

This thesis explores 3D computer reconstructions; physical models are not explored. The use of software for this project is vital, as it is the only means by which the reconstructions can be made and ultimately governs how the model is observed, the information which can be gathered and the accuracy. Three phases of software use within this project, are initial image processing, image editing and model analysis.

2.3.1 Initial image processing

This section is only relevant if POT has been used. If the dataset is of CT origin then the images will already be normalised and in the correct orientation.

The best use of SPIERSedit makes use of the automatic slice generation facilities. In order for this process to work, a high contrast between the fossil material of interest and the surrounding matrix is required. The initial image processing is the process by which this is achieved and the colour and contrast of each of the images is as close as possible, resizing is undertaken. By default, many digital camera's native image resolution is far greater than is required for reconstruction purposes, downsampling will often be required.

All of the images contained in this thesis have been corrected and processed in Adobe Photoshop CS2, all the functions used are fairly generic and any image processing software would be able to achieve the same results. All the image formatting which is now used is for SPIERSalign version 2. The previous version of SPIERSalign has very different image requirements, for instance all images had to be bitmap format and all images in the dataset had to be equal resolution. SPIERSalign V2 (see SPIERS V2 supplementary notes to Sutton *et al.* 2004) allows a much greater variety of image formats and allows a difference in resolution.

Thresholding the images is a process of educated guess work in which the parameters will change for each specimen and even through the same dataset, as lighting levels and lithology can change throughout the dataset. It is preferable to begin with the contrast levels, all that is required to make the fossil material visually stand out as much as possible. In some lithologies such as siderite, a red-brown colour is present; it can be

effective to filter some of the red light spectrum.

It is advisable to re-scale all the images to the same resolution as it provides continuity within the dataset. A resolution of roughly 1200x1200 pixels is advisable as this allows high resolution for detailed editing. A variety of image formats are permitted, however PNG files are recommended for faster computers as the file has to be decompressed then recompressed every time the file is altered, the clarity within these files is high, despite a relatively small file size. Bitmaps are preferable in most circumstances as they require a small amount of processing time and memory to be modified, however their file size is large and clarity reduced.

2.3.2 Image alignment

This is only applicable to POT reconstruction methods; scanning methodologies produces aligned data sets. This method relies on the basis of trial and improvement, by which each aligned images has to be compared to the images which pre and proceed the current image. Movement on the X and Y axis is possible, along with clockwise and anti-clockwise rotations, scaling and the removal of images.

The alignment method which is used within this thesis is a slightly modified version of from the SPIERSalign manual (Sutton 2004b). The wafers which are reconstructed are not mentioned with the manual and therefore need to be treated slightly differently than the specimens with much closer tomographic spacing.

After loading the dataset into SPIERSalign, it is important to choose an image as a datum point. The image datum point should be roughly halfway through the dataset, it is most

likely the image halfway through the dataset will also be the largest so that any scaling which needs to be undertaken can be done based on this. The image should be set dead centre, with the long axis of the specimen perpendicular to true vertical. The rest of the dataset can then be aligned. Moving quickly between an aligned image and un-aligned image will quickly show the movement required. Often, it is most beneficial to move the image on the X Y axis first then to undertake the rotational movements, much finer movements to achieve very close alignment are then possible.

Using markers based on alignment marks is by the far the most straight forward way of aligning the images. Iif alignment marks are not present then continuous structures can be used throughout the specimen, depending on the amount of change between each image.

Where a large amount of change is present between each image and alignment marks are not present, alternative strategies need to be used, if the specimen was set in resin before being cut, the right angled edges of the resin can be used as an alignment mark. Failing that a common sense approach needs to be used, where the centre of each image is aligned and then rotational corrections are made. Although this is not precise and has numerous flaws, it is making best use of the specimens available.

When the alignment has been complete the images need to be cropped This process makes all the images the same size for use in SPIERSedit, all of the specimen in each image must fall within the area covered by the crop box.

2.3.3 Image editing

After the dataset has been loaded into SPIERSedit the images all have to be thresholded to produce segments. These segments are simply highlighted areas on the image which separates the fossil from none fossil material (Figure 2.3). A number of different segments can be used depending on the number of structures that will be reconstructed. There are a number of automated systems which are available to produce segments, however these will not be as accurate as manually edited segments and even the best automated generation will require some manual editing. For its simplicity linear slice generation has been used in this project as it will distinguish between the majority of the fossil and non-fossil material. This is a simple method where the areas of high contrast will be designated areas of interest and low contrast areas will be omitted.

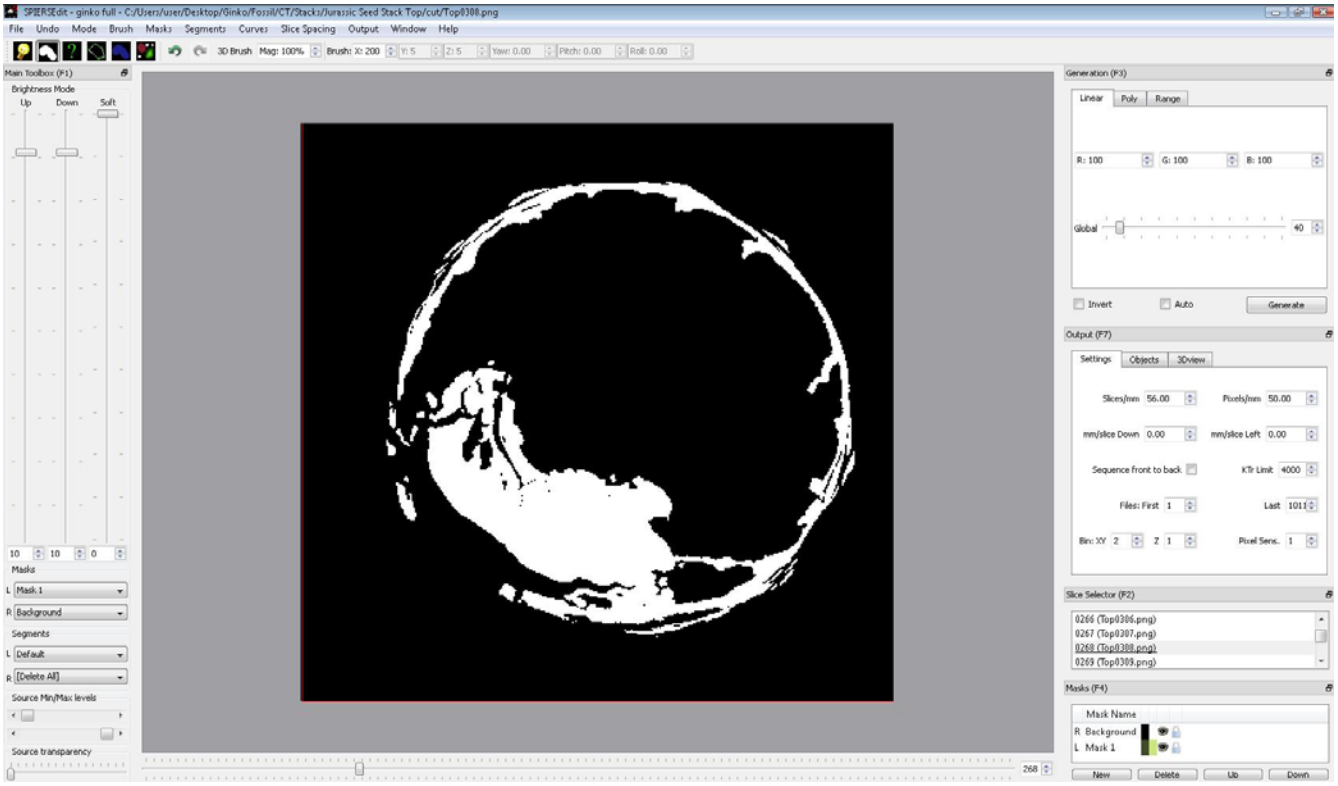

Figure 2.3 SPIERSedit screen shot showing a segment highlighted in white

Two methods in SPIERS are present for the editing of the fossil material, masks and curves. As the name suggests, using masks involves highlighting an area of a segment, the mask is applied by choosing a brush size which is appropriate to area to be masked. The structure of interest is then traced using the curser and holding the left mouse button down. The mask should be traced while using the fossil image is viewable and not the segment, it is possible to make the fossil image semi-transparent which does aide in tracing the areas of interest.

Many masks can be applied to the same segment (Figure 2.4). A mask would be applied to highlight a specific structure or organ, the same mask would need to be applied to the same organ or structure throughout the dataset in order for it to appear as complete in the final reconstruction, minimal editing of the mask is then required between each slice. A mask can be copied between slices to save highlighting the same area over and again. The 3D mask tool will apply the mask throughout the whole dataset; this does require increased processing time and is only advisable on faster computers.

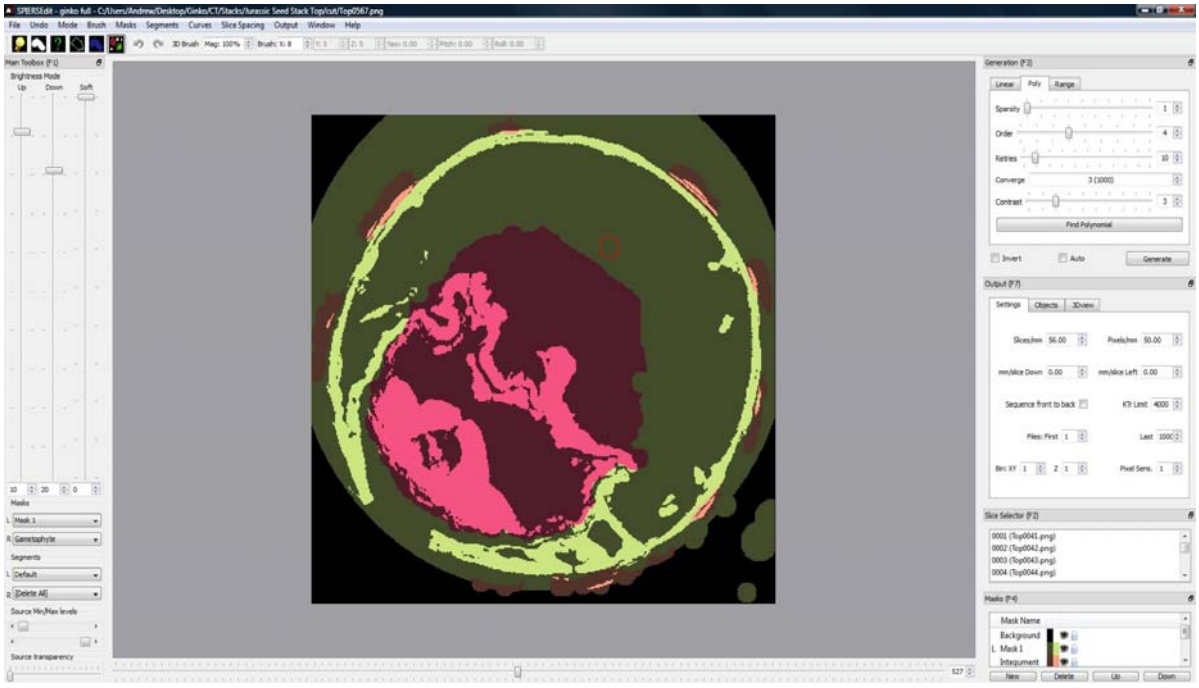

Figure 2.4 SPIERSedit screen shot showing the application of masks to a segment

Masks are created separately for each slice, therefore if the spacing is large between each of the slices, the reconstruction can take on a blocky appearance, the overall accuracy of the reconstruction is not affected. A small amount of smoothing can be undertaken using 3rd party software. Rapid prototyping software such as materialise magics and perform this, along with commercial animation software such as Maya or 3ds max.

The three types of curves are lines, closed loops and filled areas, each of which works on the same principle where a line is drawn on the area of interest and point are added onto the structure which the curve will follow. Single lines are useful on small structures such as transverse sections of sporophylls. The closed loops are used to identify structures such as cell walls and the closed loop is used to highlight whole areas in a similar way in which a mask would be used.

The masks are continuous between each slice and the missing data between each slice is interpreted, however if the gap is too large the interpretation is not sufficient and errors are likely to occur including giving the reconstruction a ‘twisted’ appearance.

SPIERSview is the package for which the reconstructions are viewed, the reconstructions can be exported as a SPIERSview file, a .DXF file and a .STL file. The DXF files can be used in CAD and animation software. The STL files can be imported into analysis software. This software is generally used in the engineering industry and does have certain limitations when dealing with fossil material. As the fossil models are not ‘perfect’ and often there is not the option to calibrate, to take accurate measurements. However measurements which do not require calibrations, such as angles, can be taken accurately.

2.4 Scanning Methods

Micro X-ray computer aided tomography (micro XCT) is the most common method used in palaeontology and has been used in the project. This is a relatively simple method in which the specimen is placed on a rotating stage, X-rays are then emitted at the specimen, a detector is behind the specimen and any X-rays which penetrate the specimen will then be detected. The specimen is rotated through 180 degrees with an image taken on average every 0.75 degrees (this can be altered). A series of filters can be used to allow different material to be scanned. The denser the filter the more dense material can be scanned. The material which can be scanned is dependent on the quality of the CT scanner used.

Limitations are placed on the size of the material which can be scanned in a micro CT scanner, although this does vary between manufactures, 2 cm diameter and 8 cm in height is usually the biggest specimen size which is applicable.

The Skyscan equipment at the University of Birmingham is not able to penetrate siderite, however newer and more advanced scanners are able to penetrate denser material, as siderite has been scanned in the reconstruction on arthropods (R. Garwood, pers. com. 2009).

2.5 Discussion

The benefits of the preparation methods used are described in Table 1. The context of the specimen and reconstruction always need to be taken into consideration when producing a reconstruction. If the specimen is one of a kind, very delicate, then a method such as serial grinding is not appropriate and a scanning method should be considered. Where a reconstruction is required on a more common specimen then a cheaper and more destructive method like wafering or grinding could be considered.

Method	**Approx. slices per MM**	**Advantages**	**Disadvantages**	**Level of destruction of the specimen**
Thin sectioning	0.2	High quality observations. Someone else	Slow. Low slide spacing. Wasteful of specimen (c. 95%	High

		does work.	ground away)	
Wafering	1-2	High quality. Regular spacing and measurable.	Intermediate speed. Hard to mount.	Low
Peel	20	Speed. Frequency of slices per MM. Do not need to mount all peels.	Can destroy soft tissues (parenchyma). Can over sample.	Low
Serial grinding	30	High resolution, excellent surface finish for digital photography	Slow and time consuming. Specimen is destroyed	Very high/total
CT scanning	50	Very high quality data, perfect image alignment, perfect tomographic spacing, specimen is undamaged	Very expensive, quality of scan can vary depending on equipment used, small specimens only. Not all material can be successfully scanned.	None

Table 1. Comparison of all preparation techniques used.

In an ideal situation scanning methods would be used, the main prohibiting factors being cost, specimen density and specimen size. With improving technology the factors will be reduced. Increasing levels of detail can be seen using scanning methods (Friis *et al.*, 2007), however use of a syncotron is extremely expensive and tightly controlled.

The physical optical tomographic methods in general show the best overall compromise. Wafering allows relatively rapid specimen preparation and greater than 60% preservation of the specimen, however the spacing between each slice is high and gives a low resolution reconstruction. When using serial grinding a high resolution reconstruction can be achieved, however all the specimen is lost and alignment time is very high. Combining serial grinding with acetate peeling would allow material to be saved, but increases the specimen preparation time and often acetate peels are not a substitute for wafers.

A common sense and pragmatic approach is highly recommended when undertaking a reconstruction, the needs of the reconstruction need to be taken into account along with the other factors mentioned within this chapter. There is no perfect reconstruction method and ultimately the governing factor on the quality of the reconstruction produced comes down to end user ability.

CHAPTER 3

TESTING RECONSTUCTIONS

3.1 Introduction

In order to generate 3-D reconstructions of sufficent quality to be able to assertain useful morphological information many considerations need to be reviewed including the required resolution of data collection, preperation methods to be use, and method of reconstruction to be used. To be able to determine these parameters, a large amount of testing needs to be undertaken. Many of these factors are discussed in Chapter 2 and in summary are the size, shape and complexity of the structures present in the specimen which need to be included in the reconstruction, the matrix in which the specimen is enclosed in, and what resources are avalibale to facilitate the reconstruction.

In this chapter, example reconstructions are shown of the cordaitean ovule *Cardiocarpus dabiziea* that was prepared by precision sectioning methodologies, the medullosan ovule

Trigonocarpus that was scanned using micro X-ray computer aided tomography, and previously prepared wafered specimens belonging to the gymnosperm genus *Araucaria* and also the gymnosperm family Ginkgoaceae. Each of these reconstructions will be reviewed mainly on their technical merit to show if the structures within the specimen are represented to an accurate degree, the type of specimen is suitable for a reconstruction and to evaluate what improvements can be made to attain greater levels of accuracy.

3.2 Reconstructions

3.2.1 *Caridocarpus dabiziae* – reconstruction from serial wafered sections

The first specimen of interest is the type and figured specimen of the cordaitean ovule *Cardiocarpus dabiziea* Hilton *et al.*, 2001 (Figure 3.1), which was orginally prepared for taxanomic and systematic investigation from an Early Permian permineralised plant assemblage in China (Hilton *et al.*, 2001).

The ovule is contained on 10 wafered sections and is visible on 18 surface tomographic planes, with each wafer being 1 mm thick, but with the cutting blade removing 0.3 mm for each cut. As the thickness of the sections and saw blade are known, spaced between successive tomogrpahic planes can be accurately reconstructed. The specimen was prepared in this way to undergo traditional taxanomic evaluation and at the time no consideration was made for it being subsequrntly used for 3-D reconstruction purposes. As a result no alignment marks are present in the preparations and all alignment had to be done on an educated but subjective basis; estimations were made to ensure there was a minimum amount of distortion in the rotation of each of the images and also on the X and

Y axis.

A datum point was measured to find the centre point of the specimen on each of the images used, each of these points was then used as the basis of alignment of the X and Y axis. Small adjustments were made if it was clear that alignment was not correct based on the structures within the specimen. To maintain consistancy in aligning the rotation of the images, the edges of the matrix block in which the specimen was contained was used as external alignment marks. This method was unable to be used to align on the X and Y axis as the outer edges were not consistant through the specimen that had an irregular outline prior to being cut. However, they do show enough accuracy for reasonable rotational alignment.

The clearly defined and continous structures within this specimen have made it ideal as a starting point to attempt serial reconstruction from previously prepared specimens as the slice generation tool within SPIERSedit (Sutton, 2001) can be used effectively to threshold the specimen from the matrix. This has two benefits; firstly it reduces the amount of time required to edit the reconstuction, and secondly it maintains consistancy throughout the reconstruction, that is assuming image exposure and thresholding levels are maintained throughout the sequences of images used to build the reconstruction.

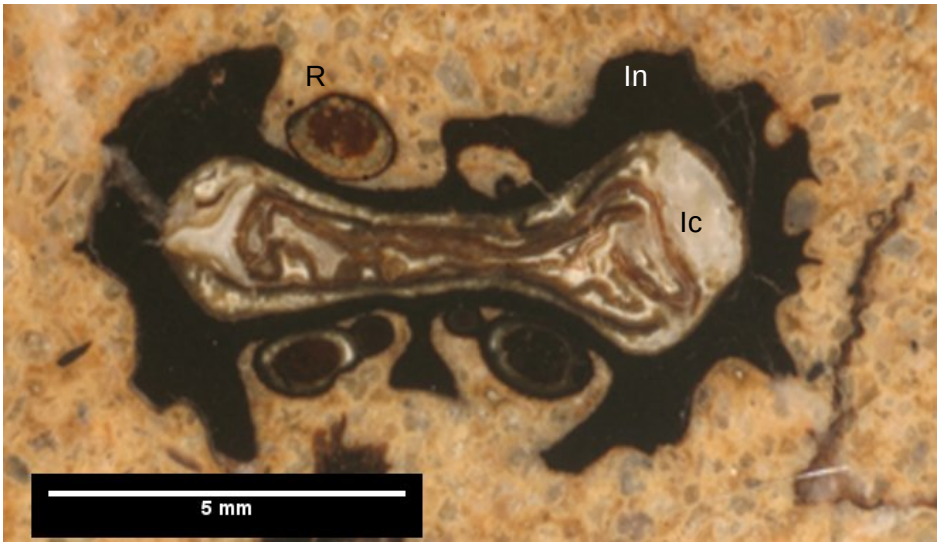

Figure 3.1 Transverse section of *Cardiocarpus dabizea* showing resin bodies (R), sarcotesta of the integument (In) and integument caviety (Ic).

Three main areas of interest have been explored within this specimen, each of which has been independantly reconstructed (Figure 3.2). These are the Integument, the ingeumentary cavity (Figure 3.3) and the resin bodies. Looking at figure 3.1, more detail is preserved in the specimen than can be shown in the reconstruction, the realativly coarse spacing in this reconstuction would make reconstucting structures on the sub mm level pointless as there is no way to make the structures continous throughout the reconstuction as the tomographic planes are more than 1 mm apart. This would provide no further clarity than studying the wafered sections in the traditional manner.

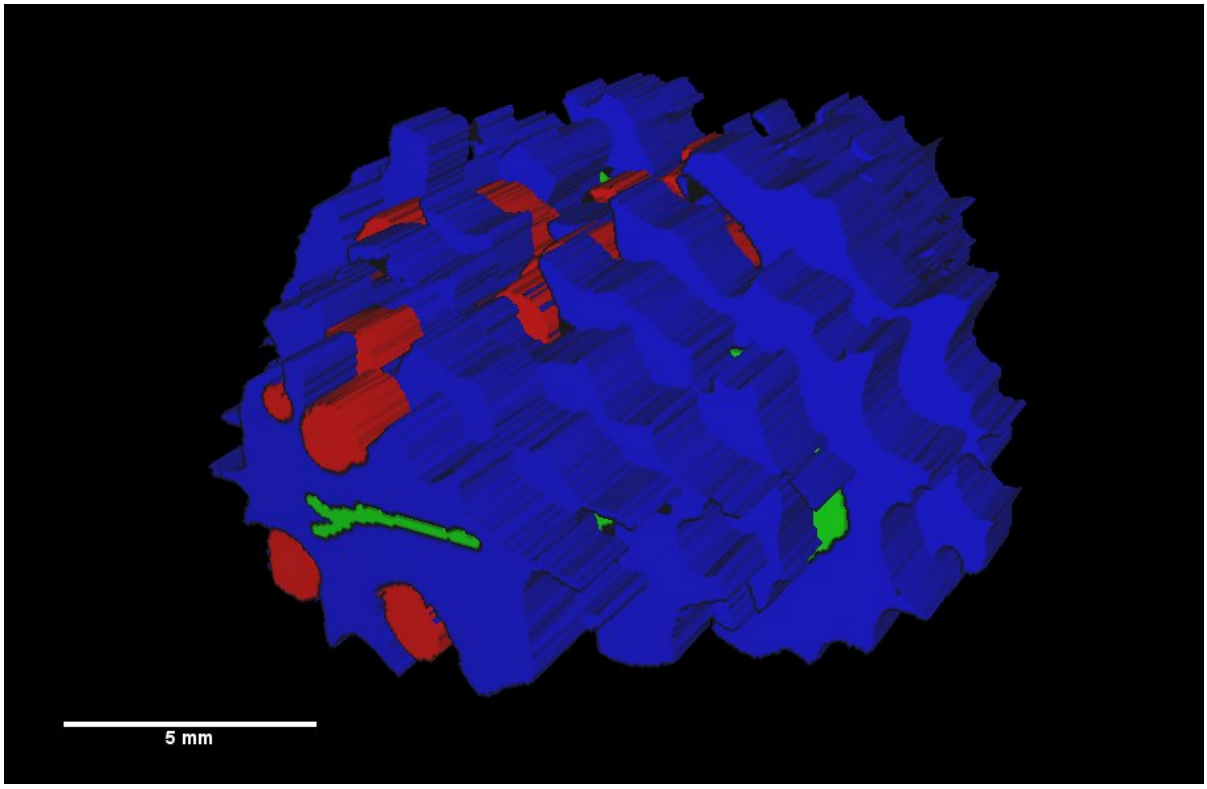

Figure 3.2 Reconstruction of *Cardiocarpus dabiziea,* oblique view with the ovule apex at the front. Showing integument (blue), resin bodies (red) and integument caviety (green).

The reconstruction has a blocky apparence that lacks fine surface details, and the overall apparence does not conform to a naturally curved, organic shape. These are artifacts of the preparation method used to construct the reconstruction, however, when studied in further deatil, the reconstruction shows that the specimen is bilaterially symetrical and that the resin bodies occur through 80% of the length of the ovule and are present in the major plane but not the minor plane of the ovule.

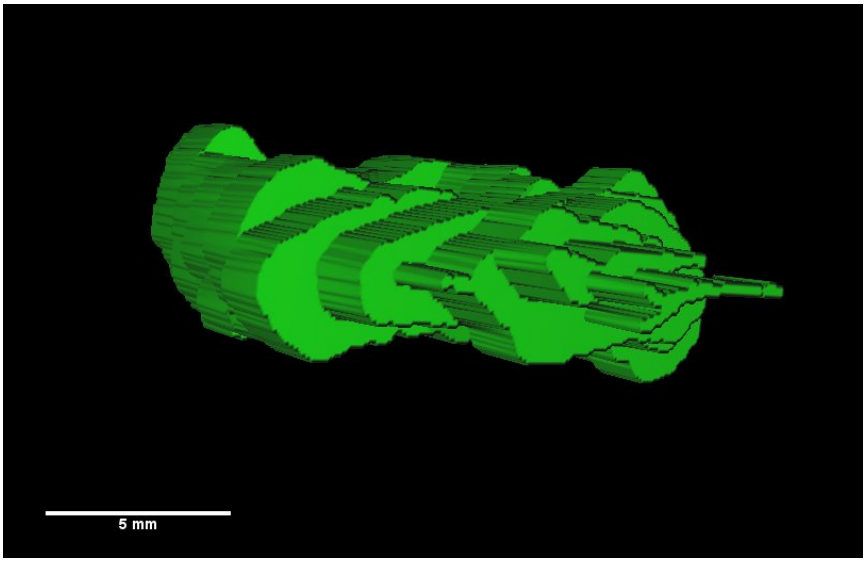

Figure 3.3 Reconstruction of *Cardiocarpus dabiziea,* oblique view showing integument (green)

To try and combat the blocky apparence and to see if a reconstruction can be made which is a more accurate representation of the morphology of the organ, smoothing methods were used on the reconstruction (Figure 3.4). Smoothing was undertaken in 3D animation software Maya produced by Autodesk. It uses Non-Uniform Rotational B-splines (NURBS) which is a method for producing complicated curved surfaces in compouter software (Foley *et al.,* 1995). This is used extensively in many industries from automative desgin to animated computer graphics. This allows a curved line to be placed between 2 points, which, in the case of these reconstructions, should produce the smoothing required for this specimen.

Not all of the internal structures could undergo the smoothing process as it is very memory and CPU intensive; the polygon count from SPIERS reconstructions is very high (Figure 3.5). Despite this, the smoothed reconstructions do provide a very good insight into the internal and external morphology.

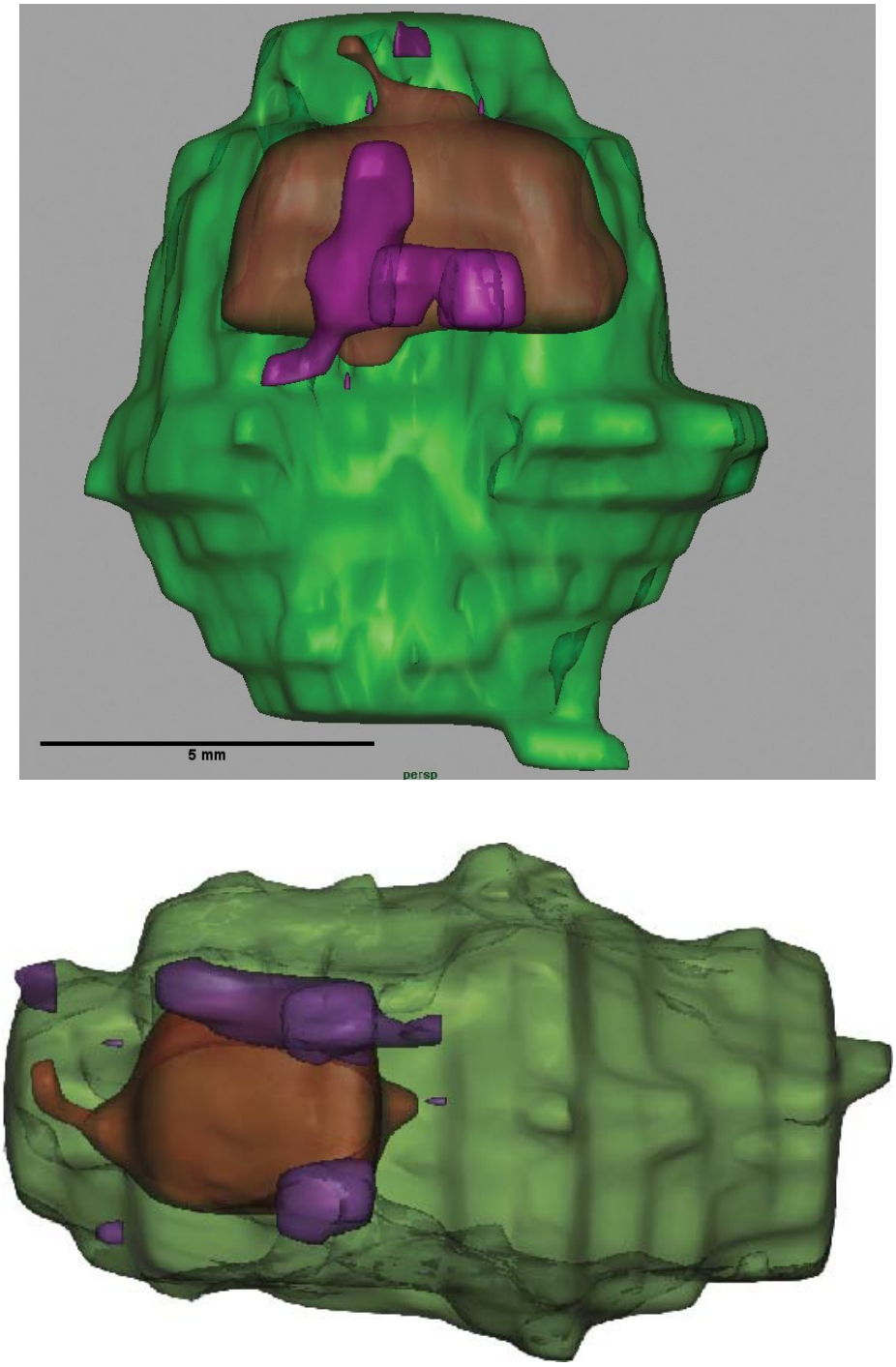

Figure 3.4 Smoothed and rendered images of *Cardiocarpus dabiziae* showing integument (green) resin bodies (purple) and integumentry cavity (brown). Top image as viewed from above (major plane) and bottom image as viewd from the side (minor plane)..

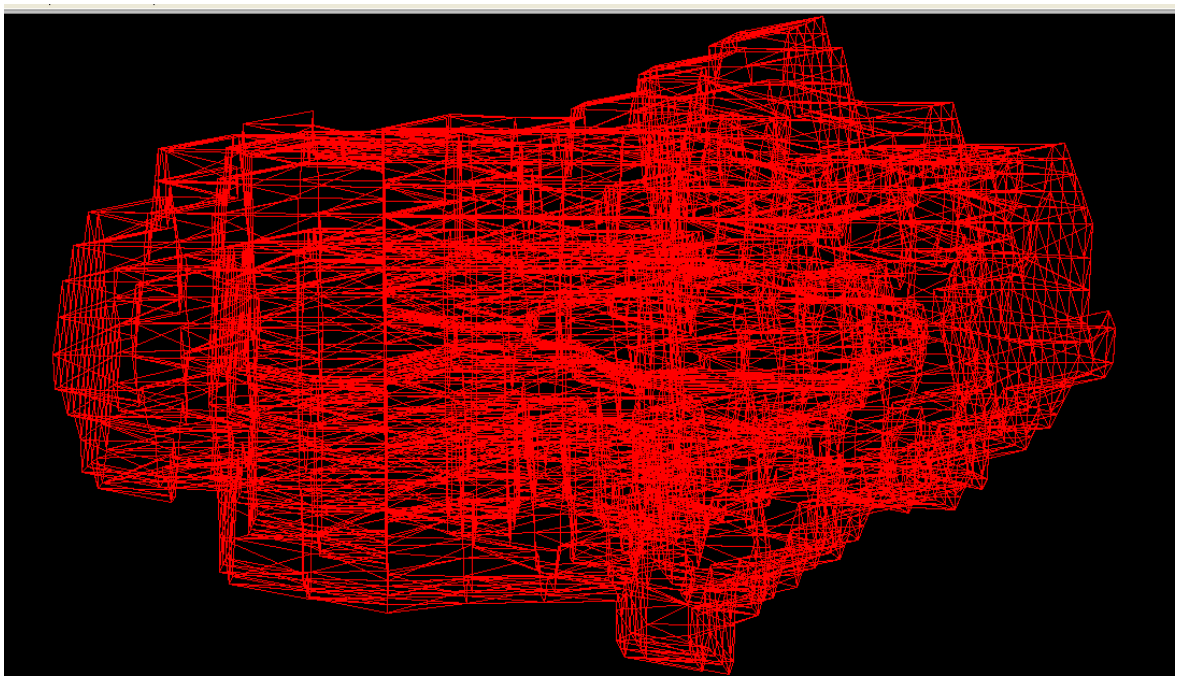

Figure 3.5 Wire frame mesh reconstruction of *Cardiocarpus dabizea*

Despite the thickness of each of the wafers and the lack of alignment marks, this reconstruction highlights that reasonably quick, simple and basic reconstructions can prove informative. This does highlight the gross morphology and interaction between tissues. There are also obvious limitations to this reconstruction, the complex internal structure within the integument has been largely ignored. This detail can be observed in sections, but as the structures are smaller than the thickness of each wafer, they would not appear as contionous structures and would be of no advantage than examining the wafered section using a more traditional method.

This material had been prepared for examination and mounted on microscope slides. Photography was easily and quickly undertaken, the main time consuming difficulty in this reconstruction is the alignment process which takes several weeks. The large level of

detail in the specimen means that applying the segments and masks is a slow process with the whole reconstruction taking just over 1 month, with the additional smoothing and manipulation taking a further month.

3.2.2 *Trigonocarpus* – Micro X-ray Tomography reconstruction

The second specimen has been reconstructed using Micro X-ray Tomography. The specimen was placed in a SkyScan desk top X-ray CT scanner in the Department of Chemical Engineering at the University of Birmingham. The specimen was chosen as it was free from any matrix or substrate, it has a broadly round shape and its size. All of these factors make the scanning process more successful as the X-rays do not have any matrix to pass through, the X-rays are penetrating a similar density and surface area through all 180º in which the scanning occurs, and the relativly small size means the X-rays are confined to a smaller area which should allow for greater accuracy. The specimen has never been formally identified and its location is unknown, however it is believed to be mid Carboniferous in age (Pers coms, Jon Clatworthy, 2009, Curator of the Lapworth Museum). From the external morphology it would be fair to assoicate the specimen with the genus *Trigonocarpus* Brongniart 1828*,* showing a particular similiarity to *T. shorensis* Sailsbury, 1913 (Salisbury, 1913). It is defined by being radially summetrical with three prominent ribs running longitudially along the length of the ovule 120º apart (figures 3.6-3.8).

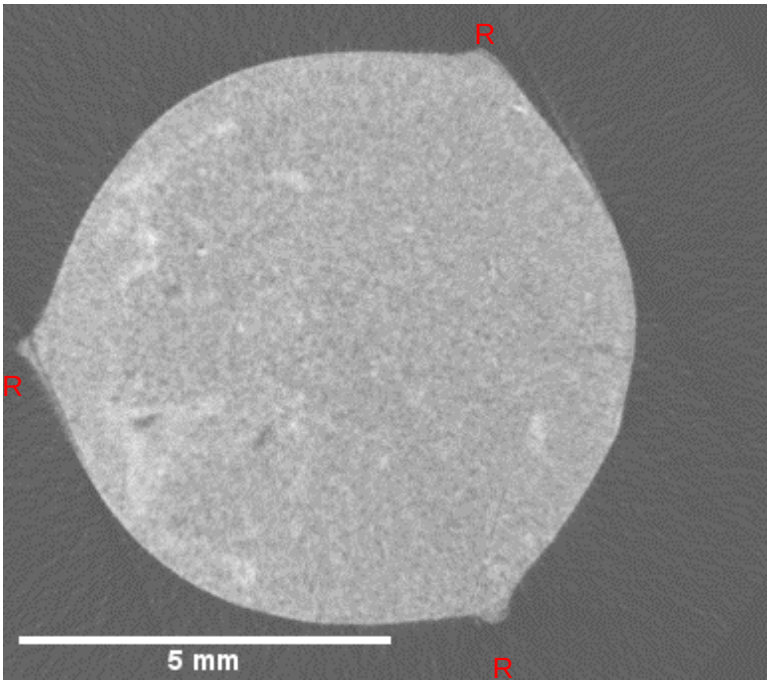

Figure 3.6 X-ray tomographic image of *Trigonocarpus.* Transverse orientation, 1.3mm from apex of specimen. Showing three ribs (R)

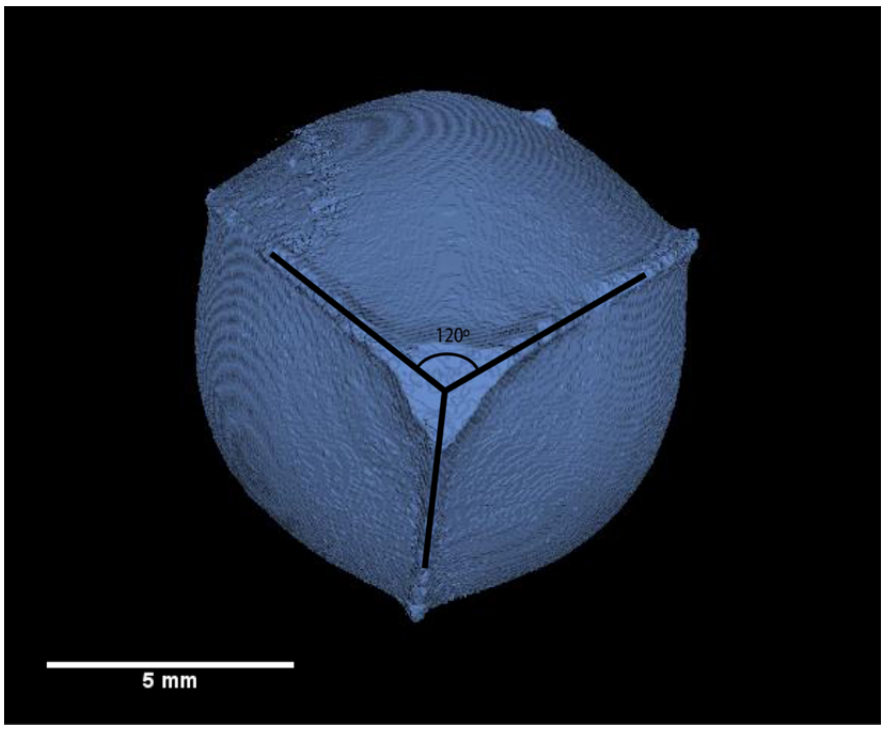

Figure 3.7 Reconstruction of *Trigonocarpus* viewed from the apex showing three ribs with an angle of 120º between each.

The reconstruction is made up of 300 images at a spacing of 70 µm and gives a total specimen length of 21 mm. Alignment of the images was achieved automatically as the tomographic images that come from this scanning method ‘pre-stacks’. Thresholding of the fossil from non-fossil material was also a simple task as there is a clear contrast allowing for auto-slice generation to be used within SPIERSedit.

There is a lack of clear internal structure within the specimen (figure 3.6), elements of some structures are present but are not continuous and can only be used to draw brief assumptions of the presence of an integument. This demonstrates that the specimen is a cast rather than an anatomically preserved specimen. As a result of this, the specimen was not investigated further and only used as a test piece to show external morphology and to understand the principles of producing a reconstruction from micro X-ray CT data.

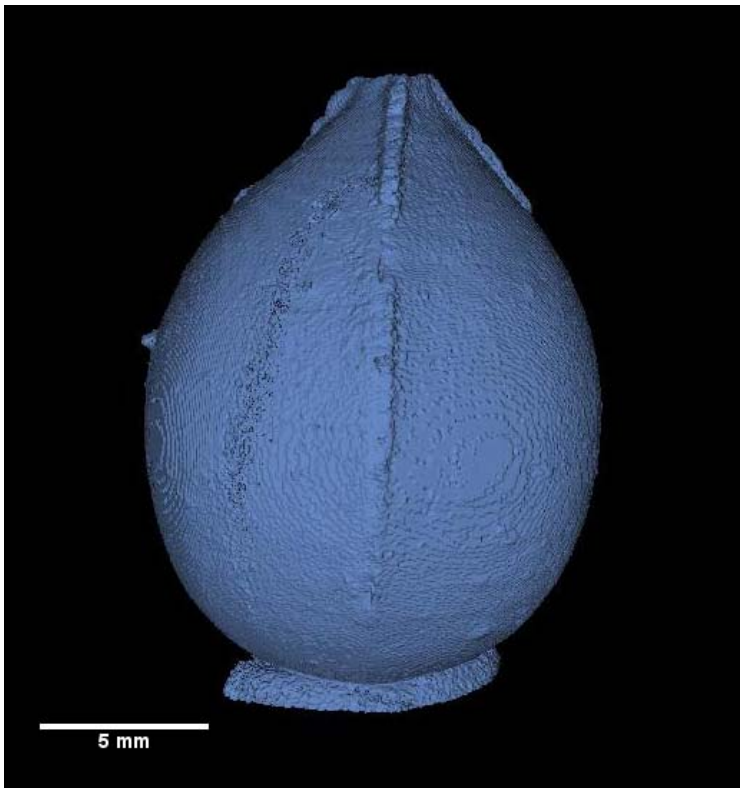

Figure 3.8 Reconstruction of *Trigonocarpus*, side view with apex at the top of the image.

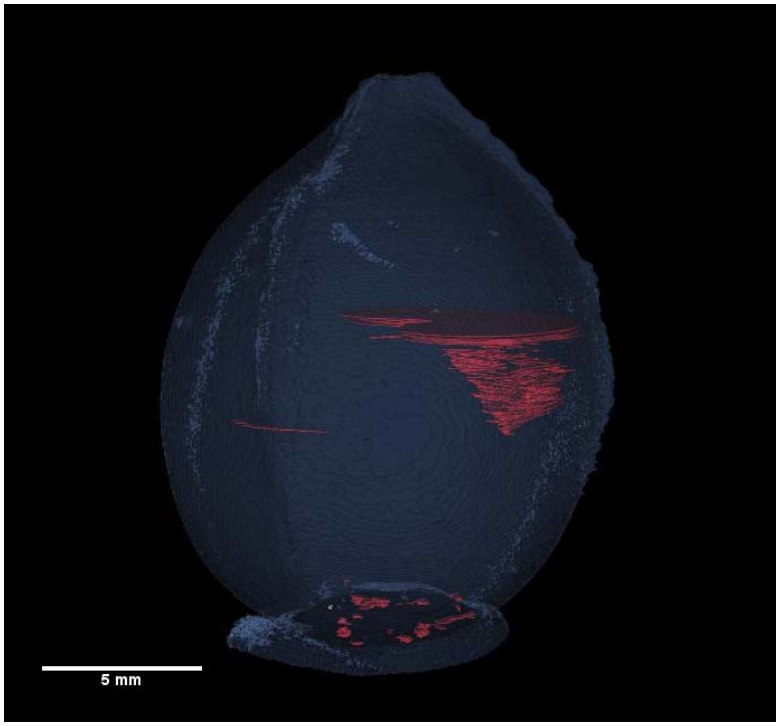

Figure 3.9 Reconstruction of *Trigonocarpus*, side view with apex at the top of the image. Outermost testa is partially transparent revealing some internal structure (red).

A small mass is present (towards the top of the image) in Figure 3.7, this is thought to be a taphonomic artifact rather than any particular structure that was present when the specimen was living. The ribs also appear to be truncated in certain areas (Figure 3.8) and they do taper towards the base. The truncation is again likely to be due to preservation, the rough edges where the ribs appear to be broken would also suggest that this feature in its current state has occurred post burial and could have occurred during specimen collection.The tapering of the ribs towards the base of the specimen is likely to be a natural occurance and is common place in living ovules of similar morphology. The extant gymnosperm *Ginkgo biloba* L. 1753, which is discussed in Chapter 5 also shares this feature.

In summary, this specimen of *Trigonocarpus* provides an excellent insight in to producing a reconstruction using micro X-ray CT data on the external morphology of specimen casts. The images are of sufficent quality and are closely spaed enough to allow a high resolution reconstruction with processing and editing times greatly reduced compared to those of *Cardiocarpus dabiziae* (see above). Where more detailed internal structures remain, the editing and processing time will increase, however this would be the same for any specimen and the type of data set will still make that process reasonably fast. The external morphology is represented in exceptionaly high detail and because the model can be manipulated and moved on screen, is of more use than simple photography.

This was the first specimen to be reconstructed using CT scanning in this project. As a result it took longer to produce the finished reconstruction than later simple CT scanned models, however it was still quicker than undertaking a similar resolution model by a grinding method. This reconstruction took about 1 week to produce.

3.2.3 Ginkgoaceae – Wafered reconstruction

The specimen (figure 3.10) was collected from St Ives in Cambridgeshire (grid reference TF 305 725) and is from the Oxford Clay Formation which in this area is Callovian (Jurassic) in age.

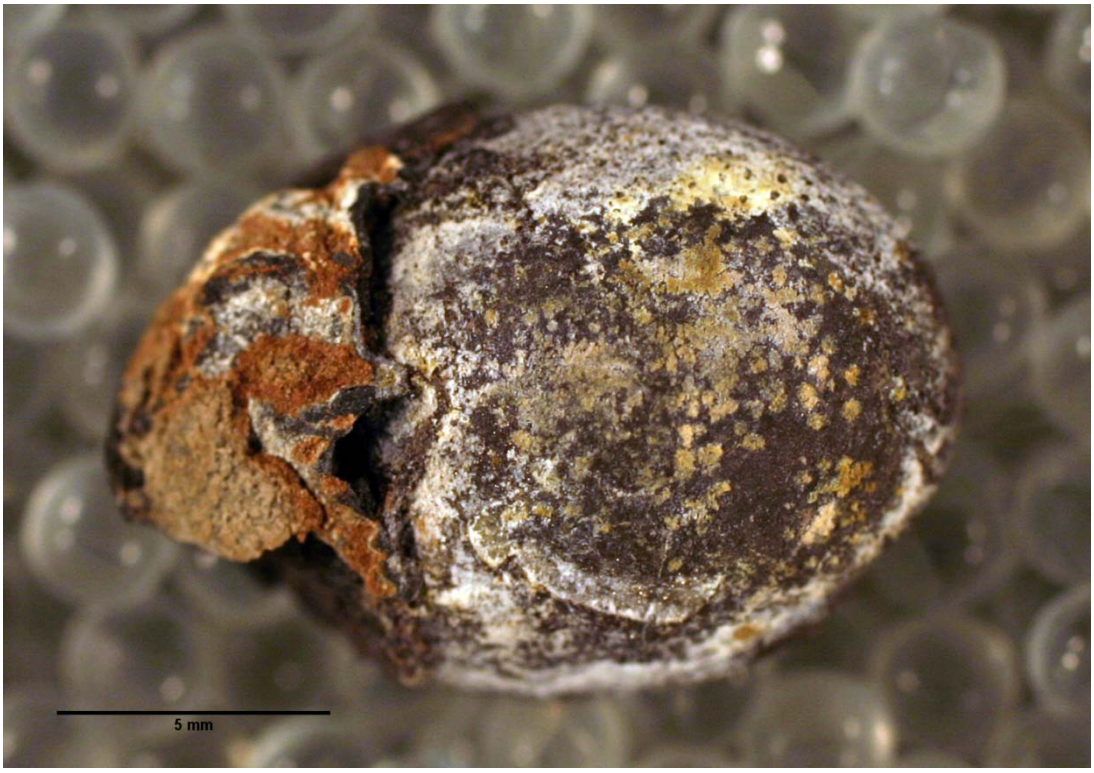

Figure 3.10 Fossil specimen of Ginkgoaceae. Lateral view.

The specimen has been serially wafered at 0.5 mm intervals (Figure 3.11) and mounted on glass slides. 42 cut surfaces were available for reconstruction. Each surface was photographed using a Canon 10D Digital Single Lens Reflex camera using a 50 mm macro lens. The specimen had been prepared for traditional taxanomic description. No alignment marks are present.

The specimen is very similar to other species of the family Ginkgoaceae which are described by Zhou (2009) and in greater detail in chapter 5.

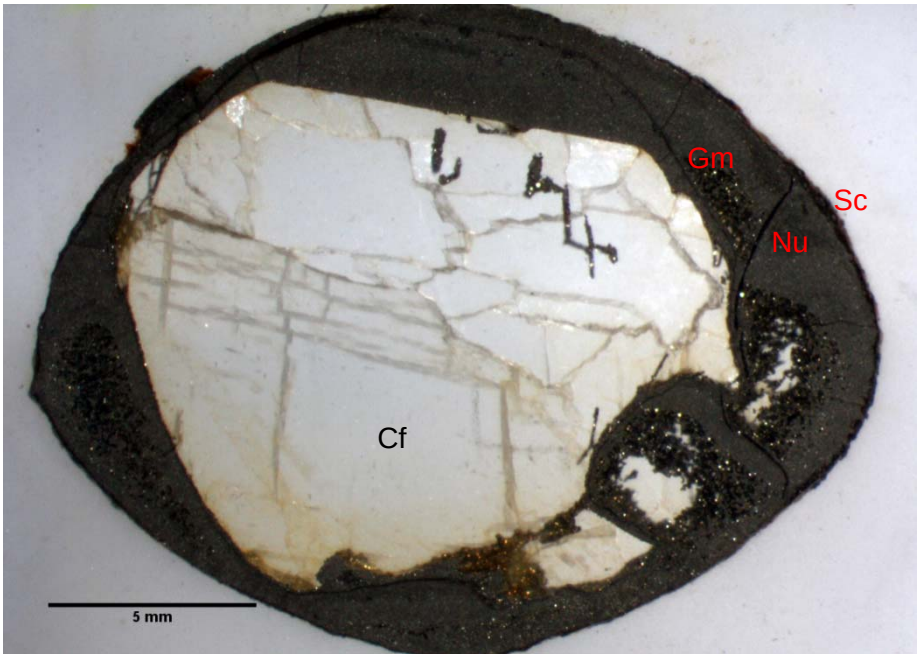

Figure 3.11 Transverse section of Ginkgoaceae ovule showing sclerotesta (Sc), nucleus (Nu) gametophytic membrane (Gm) and calcite cavity fill (Cf)

Many of the structures shown in figure 3.11 are representative of a ginkgoalean ovule (Zhou, 2009 & 2012). The scale of these structures, many of which are below 0.1 mm, make them too small to be viable for reconstruction purposes as they vary significantly between the tomographic planes present.

The alignment process was conducted in a very similar manner to that of *Cardiocarpus dabiziae* described earlier in this chapter. One of the advantages of aligning this specimen over *Cardiocarpus dabiziae* is that part of the cavity fill forms a straight edge that represernts a cleavage plane within a single crystal of calcite. This acts as a rough guide to the X and Y axis positions, but crutially, acts as a near perfect guide to any rotational movements of the images which need to occur.

The sarcotesta of this specimen no longer remains and the reconstruction shown in figure

3.12 shows the outer most remaining layer which is the sclerotesta. One rib is prominent and runs along the long axis of the specimen, another rib is present 180º to this but is much less pronounced and is far more rounded.

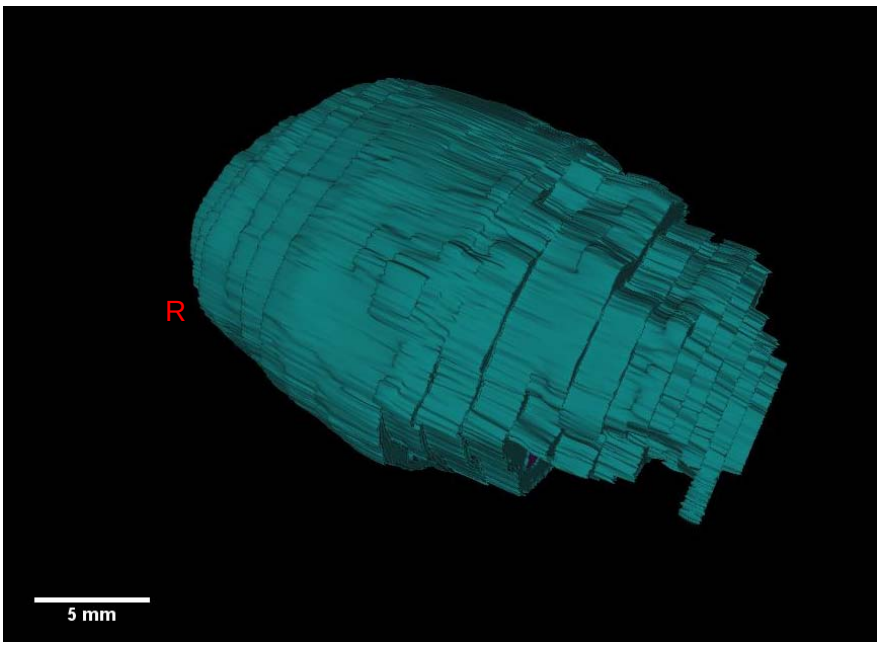

Figure 3.12 Reconstruction of Ginkgoalean ovule, oblique lateral view of exterior (sclerotesta) showing one rib (R)

When comparing the gross morphology of the whole specimen in figure 3.10 to the reconstruction shown in figure 3.12, there are obvious similarities which are maintained, however due to the nature of the preparation of the specimen, lacking alignment marks and due primarily to the relatively wide spaces between each of the tomographic surfaces, resolution and detail has been significantly lost especially at the apical part of the ovule that is incomplete.

The only internal structure which could be reasonably reconstructed was the cavity infill (Figure 3.13). This area is filled by calcite and provides an excellent contrast with the

surround area making the masking process quite straight forward. There are some similarities with the mega-gametophyte material reconstructed in chapter 5 (figures 5.13 & 5.14)

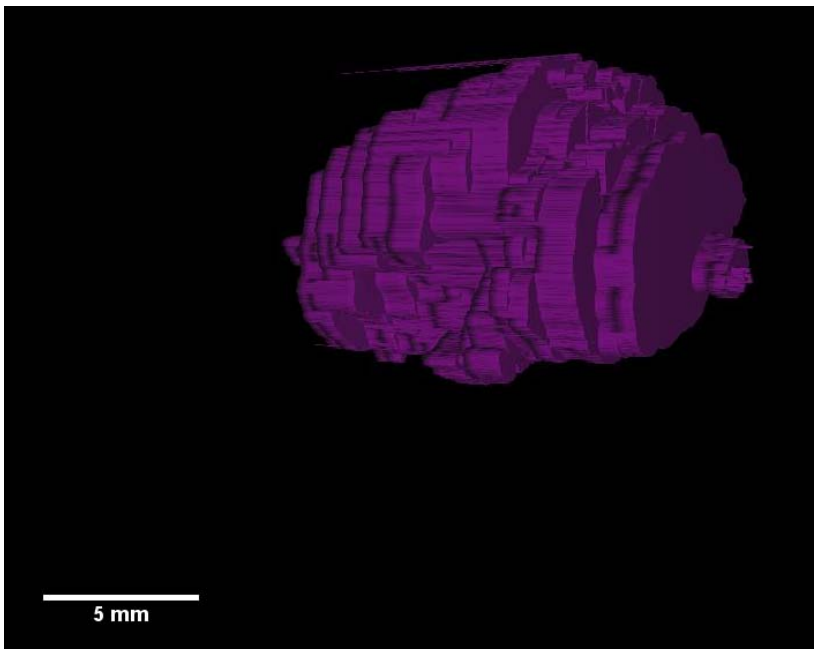

Figure 3.13 Reconstruction of Ginkgoalean ovule, oblique lateral view of interior cavity fill

This specimen of Ginkgoaceae does not benefit from this method of 3D reconstruction. The external morphology is clearly shown from the photographs of the specimen before serial sectioning was undertaken. The internal structures within this specimen are best observed under microscope from the wafered surfaced, where most detail can be observed. The reconstruction which shows the internal cavity gives little information on the morphology of any fertile tissues as the exact boundaries are not clear and the gaps between each tomographic surface are too great for them to be reconstructed as continuous structures.

This material had been prepared for examination and mounted on microscope slides. Photography was easily and quickly undertaken, the main time consuming difficulty in this reconstruction is the alignment process which takes several days. The limited level of detail in the specimen means that applying the segments and masks is a quick process with the whole reconstruction taking just over 1 week.

3.2.4 *Araucaria mirabilis* - Wafered reconstruction

This specimen of *Araucaria mirabilis* is a type and figured specimen located in the Department of Paleobotany at the Naturhistoriska Riksmuseet, Stockholm, Sweden. The specimen was described by Stockey (1975) and is made up of 12 tomographic surfaces (Figures 3.14 & 3.15). The reconstruction was undertaken to investigate whether a specimen which has been sectioned in a longitudinal orientation could be undertaken as easily as one which has sectioned in transverse orientation. The specimen also shows a clear internal structure which is well understood and described.

Alignment of this specimen was exceptionally difficult, the wafered sections were not of equal spacing, the outer edges of each of the surfaces is different and there is no common centre point. Attempts were made at alignment and were subsequently not successful.

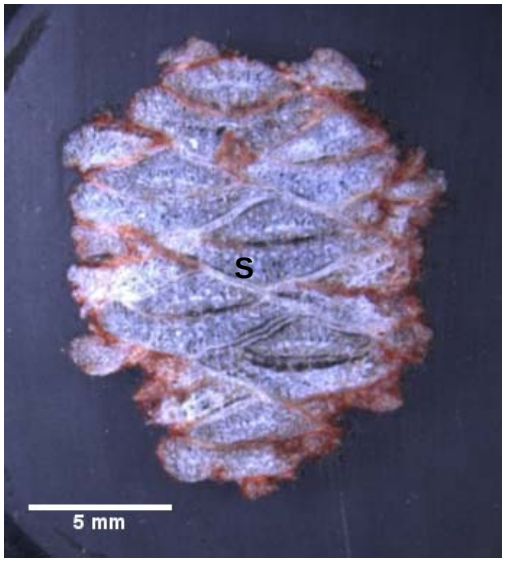

Figure 3.14 Longitudinal section of *Araucaria mirabilis,* showing sporophylls (s)

Figure 3.15 Longitudinal section of *Araucaria mirabilis,* showing central axis (Ca) and sporophylls (s).

As a result of this unsuccessful attempt to accurately align this specimen, it was decided to reconstruct each of the surface separately and to export each of these surfaces as a individual object and then attempt to align and reconstruct each of this surfaces in 3rd party software. Figure 3.16 shows 3 of these completed surfaces in which the position, size and shape of each of the sporophylls is masked. These individual reconstructions are then artificially stacked in the same way that the images are stacked during the initial image processing described in Chapter 2.

The missing data in between each of the tomographic surfaces does not allow for the continuous structures to be used for alignment as their position changes too greatly from one surface the other. This does provide a good representation of the interlocking nature of the sporophylls and a way to understand the overall structure in diagrammatic form.

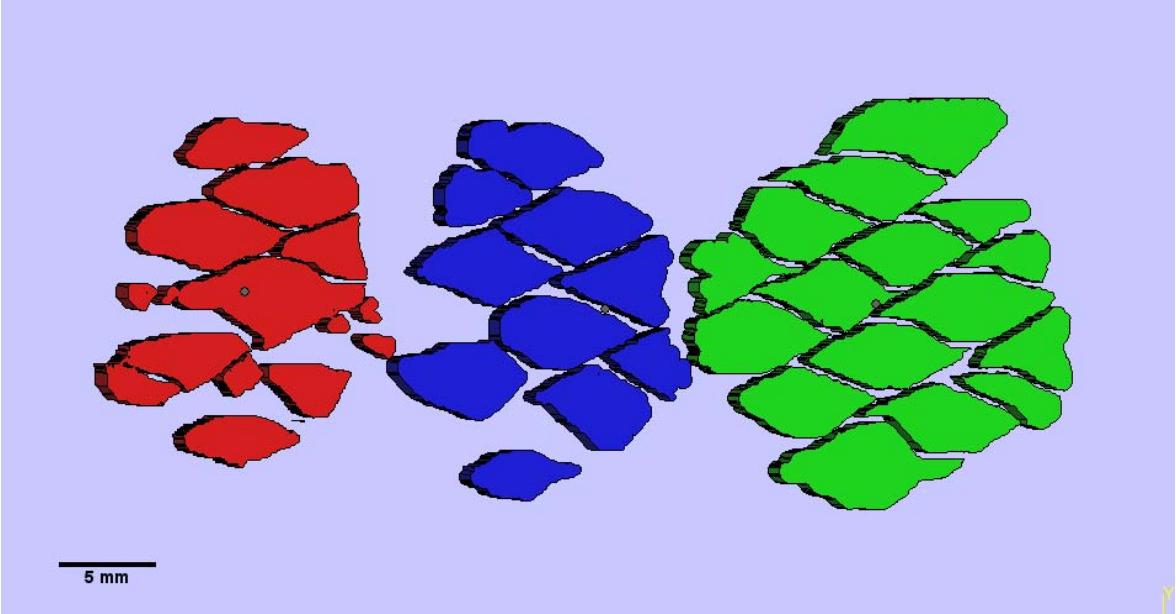

Figure 3.16 Reconstruction showing individual sporophylls, each colour represents the sporophylls located on each tomographic surface.

Due to the limited nature of this reconstruction and that the material had been prepared for taxonomic examination, this partial reconstruction was undertaken in 2 days. The manipulation in 3rd party software was for examination purposes and was undertaken in less than 1 day.

3.3 Discussion

Before undertaking a reconstruction, several factors need to be addressed. First of these is what information and data are required to be gathered from the specimen. Secondly, one must consider how the specimen is to be or has been prepared. Finally, it is important to consider the nature of the specimen itself.

In the case of *Cardiocarpus dabiziae*, the specimen has been prepared to a high standard, with each of the wafered sections at regular intervals and only a gross morphology was required from the reconstruction. The specimen has large external and

internal structures which are continous and allow for this type of reconstruction. The smaller scale internal structures were omitted from the reconstruction due to their scale; they were far too small for the overall resolution of the reconstruction to show anything informative. These fine internal structures could be adequatly investigated using traditional methods, showing that the reconsturctions should be used in combination to assertain the morphological data within a specimen.

Results from the *Trigonocarpus* reconstruction has shown that data from micro X-ray CT scanning is an excellent method for creating reconstructions. The quality of the data, pre aligned images and very low distances between each tomographic surface mean that reconstruction can be made quickly and very accurately. Problems do arise from using this method when the specimen is surrounded by a dense matrix, however this is a problem that can be spotted within minutes of the specimen being scanned. The very first scan which is undertaken produces what is known as a shadow image. This will show what the level of X-ray attenuation is within the specimen and will decide if a full scan is applicable.The other advantage of this method is that it is non-destructive with specimens not being damaged in any way. Before scanning methods were available, there would have been a very strong argument to section specimens of this kind if they were to undergo detailed systematic investigations. Such methods destroy the completeness of the specimen and allow only partial and low quality reconstructions to be made, and should be reserved only as a last resort for important specimens that do not respond to X-Ray penetration.

The Gingkoalean ovule analysed in this chapter shows that despite careful preperation, a sectioned specimen may not lead to an adequate reconstruction. The external

morphology of the reconstruction is a good representation of what is shown in figure 3.10, but this is not as accurate as a direct study of the whole specimen would have been. In a similar sense there is little gained from simply reconstructing the cavity infill as this does not fully reflect the boundaries of the internal structures. This specimen would be ideal to undergo micro X-ray scanning and then a traditional investigation through serial sectioning, but when this specimen was prepared this method was unavailable. Many of the internal structures would have been present in the scan, however, the very fine detail is unlikely to have been shown and the more tradtional approach would have been able to investigate these reigons. The speicemen, as is it currently prepared, is unsuitable for reconstruction unless only a crude morphology is required. It remains suitable for study by traditional systematic investigations.

The specimen of *Araucaria mirabilis* Stockey, 1975, shows that some specimens are not suitable to be reconstructed if they have not been prepared in a suitable way for the specimen type. Although the preservation is excellent and there are larger scale structures which seem to fall within the boundaries of scale for this preparation method, there is too little information to be able to accurately align the specimen, if alignment cannot be achieved then a reconstruction cannot be produced.

CHAPTER 4

RECONSTRUCTION OF FOSSIL LYCOPSID CONES

4.1 Introduction

During the Pennsylvanian, late Carboniferous, large regions at tropical latitudes were covered by peat forming mires (DiMichele et al., 2002) with many of these mires being dominated by arborescent lycopsids (DiMichele and Phillips, 1994; Gastaldo et al.. 2004). Many classic paleobotanical localities occur in the Carboniferous of the UK, as a result there has been a long history of investigation in to the species which dominated this environment. Traditional methods of assessing lycoposid cones have given a wealth of information on their structure and morphology.

Presented here are 3-D anatomical reconstructions of specimens from the genera *Lepidostrobus* Brongniart 1828*, Lepidocarpon* Brongniart 1828 and *Flemingites* Brongniart 1828,. Different reconstruction methods have been used on each specimen and emphasis has been placed on maximising data collection of each reconstruction method used. It is

not expected to be able to collect the same specific data from each specimen as the nature of the specimens, preparation and reconstruction method will make this vary. It is hoped this will detail a frame work of what is possible to be understood.

4.2 *Lepidostrobus sp. A*

4.2.1 Introduction and geological setting

A formal identification of this cone has not yet been achieved as the main distinguishing features of lycopsid cone taxa are the spores contained (Brack-Hanes & Thomas, 1983; Bec, 2004) and in this specimen sporangia have abscised such that spores have been shed prior to preservation. However, for the purposes of the reconstruction, identification is not critical and the likely genus is *Lepidrostrobus* (Brack-Hanes & Thomas, 1983)

Crock Hey open cast coal mine is situated in the North West of England approximately 3 KM NE of Saint Helens (SJ 530 975). The area is a Konservat-Lagerstätten with the majority of exceptionally preserved plant material being found in siderite concretion, occasional *in-situ* calamites and *Lepidodendron* Brongniart 1828 stems are found in the coarser sand bodies, which generally show a small amount of inclination (Anderson *et al.*, 1999) that possibly indicates low energy current flow direction. The thinly-laminated siltstones, with intermittent sandstone layers and the occurrence of fresh water fauna would indicate that this is a lacustrine deposit.

Three coal seams were worked at this location; they are the Wigan Nine-foot, Two-foot, and Four-foot seams. Due to the complicated nature of the faulting many of the coal seams now appear discontinuous and the naming has become blurred. The Wigan Nine-foot seam has two alternative names, the Wigan Six-foot seam and the Trencherbone seam.

Back filling of the mine started in 2006 and access to the coal seams was denied during a previous visit due to safety concerns. Material collected was taken from spoil heaps, therefore all collected material is *ex-situ*. Previous work (Braznell, 2006) will be used as one of the main locality descriptions. Other locations within the area have mined the same seams, namely Westhoughton (Anderson *et al.*, 1999) 10Km NE of Crock Hey

All of the material for the 3-D reconstruction work from Crock Hey has come from siderite nodules rather than from the coal material. The source of the nodules is a series of siltstone beds which occur above the Two-foot seam and above the Four-foot seam. It is not known from which of the above seam deposits the nodules have come from. Work done by Anderson *et al.* (1999) at Westhoughton states that the nodules often show a grading pattern and rapidly coarsen upwards from between 2-3 cm in diameter to up to 50 cm within the siltstone above the Four-foot seam. This pattern is not noted in the work done by Braznell (2006).

Majority of the plant material found in the West Lancashire coal fields is found in nodules directly above the Two-foot and Four-foot coal seams, the amount of plant material occurring in nodules decreases with distance away from the coal seam (Anderson *et al.*, 1999). Above the Four-foot seam occurs *in-situ* tree stumps of *Lepidodendron,* they are commonly at a slight inclination of approximately 10- 15 degrees relative to the bed they occur in. The sandstone which they occur in are indicative of a short term increase in energy level, likely to be as a result of an overbank deposit (Braznell, 2006). It is reasonable to assume the inclination of the stems is as a result of the current flow. This is very similar to the succession see in Joggins, Novia Scotia (Calder *et al.*, 2011) and also a lot of the environments described by DiMichele *et al.* (1985).

The type and level of preservation seems to depend greatly on the genera. The more

substantial cones from *Lepidodendron*, such as *Lepidostrobus* and *Lepidocarpon*, do generally have well preserved 3-D structure, showing small amounts of decomposition and deformation, but as a whole are intact.

The top and bottom of the nodule were lost during collection of the specimen and only a partial reconstruction is shown here. This reconstruction represents the centre 60% of the specimen and has been produced from 550 images which have been acquired through serial grinding and photographing the fresh surface. Acetate peels were taken after every 5 photographs so a permanent record could be kept of the specimen. This method is described in more detail in chapter 2.

Leipdostrobus is a genus which was first assigned by Brongniart and has been later modified by Brack-Hanes & Thomas (1983) so the genus is assigned in the presence of microspores only (Brack-Hanes & Thomas,1983). No megaspores were observed in the sections, with a tentative possibility of microspores being present in one of the ground sections. The specimen has not been macerated to obtain spores as that falls outside of the scope of this thesis, as the aim of this thesis is to reconstruct the gross morphology and not to identify species based on palynology. On this basis the specimen will be assigned to the genus *Lepidostrobus,* however if any further investigations do take place, and megaspores are found then this could be re-assigned to *Flemingites.* Like many examples of *Lepiodstrobus*, identification down to a species level requires the identification of spores (Thomas *et al.*, 2009) as many of the cone structures are quite generic.

4.2.2 Description and Results

Lepidostrobus sp. A was found in a siderite nodule, which is very typical of the area and

indeed coal measure successions as a whole. The specimen is contained within the centre third of the cobble and has been heavily compressed in the transverse orientation (Figure 4.1). The specimen now has a rectangular cross section, the width being approximately 8 mm and length 28 mm. There is a small amount of variability throughout the length of the specimen. The compression would have occurred soon after burial and was the result of a sustained load rather than sudden impact as the deformation has preserved the original structures and there are no obvious breakages, just a modification in shape. This would have been helped by the specimen falling into a wet substrate in which the desiccation would have occurred slowly and after the compression has taken place.

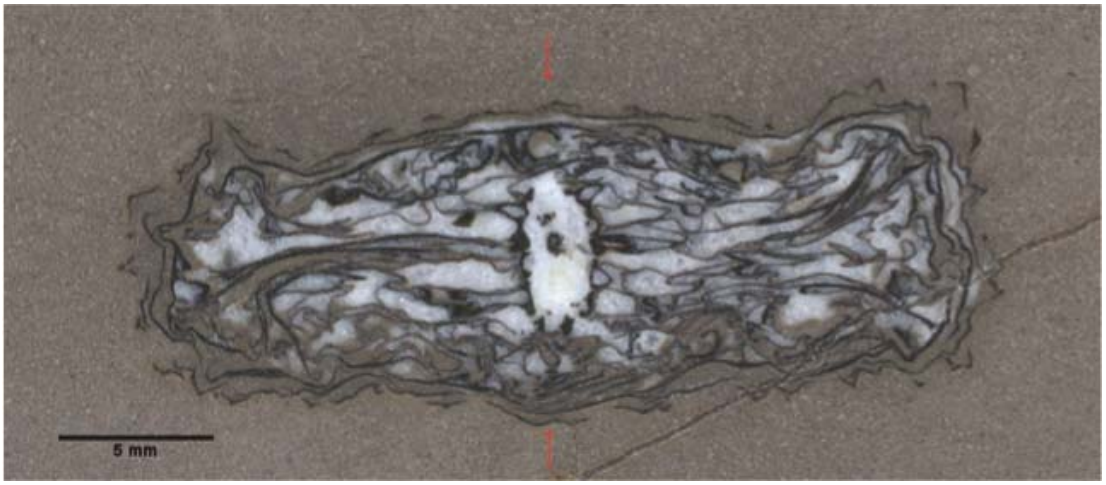

Figure 4.1. Transverse view of the centre of the *Lepidostrobus* sp. A, red arrows showing direction of compression.

The specimen shows a highly complex but ordered structure which is based around a central axis which shows a basic stele which is similar to an actinostele (Figure 4.2) The sporophyll traces emerge from the vascular material in a typical spiral arrangement.

The organic material is shown with high contrast as the black material within the specimen. The white material (calcite) readily dissolves in HCl leaving the organic material behind. The calcitic material seems to have been trapped, or is at least more closely associated with the sporophylls closer to the centre of the specimen and is not evenly distributed.

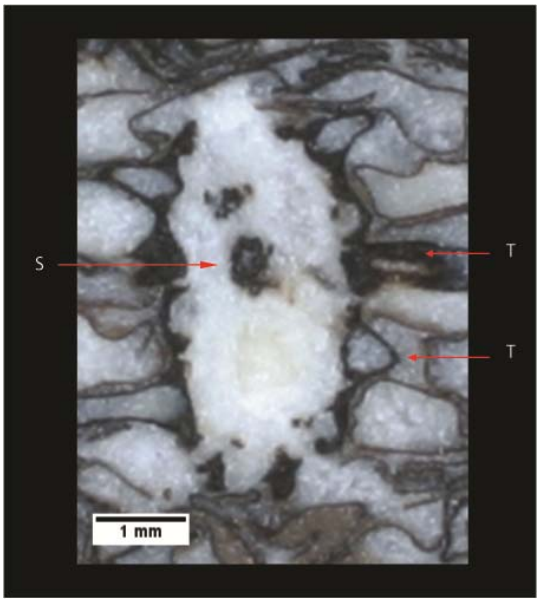

Figure 4.2 Transverse orientation of *Lepidostrobus* sp. A. showing the central axis, stele and emerging sporophylls

From looking at both the photographed sections and the reconstructions (Figures 4.1-4.5) the tight arrangement of the sporophylls can be seen. The sporophylls have a length of up to 20 mm and a maximum width of 3 mm. Their arrangement is very similar to that described by Scott (1901) with a very tightly packed sporophyll arrangement.

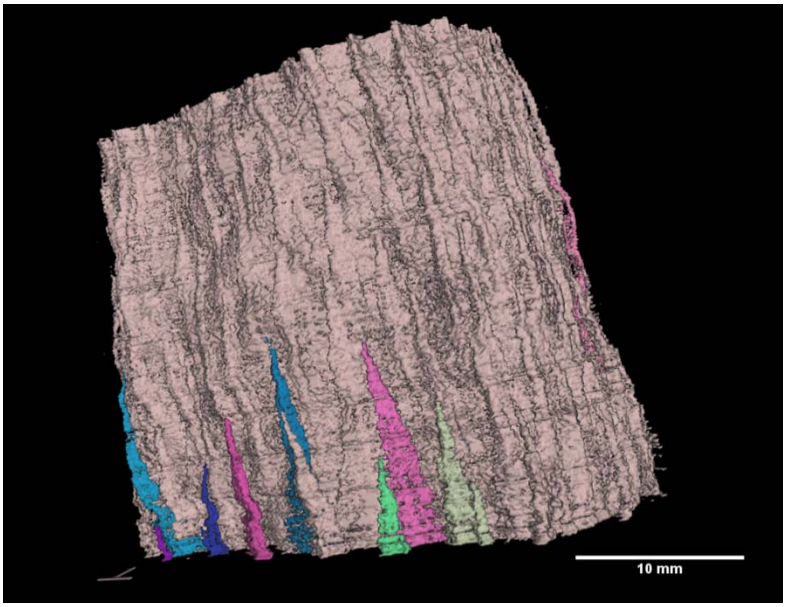

Figure 4.3 Partial reconstruction *of Lepidostrobus sp. A,* oblique view, showing external morphology and selected highlighted sporophylls

The sporophylls are not regular and homogenous in terms of their morphology. Some of the sporophylls have a curve from the axis to the distal at the apex in the transverse plane; this is shown in some of the curved structures seen in Figures 4.4 and 4.5.

.

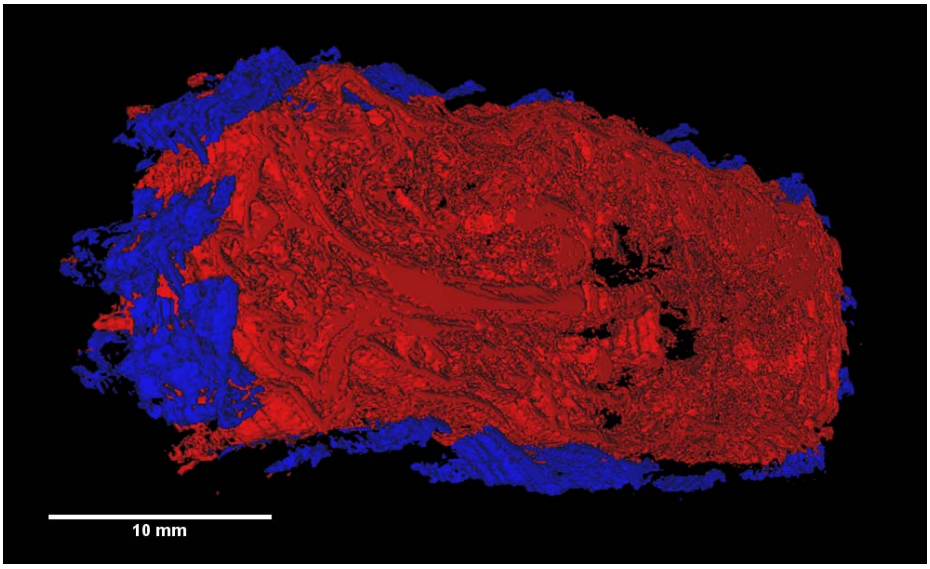

Figure 4.4 Partial reconstruction *of Lepidostrobus sp. A.* Oblique view, showing outermost sporophyllls (blue) and internal structure (red).

The curves in the sporophylls are in the same orientation as the compression, this would indicate that this morphology is not an artefact of compression, indeed the compression would reduce the amount of curvature seen, indicating that it is likely that more of the sporophylls would have been curved. The distribution of the sporophylls does not seem to have been adversely affected. The most distal parts of the apex of each sporophyll are highlighted blue in Figures 4.4 and 4.5, and no large gaps are present. Where gaps do seem to appear, the likely cause of this is as a result of the helical nature of the arrangement of the sporophylls.

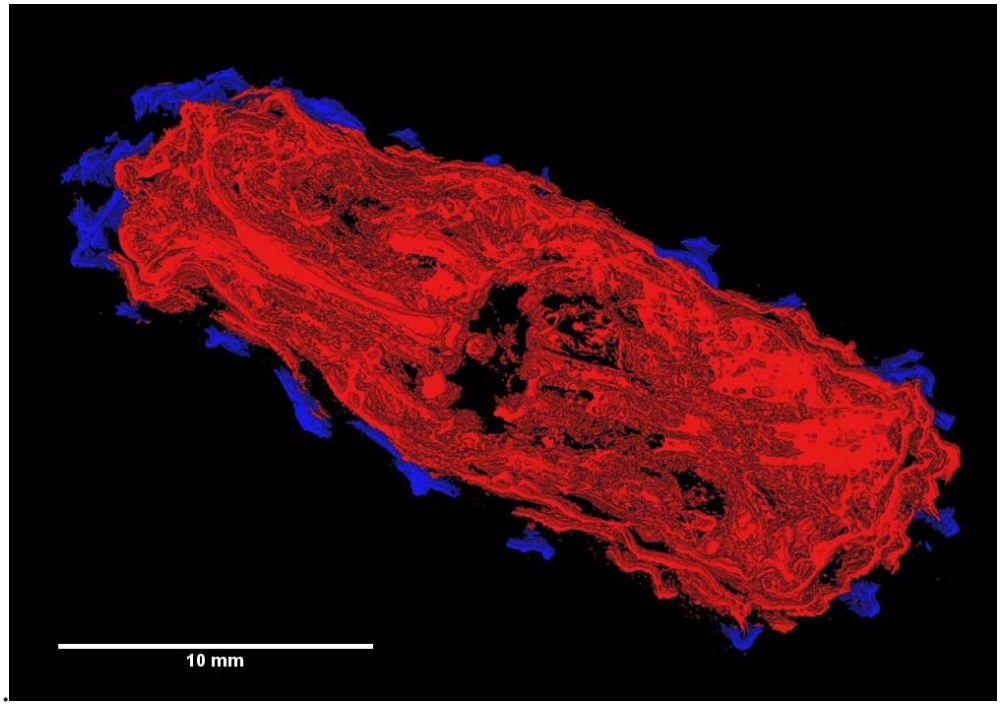

Figure 4.5 Partial reconstruction *of Lepidostrobus* sp. *A.* Oblique view, showing outermost sporophylls (blue) and internal structure (red).

The sporophylls share many similarities with those described by Reed (1941) but also have some differences. There is consistency in the angle of the sporophyll from the axis to the apex. The majority have an average angle of between 30º and 40º, however this can be variable along the length of the sporophyll as a number of sporophylls will emerge at near vertical and parallel to the axis and then the angle will shallow.

The reconstruction using curves (Figures 4.6-4.8) shows individual elements of the specimen in high detail. The basic shape and morphology can be clearly observed, although any surface texture is completely lost in this reconstruction method. It was decided to conduct a partial reconstruction using this method to attain a highly detailed view of a sporophyll and their arrangement. For this specimen the amount of data and 'noise' contained within each photographed surface did not allow for any automatic

thresholding or automatic mask generation with sufficient resolution. Although highly time consuming using masks does allow for detail reconstruction of small facets. More interpretation from the end user is required at this stage as each mask is place manually and is not generated.

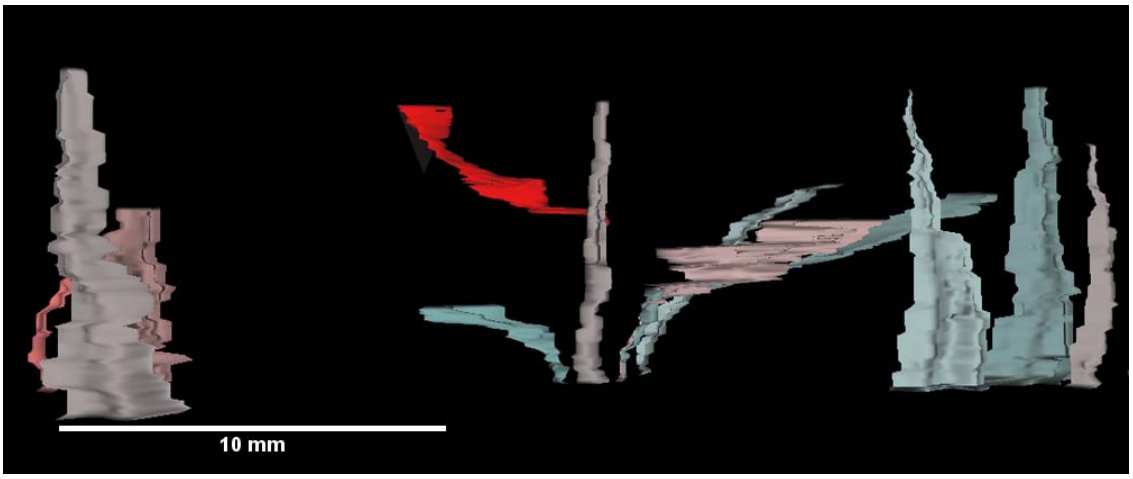

Figure 4.6 Partial reconstruction of *Lepidostrobus* sp. A made using curves. Showing apical parts of sporophylls, emerging sporophylls and the vascular strand.

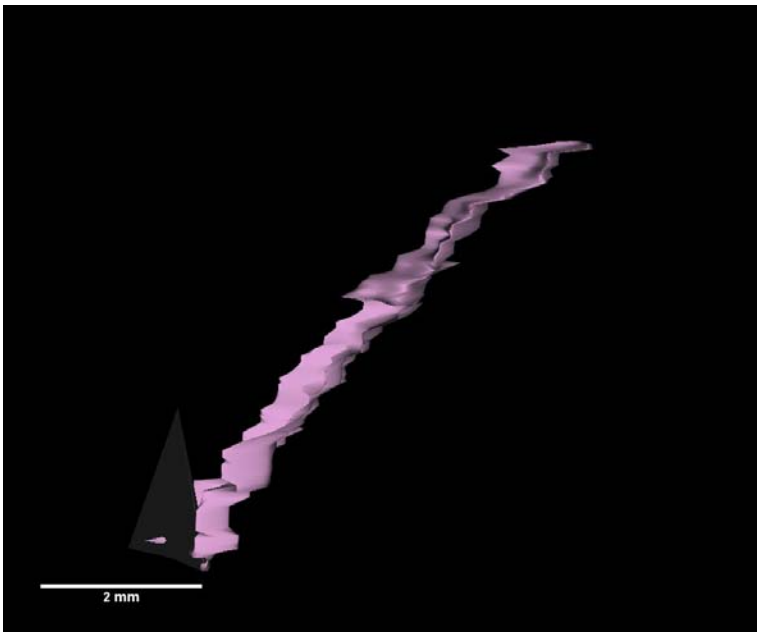

Figure 4.7 Partial reconstruction of *Lepidostrobus* sp. A made using curves showing an individual

sporophyll partial reconstruction.

The central axis is seen as a near linear structure which tapers towards the apex, the slightly disjointed appearance is due to errors in the alignment process and small error in the placement of the mask, in some cases less than 2 pixels.

The curve reconstructions (Figures 4.7 & 4.8) shows the general shape is conduplicate (Hickey and King, 2000) in cross section with a prominent keel. The sporangia are very rare and the evidence for one can be seen by a thickened surface of a

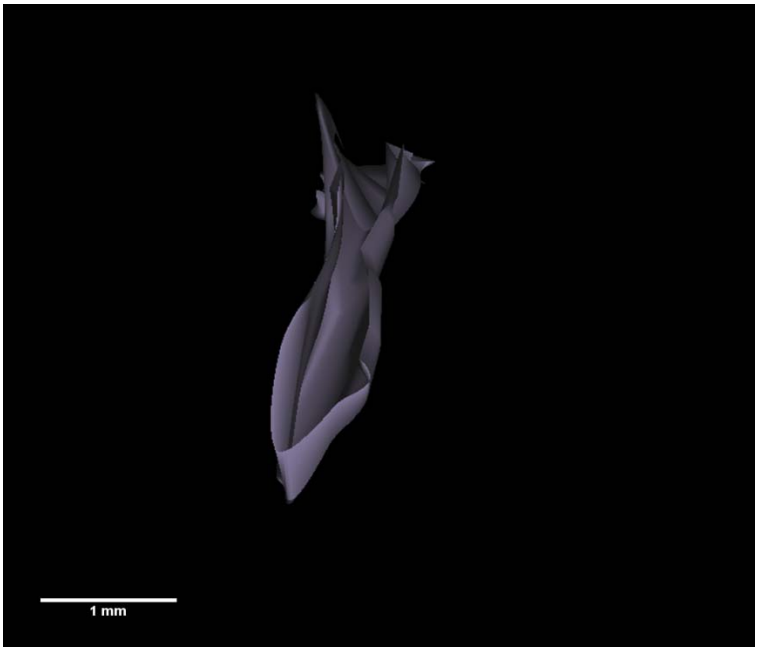

Figure 4.8 Reconstruction of *Lepidostrobus* sp. A made using curves showing an individual sporophyll.

Sporophyll in figure 4.6. The example in figure 4.8 shows how the angle shallows greatly towards the apex and has a structurally rigid design which would support the weight of a sporangia.

In addition to the reconstruction made here, a second reconstruction was attempted from

part of the specimen which was serially sectioned. The alignment marks were not present in this part of the specimen and a reliable reconstruction was not produced. The resolution required to make sense of the internal structure was not attainable with section spacings as large as 1 mm.

This was the most time consuming of all the reconstructions within the thesis, the specimen preparation and mask reconstruction time was approximately 6 months with an addition 2 weeks taken on producing the curve reconstructions.

4.3 Lepidocaropon Sp A.

4.3.1 Introduction

A specimen was found by an amateur collector in the spoil of the Crock Hey open cast coal mine. The specimen is contained within a siderite nodule and shows exceptional 3-D preservation. There are two incomplete cones within the nodule, both of which show a very high level of morphological similarity and due to their very close proximity it can be assumed they are from the same plant and therefore of the same species.

Only one half of the nodule is present so a full reconstruction cannot be undertaken. The specimen underwent high resolution X-ray Computer Aided Tomography at the Natural History Museum in London. Due to the high levels of density of the specimen and the irregular shape, X-ray attenuation was shallow allowing for only 2-3 mm of penetration (figure 4.9)

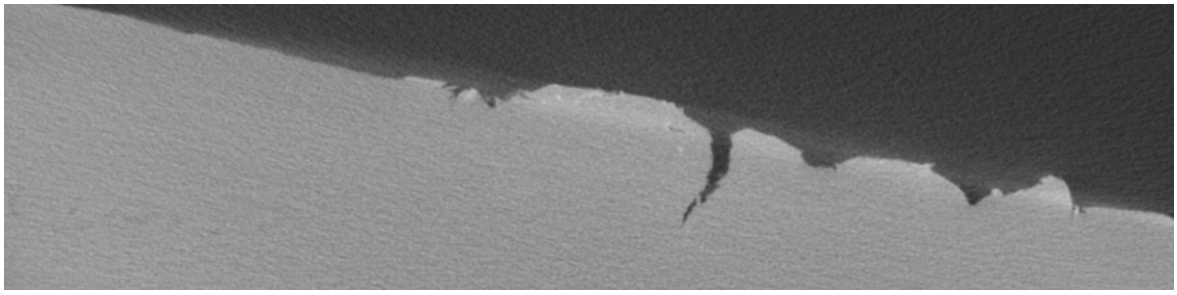

Figure 4.9. Typical tomographic image of *Lepidocarpon* sp. A. Actual image width 15mm

As a result of this poor penetration and the counterpart of the cobble not being available, the reconstruction was very difficult to undertake as no recognisable structures were visible, making masking virtually impossible. The issues which this presents is that individual facets of the specimen cannot be individually reconstructed and the majority of the background material cannot be removed from the reconstruction as it is virtually impossible to tell from the tomographs which areas are key for the reconstruction.

As a result, this reconstruction should be viewed more as a highly detailed surface scan (Figure 4.10) rather than a 3-D reconstruction as has been described previously within this thesis as it is more akin to an SEM, just on a bigger scale.

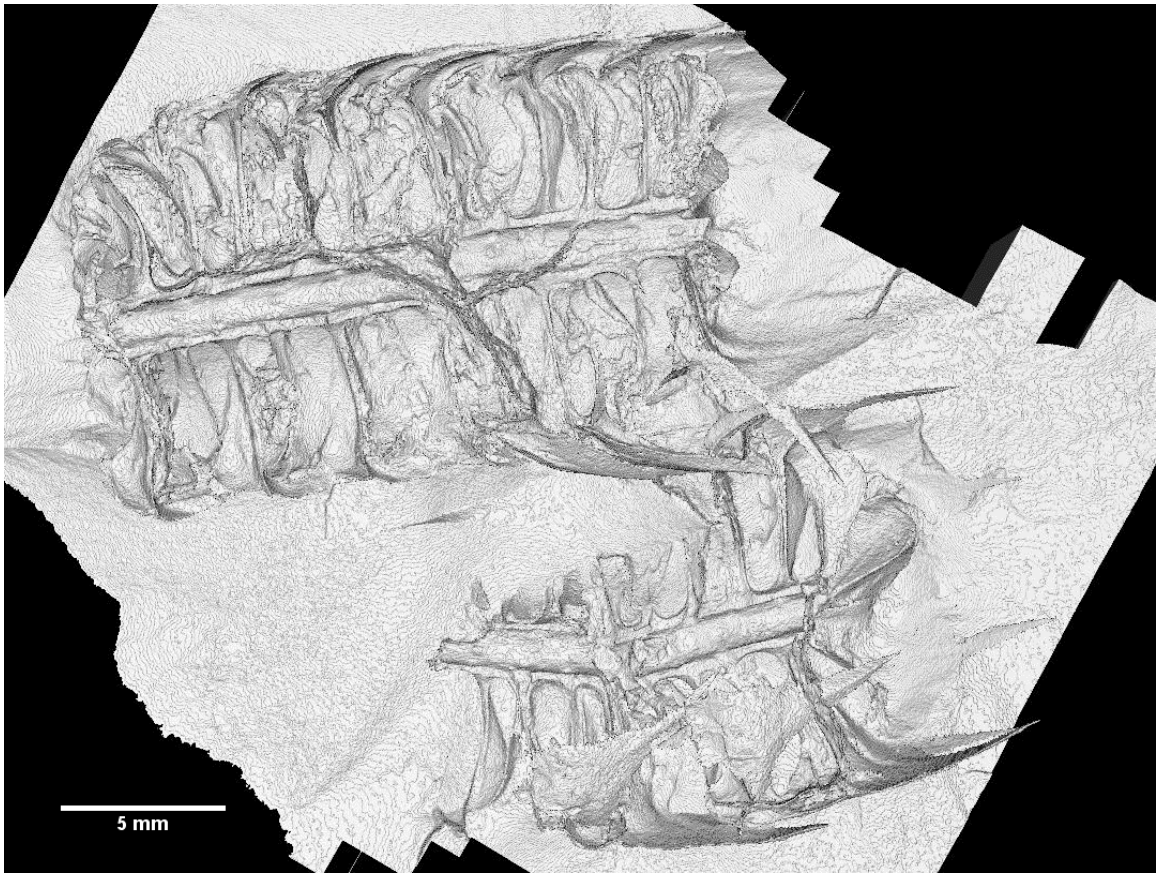

Figure 4.10 Reconstruction of *Lepidocarpon* sp. A. Longitudinal orientation, showing both cone positions and gross morphology.

4.3.2 Description and Results

Each cone has a central axis which is 2 mm wide with the walls of each axis approximately 0.25 mm, on the larger of the two cones the axis length is 19.2 mm, on the smaller cone the axis length is 12.4 mm. On the larger cone the axis is complete but is broken on the smaller cone and is disarticulated (Figure 4.11). Every 0.75 mm along the axis length is a sporophyll visible with many more scars present (Figure 4.12) indicating more sporophylls were present than what is visible from the reconstruction. There are 19 sporophylls present on the larger cone of which 11 have visible sporangia and 8

sporophylls are present on the smaller cone of which 4 have visible sporangia.

Each sporophyll radiates perpendicular from the central axis and shows a steep angle at the keele leading to the apex. The maximum angle shown is 120º, the minimum 84º with the average being 99.3º. The maximum length from the axis to the keele is 4.9 mm, the minimum length is 4.4 mm with the average being 4.67 mm. The maximum distance from the keele to the tip of the apex is 6.1 mm, the minimum length is 4.9 mm with the average being 5.53 mm

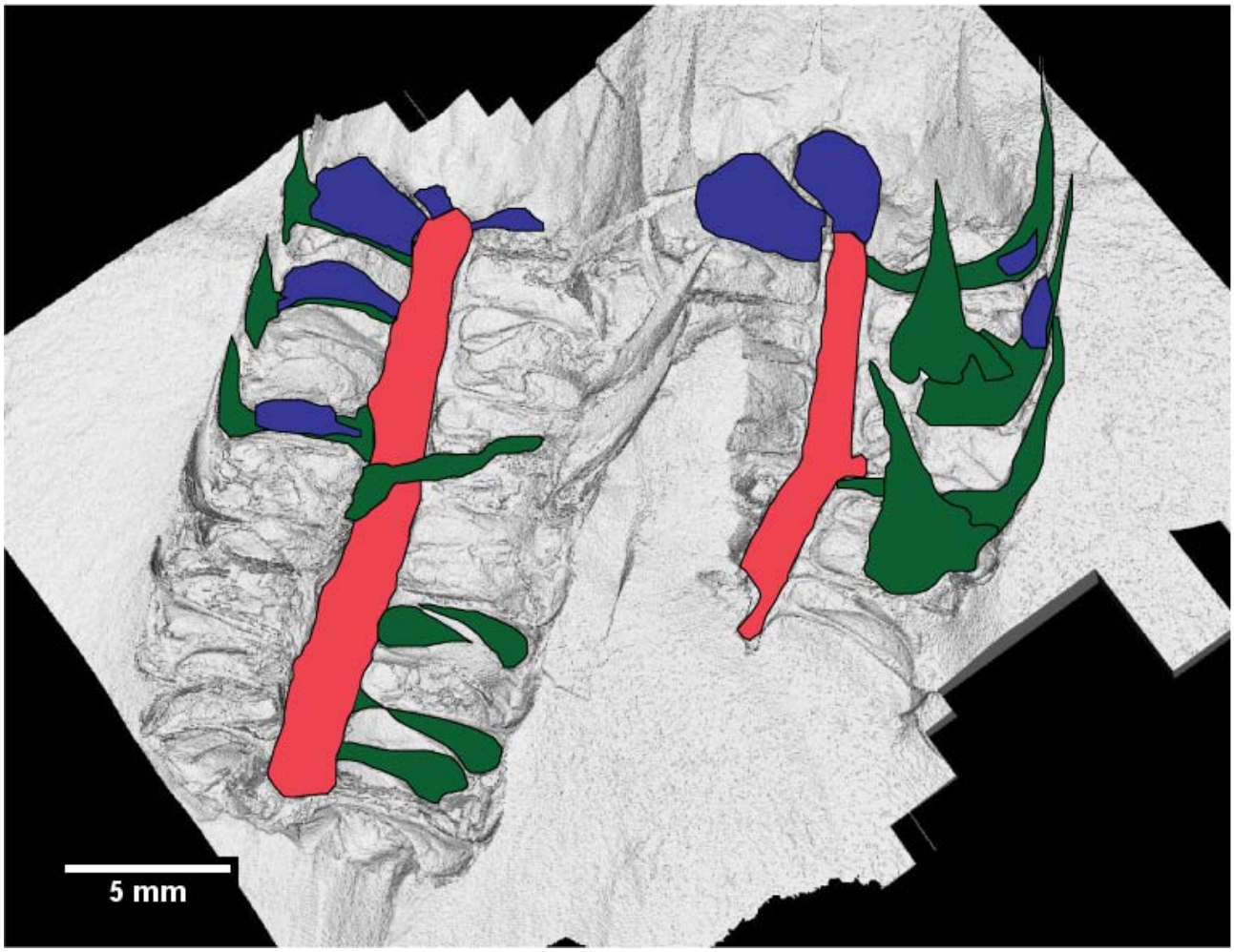

Figure 4.11. Reconstruction of *Lepidocarpon sp. A*. Longitudinal orientation, with interpretation showing central axis (red), sporophylls (green) and sporangia (blue)

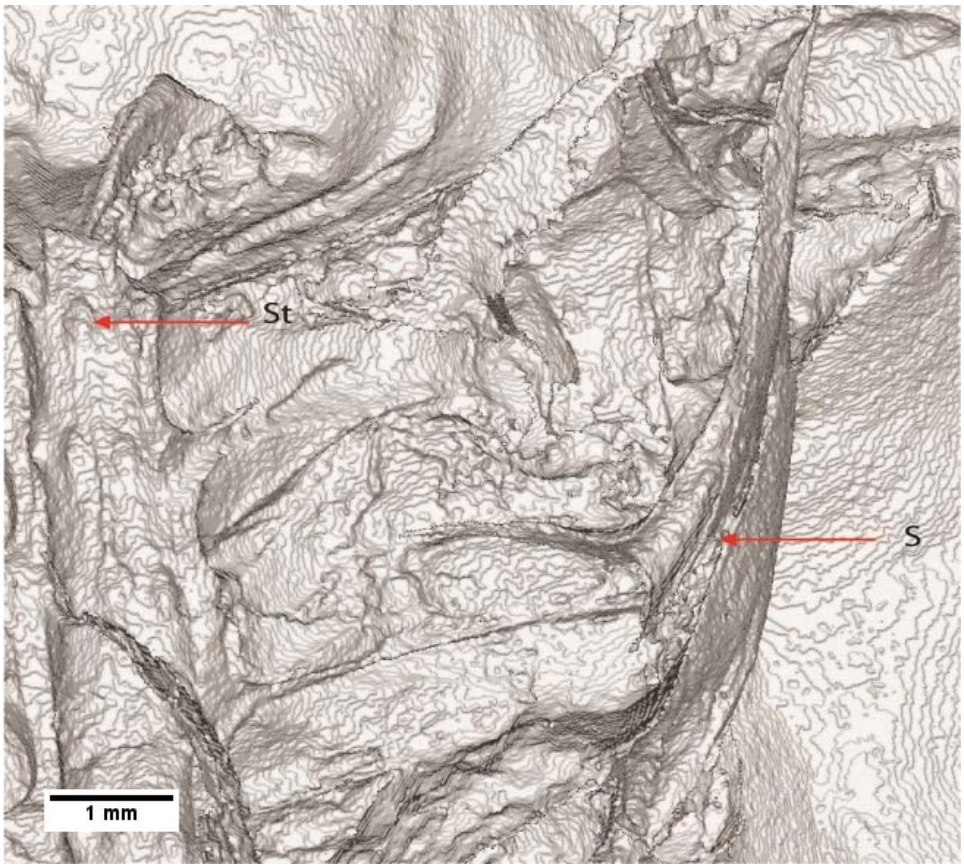

Figure 4.12 Reconstruction of *Lepidocarpon* sp. A. Longitudinal orientation, showing sporophyll (S) and sporophyll traces on the main axis (St)

The sporophyll shape is very distinctive, a pedicule comes from the axis at 90º which is not supported by a bract, when it reaches the keel the sporophyll changes angle steeply towards its apex and is subulate in overall shape but also has a concave curve, forming a hollow for the sporangia to sit on the adaxial surface.

The large size of the sporophyll is likely to aid distribution of the megaspore as a large surface area is required to catch the wind and to be carried and to allow for some floating to occur (Habgood *et al.,*1998)

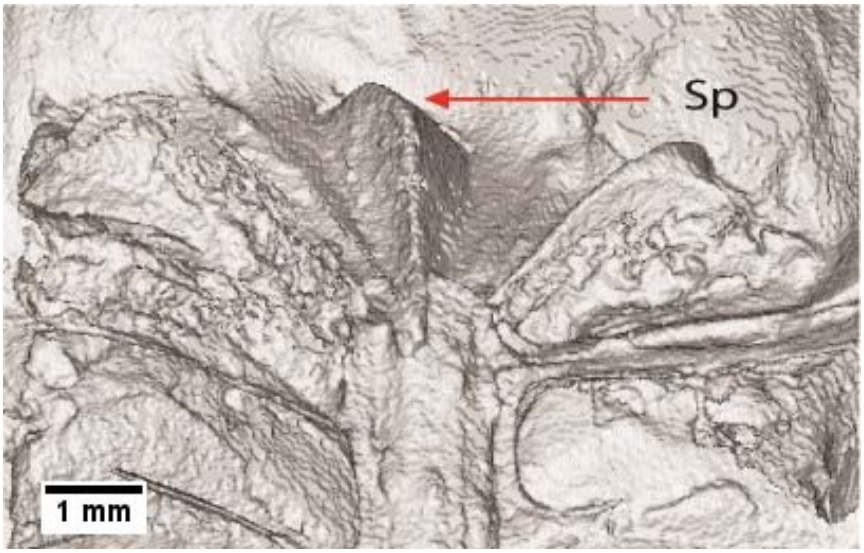

Figure 4.13 Reconstruction of *Lepidocarpon* sp. A. Longitudinal orientation, showing the apex of the specimen and megasporangia (Sp)

The megasporangia are large and occupy most of the length of the pedicle, they have a triangular cross section and show reflective symmetry along the sagittal plane. The prominent ridge which is displayed would represent the main line which abscission would occur to release the megaspore.

With the presence of the prminante scars on the axis, one large sporangia being present on the adaxial surface of the sporophyll, which in turn has a very steep angle leading from the pedicule, this specimen is to be assigned to the Genus *Lepidocarpon*. All of the features are consistent with those described by Scott (1901), Philips (1979) and Habgood *et al.* (1998).

Despite the high resolution of the reconstruction, the competition time was short. The Specimen took 2 hours to be CT scanned with 12 hours of data processing. Time taken to edit and complete the reconstruction was 2 weeks in total.

4.4 *Flemingites arcuatus*

4.4.1 Introduction

A unique silicified cobble collected ex-situ from the Yorkshire coast was prepared for systematic purposes by (Stevens et al., 2010). The cobble contained various plant (Stevens et al., 2010) and crustacean (Womack et al., 2012) fragments of which one is the species described here. The cone is incomplete and partially fragmented and was named *Flemingites arcuatus* Stevens *et al.* 2010. Reconstructed here is a partial reconstruction based on 8 sections of which 16 tomographic planes were available for use, with this reconstruction being included in the publication of Stevens et al. (2010) (See appendix 1). Due to the nature of the specimen, not all of the surfaces could be used for the reconstruction; artefacts from the reverse surfaces in the clear matrix often interfered with the images for the reconstruction, and as a result of this 14 of the 16 available surface were used. The specimen was previously prepared by serial wafering with each slice separating tomogrpahic planes being 0.7 mm in thickness.

The reconstruction was chosen due to the highly detailed megasporangiate sporophylls and detailed morphology within this part of the cone. Practical implications played a part too, although no alignment marks were present within the specimen, the central axis provided a fixed datum within the dataset and other parts of the cortex allowed alignment to be achieve to ensure as little rotational movement as possible.

This cone of *Flemingites arcuatus* and the associated material is discussed in Stevens *et al.* (2010) in greater detail including a full phylogenetic analysis, which falls outside of the

scope of this thesis. The main focus of this section will be devoted to the information gained from the reconstructions with additional information on structures taken from the photographed wafered section.

4.4.2 Description and Results

Unlike most lycopsid cones, the sporophylls lack differentiation in to pedicel and distal lamina, but curve away from the main axis and inwards towards the apex of the cone. The reconstruction shows that the sporophyll-megasporangia complexes are very close together and compact, and that they abut against each other. Large pelate to cunate shaped sporophylls dominate the cone, with each sporophyll containing a single megasporangia. At the centre of the come is the central axis (Figure 4.14) which is surrounded in turn by a cortex. The cortex has leaf traces (Figures 4.15, 4.16 & 4.17) which lead into the megasporophylls (Stevens *et al..,* 2010).

The megaspores are positioned in the upper half of the sporangium and are at various stages of ontogeny, and the reconstruction demonstrates that each megasporangium contains a maximum of four tetrads each containing four megaspores in a tetrad (Stevens *et al.,* 2010).

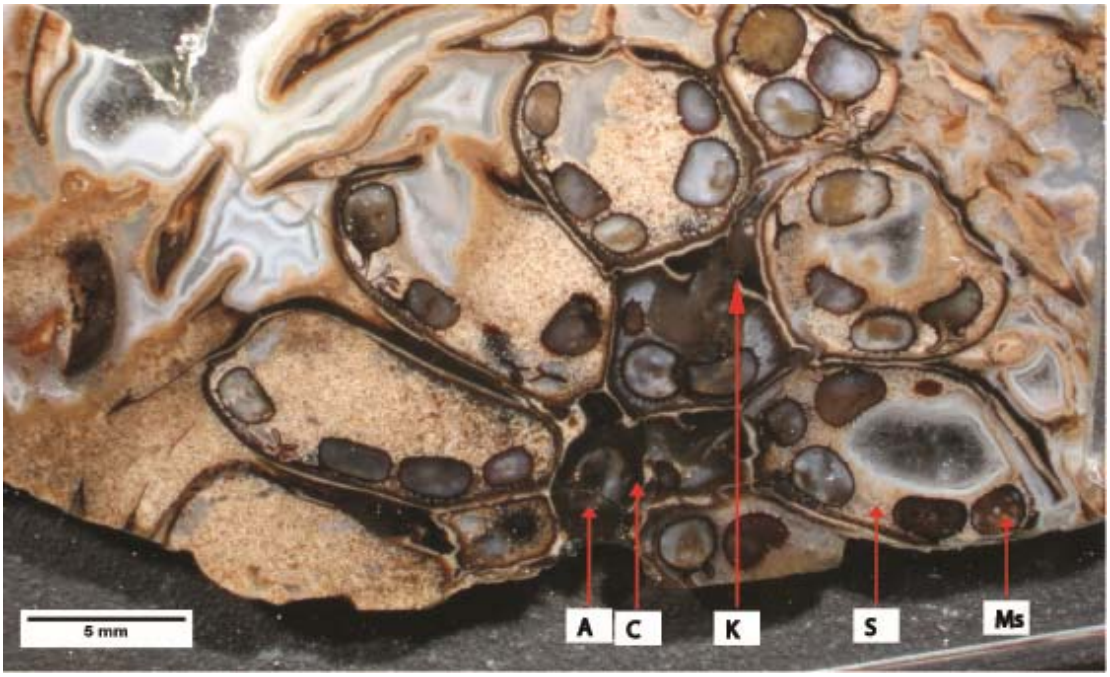

Figure 4.14 Transverse section of *Flemingites arcuatus* show axis (A) cortex (C) sporophylls (S) and Megaspores (Ms).

The sporophyll and megasporangium along with the keel form the sporophyll-megasporangia complex, this is a term which is being applied to this as it allows the single structure to be broken up in the reconstruction to show the element of the sporophyll which has the primary function of producing and releasing the megaspores and the part of the sporophyll which has the function of structural support.

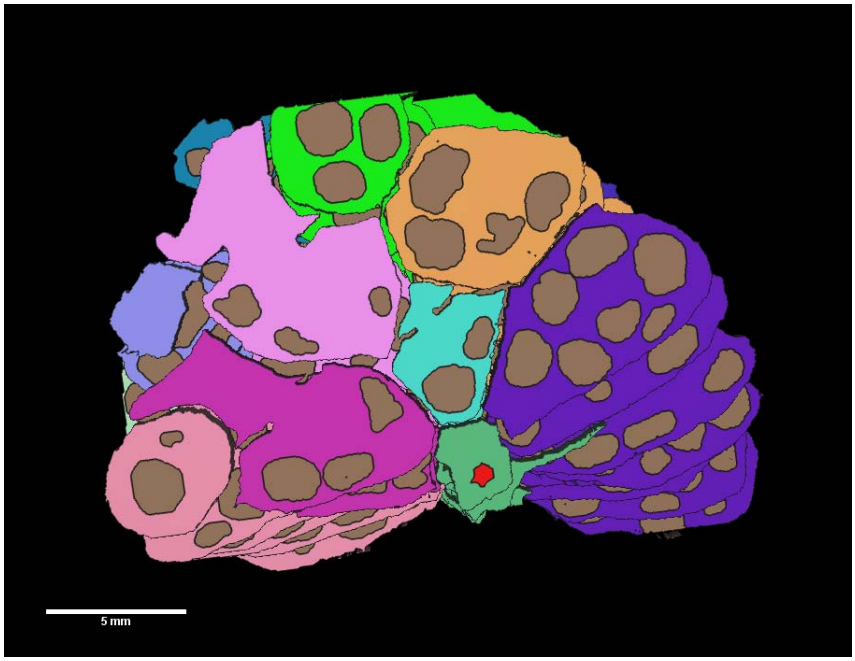

Figure 4.15 Reconstruction of *Flemingites arcuatus* in transverse section showing Axis (red), Cortex (dark green) individual megasporophylls (dark blue, light blue, orange, light green pink and purple) and Megaspores (brown).

Each of these sporophyll-megasporangia complexes have been highlighted a unique colour with the position of each megaspore shown. The representation of the megaspores on each section is how they appear on each image and does not represent a unique individual. One individual megaspores may be represented up to 3 times in the reconstruction as they could be exposed on more than one tomographic plane. The megasporophylls are arranged in a spiral (Figures 4.15 & 4.16) with 6 sporophylls per 360º making this species spirally symmetrical. The angle at which the sporophylls emerge from the axis averages at 47º with the maximum being 51º and the minimum being 45º. The total length of each megasporophyll is unknown as a complete example was not available to be reconstructed.

Although only consisting of 16 surfaces, the nature of this reconstruction being very labour intensive and detail meant the total time to produce this reconstruction was 2 months.

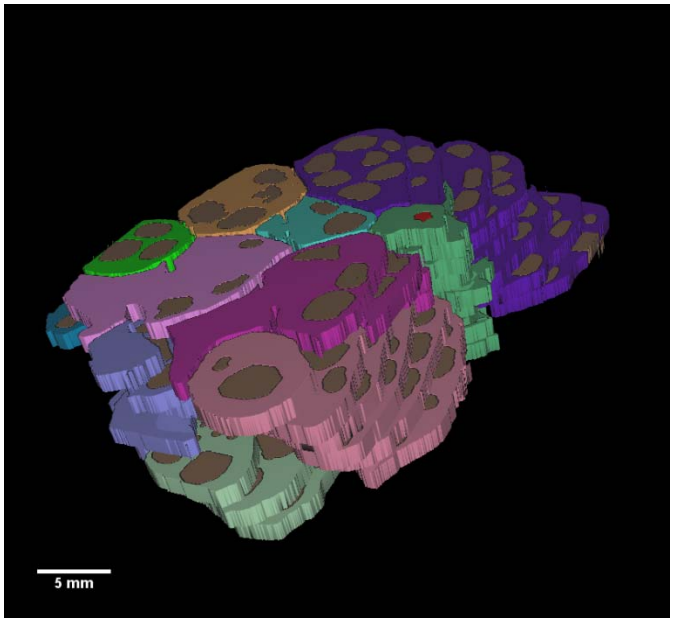

Figure 4.16 Reconstruction of *Flemingites arcuatus* from transverse sections in an oblique view highlighting megasporophyll arrangement.

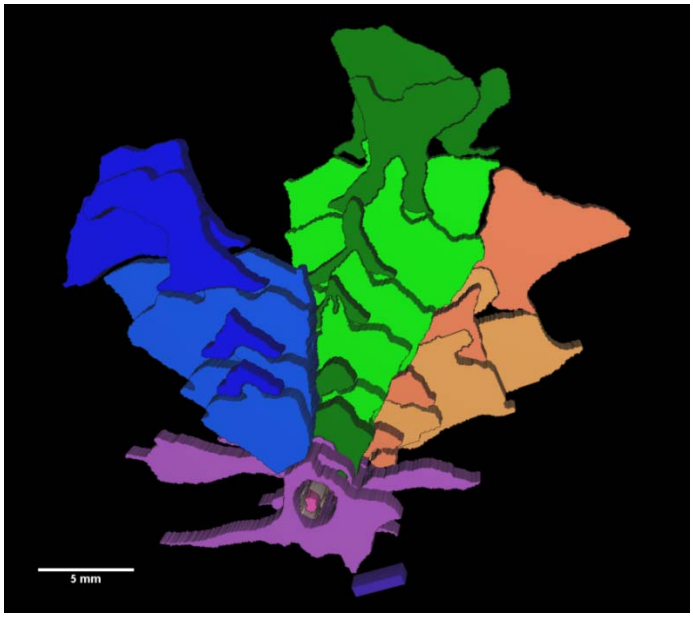

Figure 4.17 Reconstruction of *Flemingites arcuatus* from transverse sections in a transverse view highlighting sporophyll complex arrangement, the lighter shade represent the sporophyll and darker shade representing the keel.

4.5 Discussion

Each of the three specimens shown within this chapter are very different in their morphology and have been reconstructed using very different methods, with each method chosen to suit the data that can be ascertained from the specimen.

Lepidostrobus sp. A was imaged by using a destructive method and imaged at the highest resolution possible using physical optical tomography. Using high resolution scanning methods would not have been applicable for such a specimen as the siderite is very dense and the specimen does not provide an adequate density contrast as areas within the specimen and between the organic material are filled with similarly dense material.

Where the morphology of the internal structure is very complex and densely packed facets were individually reconstructed to allow for certain characters of the specimen to be studied in detail. It would be preferable to be able to examine all areas of the specimen in such detail but for reasons outlined this is not possible. The manual imagining, alignment, slice generation and reconstruction process made this reconstruction extremely time consuming and is only applicable for a specimen which fits the criteria of being highly complex and unsuitable for scanning methods.

The reconstruction shows this to be a very compact cone with a large number of small microsporangate sporophylls, there is a degree of variability with in the sporophylls in regards to their shape, pedicle length, and overall morphology. In general terms the sporophylls which are borne more apically on the axis tend to have a pedicle which quickly runs near parallel to the axis then branches toward the exterior of the cone, whereas the sporophylls born near the base seen to emerge at a much shallower angle.

Lepidocaropon sp *A.* was considered for the physical optical tomography used in the

Lepidostrobus specimen. However as there was no counterpart to the nodule and some of the structures were clearly free standing and delicate it was decided that a scanning method should be used to try and preserve as much of the detail as possible. Although initially deemed a failure when the CT data was first viewed, the final reconstruction revealed a highly detailed view of megasporophylls and some very detailed morphology and how the structures interact with each other. The shallow x-ray penetration did not allow for a full reconstruction of all the material but this did allow for a higher resolution scan to take place to record more surface detail. This is the only 3-D view of an intact megasporophyll from the fossil record.

Flemingites arcuatus had to be reconstructed using serial sectioning as the matrix of the cobble is far too hard to undertake serial grinding and is too large and too dense to consider any form of scanning method. Due to the huge amount of material within the cobble the sectioning process was long and had to be considered carefully to ensure that no damage was done to potentially important specimens, this process did limit the number of sections available to be reconstructed however it was necessary in the wider context.

As the specimen has large megasporangia and a wide helical structure a low resolution reconstruction method was perfectly applicable. The majority of the information required from the reconstruction could be gained this way and traditional approached would be used for the rest of the analysis (see Stevens et al., 2010).

Understanding the context for which a reconstruction is to be used is key in choosing how it should be undertaken and the three examples shown within this chapter aid in the understanding of three different genera. This also shows how specimens that can be CT scanned are much more time efficient in terms of producing a finished reconstruction in which viable data can be retrieved.

Chapter 5

RECONSTRUCTING GINKGOALEAN OVULES: COMPARING EXTINCT AND EXTANT SPECIES

5.1 Introduction

This chapter further develops research on gymnosperm ovules (Chapter 4) and investigates specimens of living and fossil ovule Ginkgoalean species using X-ray computer aided tomography. Both specimens have been subjected to the same scanning and reconstruction methods to allow for a direct comparison of their morphology. Where possible, the same structures will be shown and described and both species characterised in full in comparable detail. An additional example from published literature of a fossil Ginkgoalean ovules has been used as an example of how the results developed here can benefit the interpretation of additional species for which 3-D reconstruction has not occurred but for which 3-D reconstruction may be beneficial.

The gymnosperm family Ginkgoales had considerable diversity during the Mesozoic and Cenozoic but are represented in the present day flora by the sole remaining species, *Ginkgo biloba.* (Seward & Gowan 1900; Sporne, 1967; Taylor *et al*., 2009; Zhou *et al*., 2012). *G. biloba* is frequently

described as a living fossil as it is one of the most primitive extant seed plants (and appears to have shown considerable stasis in its evolutionary history (Seward & Gowan 1900; Holt & Rothwell, 1997). During the Mesozoic, nine genera of Ginkgoalean ovulate organs have been recognised to date (Zhou, 2009), namely *Avatia* Anderson & Anderson 2003, *Ginkgo grenana* Samylina 1990, *Karkenia* Archangelsky 1965, *Schmeissneria*(kirchner & Van Konijenburg-van Cittert 1994, *Toretzia* Stanislavsky 1973 *Umaltolepis* Krassilov 1972, *Nehvizdyella* Kvacek *et al*. 2005 and *Yimaia* Zhou & Zhang 1989. A diversity of other ginkgoalean organs have also been recognised including foliage (Zhou, 2012; Harris and Millington, 1974).

Extant *G. biloba* is a tree that has stems with pycnoxylic wood and has prominent short and long shoot differentiation. Its leaves are strap or fan-shaped and are deeply divided, with dichotomous venation. Ovules are borne on short shoots and are pedunculate, with as many as four ovules borne per short shoot. Individual ovules have a fleshy outer layer (sarcotesta) and a stony middle later (sclerotesta) (Seward & Gowan, 1900; Chamberlain and Coulter, 1932), with the sclerotesta having either two or three longitudinal ribs. Pollen organs bear microsporangiophores with pendulous microsporangia that contain smooth, monosulcate pollen grains. However, much less is known about extinct members of the family. For instance, while the anatomy and organisation of extant *Ginkgo* ovules are known in detail from traditional systematic investigations (Chamberlain and Coulter, 1932, Sporne, 1967) anatomically preserved Ginkgoalean ovules have not previously been documented such that they are known only from compression/impression specimens that reveal only features of their external morphology (Harris and Millington, 1974) or sometimes reveal limited inferences from their internal morphology (Kvacek *et al*., 2005).

In this chapter previously undescribed anatomically preserved ovule from the Callovian (Jurassic) aged Oxford Clay Formation is investigated (see Chapter 2). A living ovule of *Ginkgo biloba* has been collected post fertilisation from a central Birmingham specimen for comparative purposes. On

initial inspection the ovules are of a comparable size and external organisation to the sclerotesta of extant *G. biloba*, so the purpose of the investigation is to determine their structure and identity. In doing this, it has been necessary to study ovules of extant *G. biloba* using the same techniques to allow detailed comparison to be undertaken rather than comparing results against information available from traditional systematic investigations. To achieve this, the extinct and extant ovules have been scanned using high resolution computer tomography, reconstructed and interpreted using the same methods (see Chapter 2). Due to the difference in density between fossil and extant specimens, the resolution of the CT data will also be different - the lower density extant specimen is expected to show greater resolution - so using the same technique will allow this variation to be assessed.

5.2 Description of extant *Ginkgo biloba* ovule

5.2.1 Gross morphology

The ovule investigated is post-pollination and is fertile as a cotyledon is present. The outer-most fleshy layer of the ovule, the sarcotesta, has been removed from the majority of the ovule prior to study although vestigial remains of it occur in some areas. The outermost layer present for most of the ovule is the stone layer, the sclerotesta. The sclerotesta has a rounded base and attenuated apex and has two longitudinally orientated ribs, one to either side of the ovule (Figure 5.1). Individual ribs have a maximum relief of 3 mm and become less prominent towards the chalza where the ovule becomes more rounded, with the ribs slowly tapering out.

The sclerotesta tapers towards the micropyle where it forms a bluntly rounded apex (Figure 5.1) surrounding a recessed micropyle that is sealed. The position of the ribs gives the seed 180˚

rotational symmetry (Douglas *et al.*, 2007) rather than being radially symmetrical as the species is typically considered. The outer surface of the sclerotesta is relatively smooth, except where vestigial remnants of the sarcotesta are attached (Figure 5.2).

Within the sclerotesta occurs a thin membrane that envelops the nucellar membrane (Figure 5.3). The nucellar membrane is complete and continuous, and splits slightly to form a secondary structure around the gametophyte. Towards the centre of the ovule the cotyledons are present (Figure 5.4). Apically the nucellus has a nucellar beak (Figure 5.5) that contains a bolus (Figures 5.2, 5.6 & 5.8). Cotyledons are reniform in cross section (Figure 5.7) (Figure 5.7) and taper towards the distal apex (Figure 5.9). This structure is composed of mucilage, forms to stop invasion from foreign objects into the micropyle post fertilisation.

From the scanned data, it has been possible to differentiate 7 tissue layers, namely (1) vestigal sarcotesta, (2) sclerotesta, (3) nucellus, (4) megagametophyte, (5) cotyledons, (6) pollen chamber, and (7) bolus. Each of these have been masked to form the reconstruction.

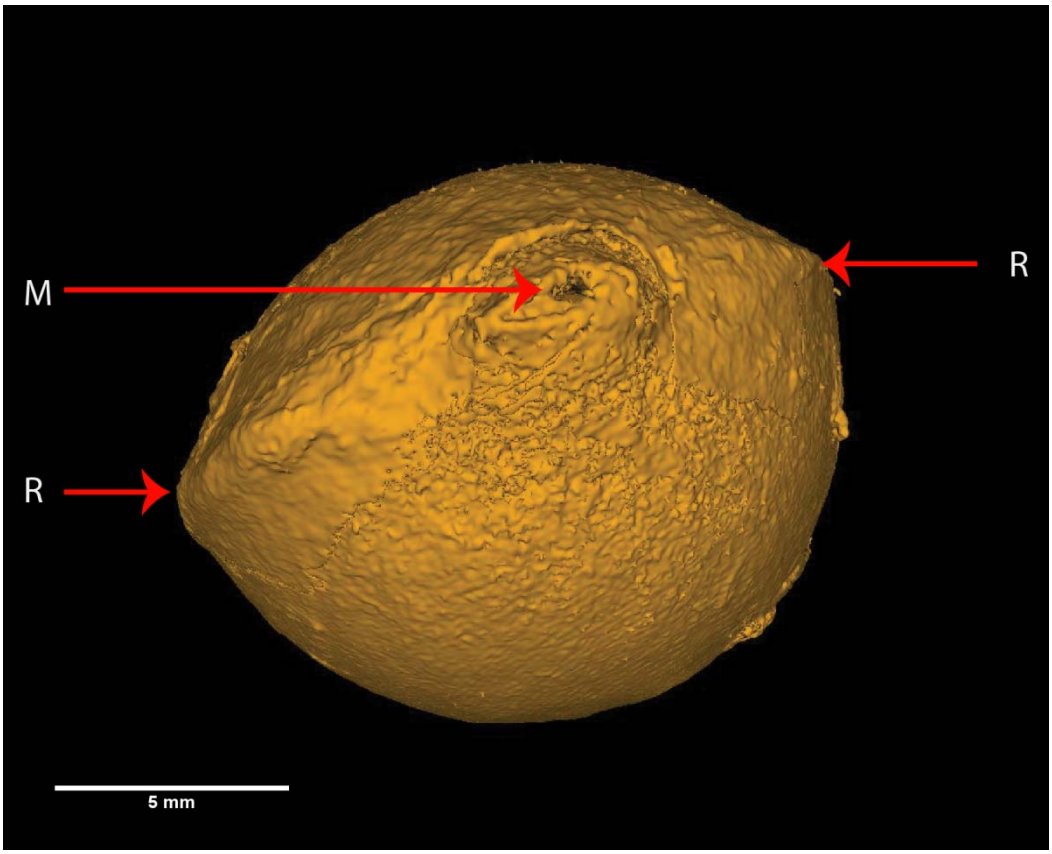

Figure 5.1. Reconstruction of the outer surface of the sclerotesta of an extant, two ribbed ovule of *Ginkgo biloba*, viewed from the micropyle. M = micropyle, R= rib.

5.2.2 Detailed description of 3-D data.

To understand the 3-D data, the 2-D sections which have been created from the tomography data will be discussed and analysed. Traditionally the majority of anatomical descriptions have been undertaken by using 2-D both in the form of diagrams and photography. One of the first detailed discussions on the anatomy of ovules of *G. biloba* was undertaken by Linneaus in his original description of the species and then was developed subsequently by Seward & Gowan in their book *Maidenhair Tree* (1900). To keep consistency with these works and subsequent published material traditional 2-D sections will be shown and interpreted.

The outermost layer included in the reconstruction is the inner membrane of the sarcotesta (Figure 5.2). This is non-continuous through the specimen and is confined to the upper right side (in relation to the orientation of the X-CT images.

A gap of 0.5-1mm separates the sarcotesta from the stony inner layer (sclerotesta). The sclerotesta is dark on the x-ray data showing it to be dense, consistent with it being composed of sclerenchyma. The sclerotesta is approximately 2mm thick and does not markedly vary through the ovule.

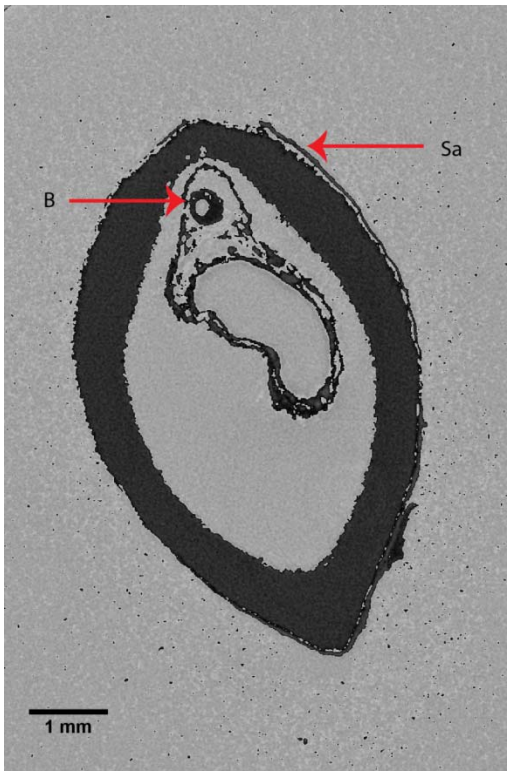

Figure 5.2. X-CT image of extant *Gingko* ovule (position, orientation) showing vestigial sarcotesta (Sa) and bolus (B).

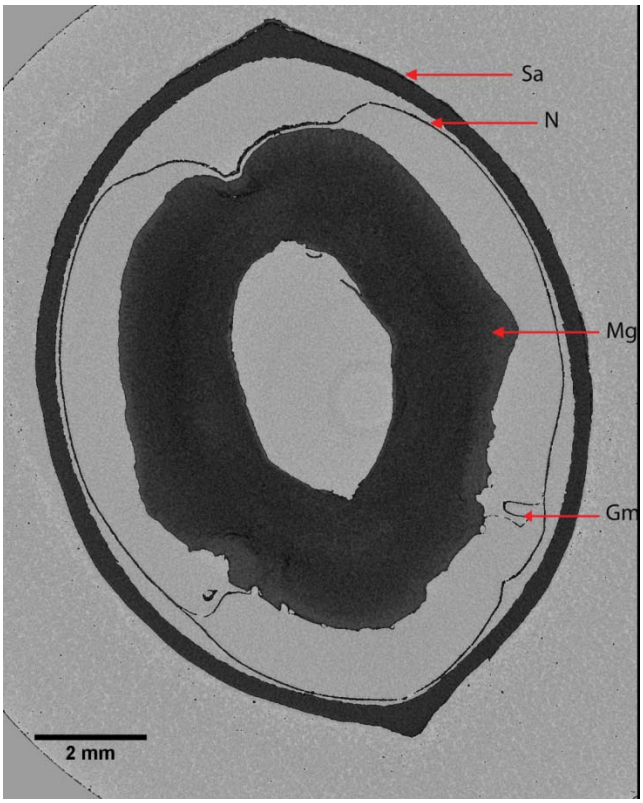

Figure 5.3. X-CT image of extant *Gingko* ovule (8 mm from apex, slightly oblique transverse) showing sclerotesta (Sa), nucleus (N), mega-gametophyte (Mg) and gametophytic membrane (Gm).

The nucleus (Figure 5.3) is frequently described as a papery layer, this forms a continuous membrane around the gametophyte and is shown as being detached from the sclerotesta, which is likely a result of the ovule becoming dehydrated and non- sclerenchyma cells undergoing shrinkage.

The gametophytic tissue (Figure 5.3) is the largest single tissue within the ovule making up 15% of the total ovule volume. Tissues of the megagametophyte shows a lower x-ray attenuation than other tissues, indicating a lower density. This would be consistent with it being made up predominantly by parenchyma cells. The other structure which shares a similar X-ray attenuation is the hypocotyl (Figure 5.4).

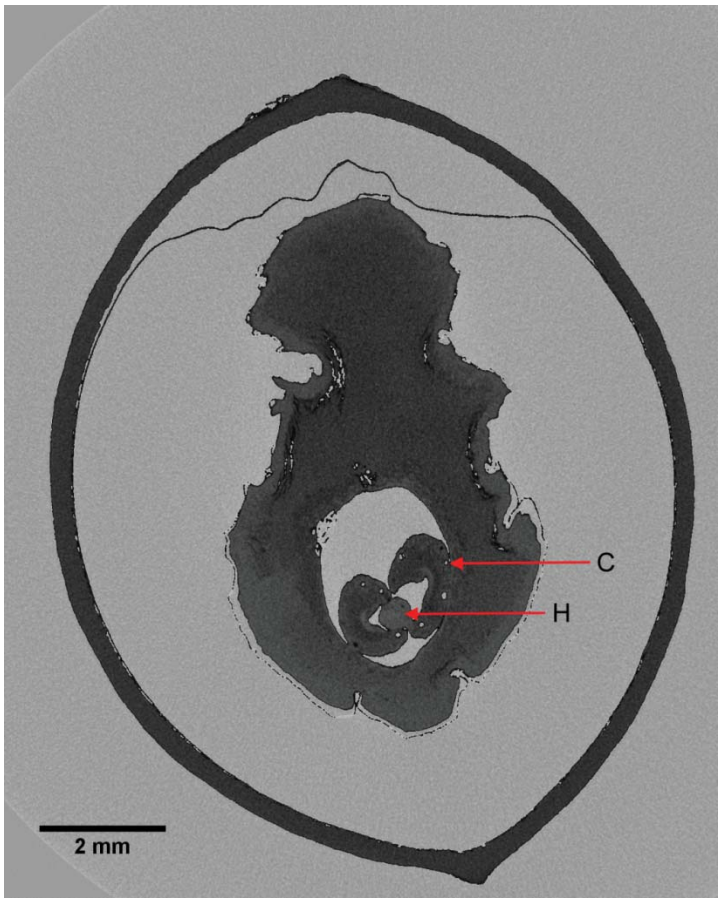

Figure 5.4. X-CT image (half way through specimen, slightly oblique transverse section) showing cotyledons (C) and hypocotyl (H) within the nucellus.

The appearance of the gametophyte is consistent with dehydration of some form, the nucleus is coming away from the sclerotesta and the gametophyte having a very irregular, contracted shape, but the resolution is not fine enough to resolve the outlines of individual cells. The cause of the contraction is going to be one of two possibilities. The first is the removal of nutrients and moisture by the developing cotyledons, or as a result of storage in a dry environment and the natural osmotic effect drying the specimen out. In all likelihood a combination of both is the likely cause.

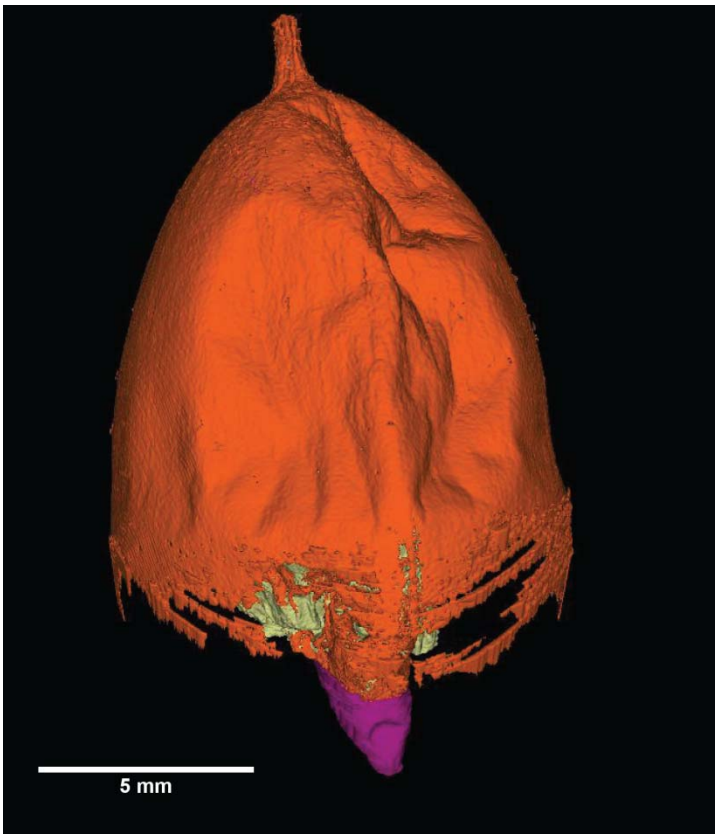

Figure 5.5. Reconstruction of extant ovule showing nucleus (orange) distal tip of the cotyledon (purple) and gametophyte (pale green).

The nucellar beak occurs apically in the nucleus and is contained within the sclerotesta, and comprises a pollen chamber and tube in to the pollen chamber. The pollen chamber contains the bolus, the beak is further contained within the sarcotesta, which does not seem to possess the same external morphology of the nucleus.

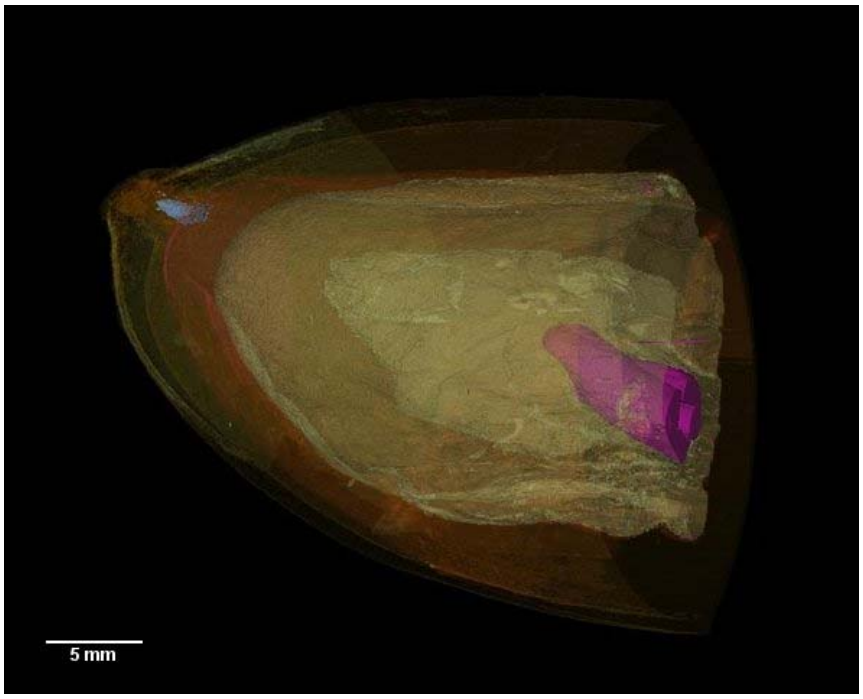

Figure 5.6: Reconstruction showing internal anatomy of the extant *Ginkgo* ovule. Nucellus (orange), bolus (blue), gametophyte (pale green) and cotyledons (purple).

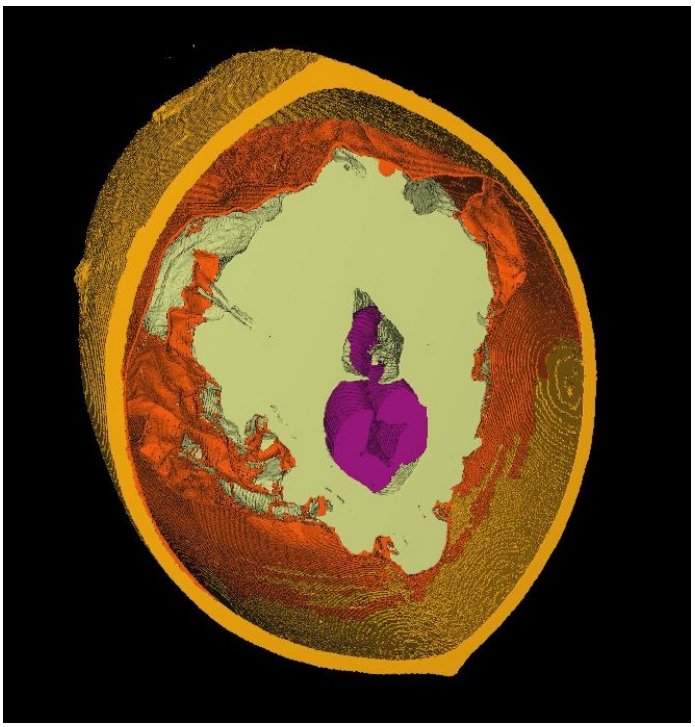

Figure 5.7. Virtual cross section of the extant *Ginkgo* ovule in transverse section through mid-point of ovule showing organisation of the tissues; nucellus (orange), mega-gametophyte (pale green) and cotyledons (purple).

The gametophyte (Figures 5.6 – 5.7) surrounding the cotyledon is the single largest tissue in terms of total volume with the seed in this state of maturation. The tissue is white in colour and low density, its function would have been as a starch and liquid supply for the developing cotyledons and hypocotyl. This specimen is beginning to show a few convolutions in its appearance due to dehydration, both due to drying and the development of the embryo.

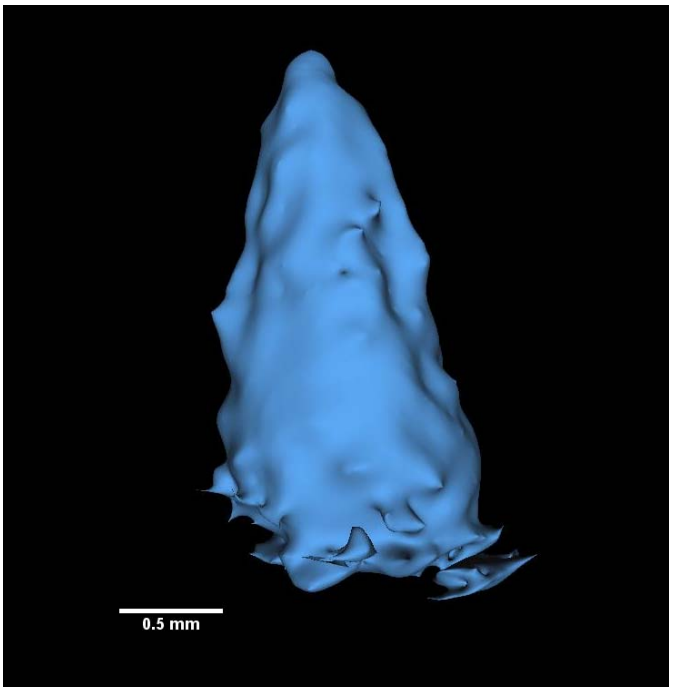

Figure 5.8 Reconstruction in longitudinal view of the bolus.

The bolus (Figures 5.2, 5.6, 5.8) is small, approximately 2mm long, round in cross section and has an overall conical shape. The structure is hollow (Figure 5.2) and shows a high x-ray attenuation as is shown by the very dark appearance in the tomograph, The walls appear thick (0.2mm) for a structure of this size indicating that is needs to resist a force of some kind. The surface appearance of the bolus seems to increase the surface area allowing it a more firm fit into the micropylar canal. Although it is not possible to tell from the reconstruction it would be fair to assume that the external surface of the bolus is a positive of the inside of the canal which it fits in to forming a tight seal, thus preventing any structures from entering the micropyle after fertilisation has occurred.

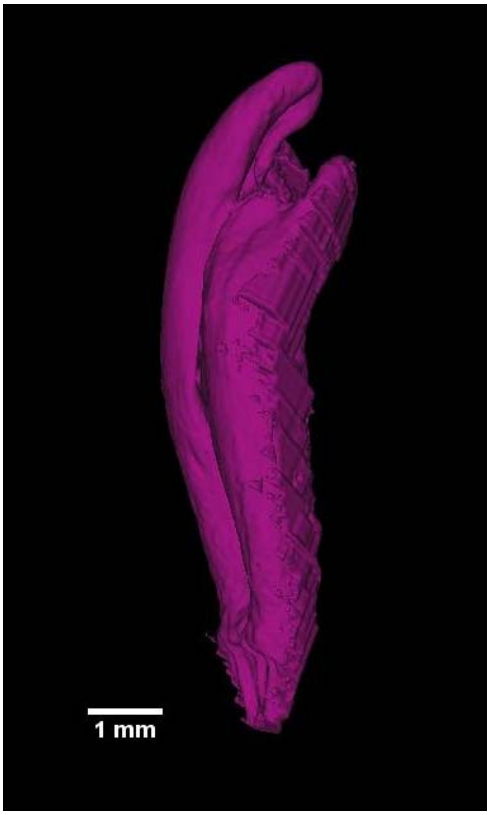

Figure 5.9: Reconstruction of the cotyledons in longitudinal view.

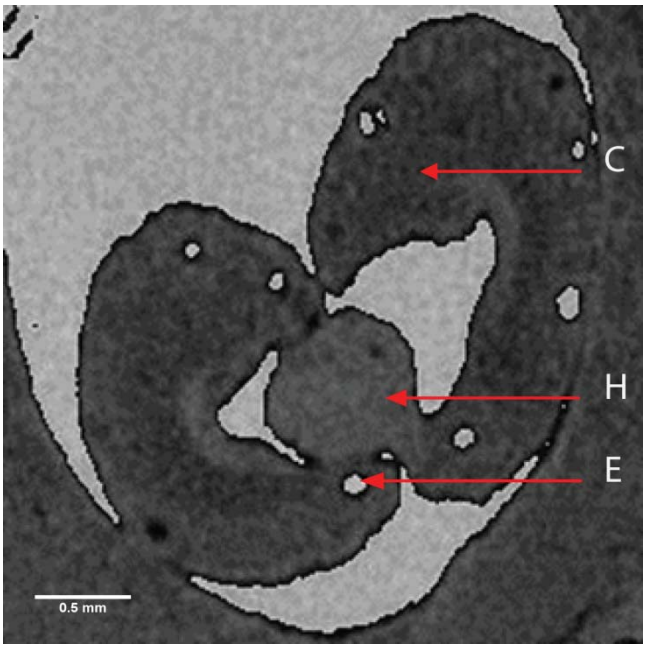

Figure 5.10. X-ray image showing structure of the cotyledon (C) with glandular epithelium (E) and hypocotyl (H).

Two cotyledons are present (Figures 5.9 – 5.10), these are the first leaves formed by the embryo, with the word derived from the Greek for seed leaf. A supporting structure, the hypocotyl, is also present (Figure 5.10) within and opening surrounded by the gametophyte. Each of the cotyledons has a closed sheath appearance with a loose helical structure (Figure 5.9). In cross section, both cotyledons are reniform in shape with a deep inward curve, joining to hypocotyl, each showing between 3-5 glandular epithelia, denoted by the higher density (greater x-ray attenuation; black coloured) lining containing a resin duct. The exact function of having such a large resin carrying capacity is largely unknown, however, *G. biloba* is very tolerant of a wide variety of climates and is resistant to many forms of pollution; this extra metabolite within the vascular system could be used to concentrate up compounds to aide in sub zero temperatures to prevent cell wall damage, be used in summer to increase osmosis to allow greater water extraction from the surrounding areas and also can act as an excretionary system for many pollutants, *G. biloba* shows very high

resistance to most pollutants (Karnosky, 1981).

The large volume of resin channels within the ovule would suggest they carry nutrients, the cotyledons have a large nutrient requirement from an early stage of development, unlike in many species *G. biloba* only has a fair basic vascular system, with little in the way of vascular traces within the ovule. This is in sharp contrast to the cotyledon which appears to have a much more developed vascular system which, is a great benefit during this rapid growth phase where completion is an important factor. This rapid growth also includes the hypocotyl, which has been included as part of the cotyledon in this reconstruction, as there was no distinct boundary to separate the two structures.

Each resin duct is an irregular oval shape in oblique section, with a difference in the diameter between the largest and smallest of 60%. The hypocotyl is circular in section and shows a strong attachment to both cotyledons, no detailed internal structure of the hypocotyl can be seen as x-ray attenuation appears homogeneous. Attachment of the cotyledons is to the inner wall of the mega gametophyte but no distinct boundary is present or obvious signs of differentiation in the tissue.

Although the specimen preparation time for this reconstruction was quite short, 2 days, the time taken to produce the reconstruction was very long. Each image had to be extensively hand edited in order to distinguish between the tissue layers resulting in a total time to produce this reconstruction of 4 months.

5.3 Description of Extinct ovule

5.3.1 Gross Morphology

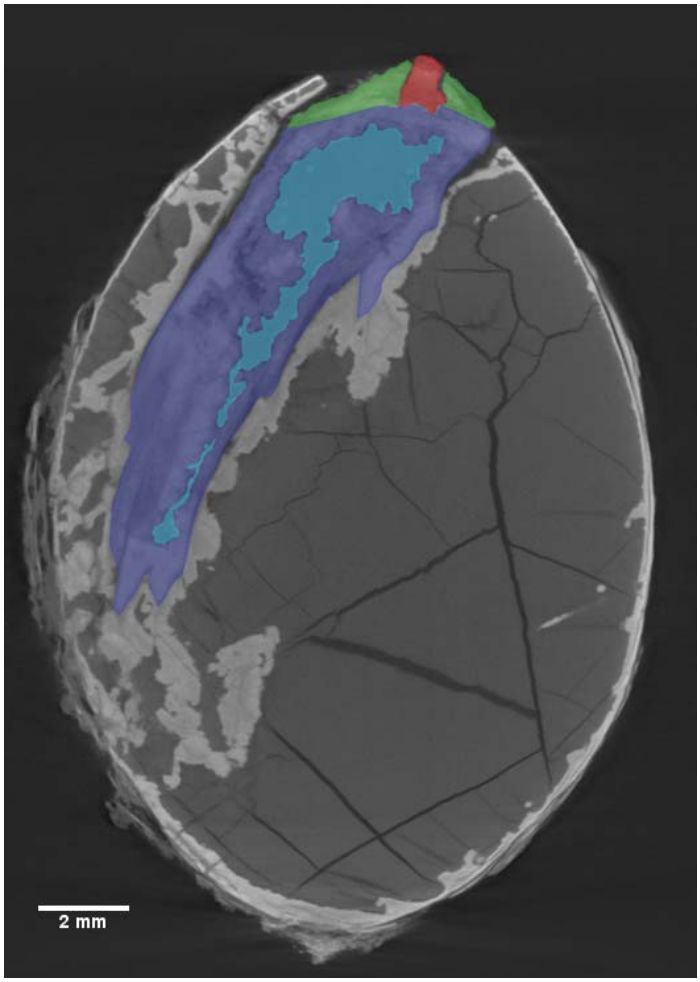

Figure 5.11 Micro-XCT image in longitudinal section through the mid-point showing Bolus (Red) nucellar beak (green) megagametophyte (dark blue) and void space (light blue).

The fossil ovule measures 23mm in length with a maximum diameter of 16mm making it smaller that the living ovule examined, however it is reasonable to assume that such a small variation in

size would be within natural variation with a species or indeed genera, therefore it is being treated as comparable in size. The overall shape is largely comparable as both ovate in longitudinal section with the area most proximal to attachment being the most rotund and the apical end being comparably pointed.

The grey area which is not highlighted (Figure 5.11) has a cracked appearance, this is due to calcite infilling which is comparable to that found in a specimen reconstructed in chapter 3. This calcite infilling represents a former void space within the ovule which would have been used by the later expansion with the development of the megagametophyte.

The nucellar beak is much less pronounced and indeed shows a much more curved appearance at the apical end (Figures 5.11 & 5.12). It is worth noting that part of the sclerotesta is not present at the apex, which could be due to natural decay or even predation, which does not allow for a total comparison of the external morphology. As the nucellar beak not as pronounced in this specimen then it is unlikely that the sclerotesta would end in a pronounced point as occurs in extant *G. biloba*.

Small amounts of remnants of a sarcotesta to show in Figure 5.11, which a very clear sclerotesta being made visible by a high x-ray attenuation layer which appears as bright white. This layer seems significantly thinner than in the extant specimen measuring 0.5mm. This is likely to be as a result of decay and subsequent preservation, so a direct comparison in sclerotesta thickness is not applicable. There are also small traces of the remains of the nucellus which appears to be consistent with the living specimen and that described by Douglas *et al.* (2007).

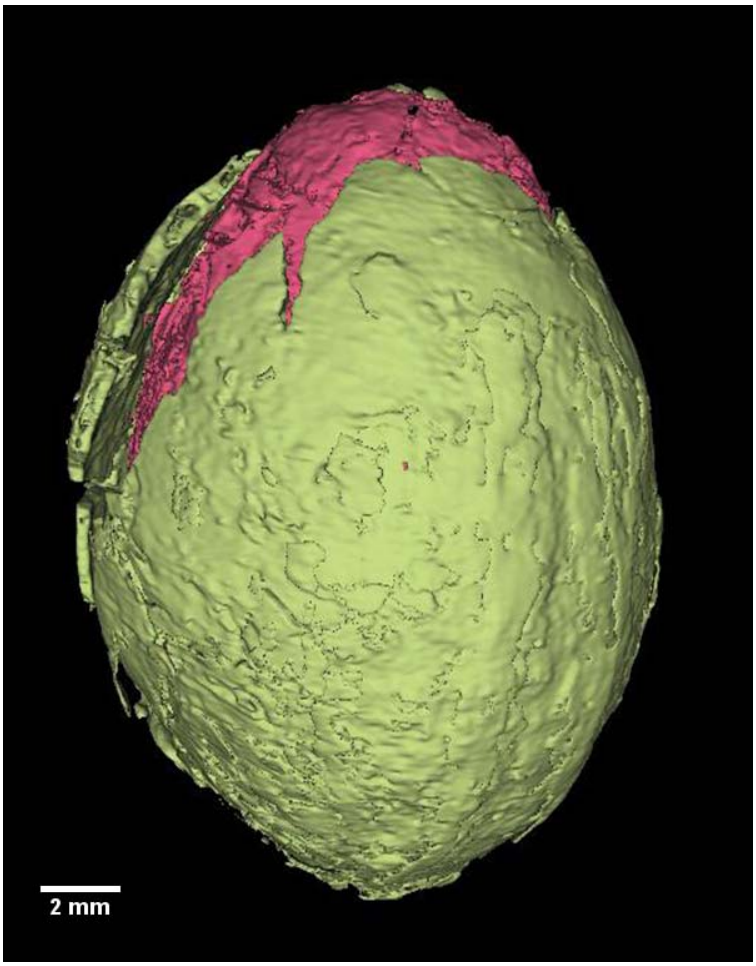

Figure 5.12. Reconstruction of fossil specimen. Showing sclerotesta (green) and megagametophyte (pink).

A split in the sclerotesta is present (figure 5.12) of which the cause is unknown. The apical end of the sclerotesta is missing with the gametophyte being exposed.

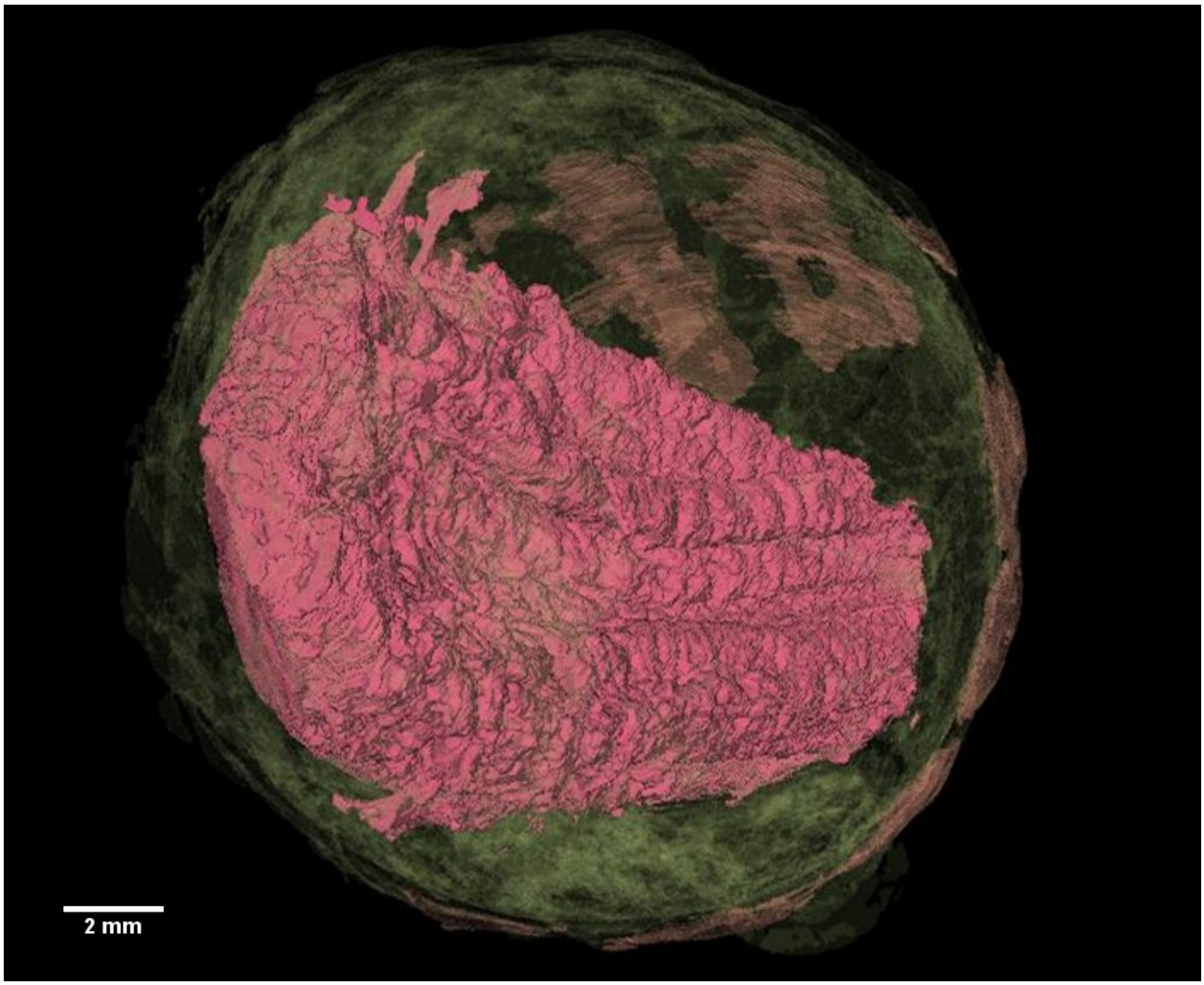

Figure 5.13. Reconstruction showing organisation of tissues megagametophyte (pink), sclerotesta (transparent green) and artefacts remaining of the sarcotesta (transparent light brown).

The megagametophyte is a tongue shaped structure within the nucellus which is smooth on the side closest to the scerlotesta and ribbed or corrugate on the opposite side (Figures 5.13 & 5.14). The megagametophyte occupies approximately 40% of the volume of the ovule (Figures 5.13 & 5.15), when as a living specimen this percentage would have been significantly great, reaching similar levels to that of the living specimen presented in this chapter. The megagametophyte has developed a series of corrugations (Figures 5.13 & 5.15) which would indicate that the

gametophyte was fully fertilised and expanding; the corrugations would have allowed the megagametophyte to inflate during the growth and development of the cotyledons. There is no evidence for the development of the cotyledons at this stage, however there is a cavity in the tissue which would have given ample space for them to develop (Figure 5.14). The cross section morphology of this cavity would suggest that a cotyledon would form in each side with a hypocotyl forming in the centre.

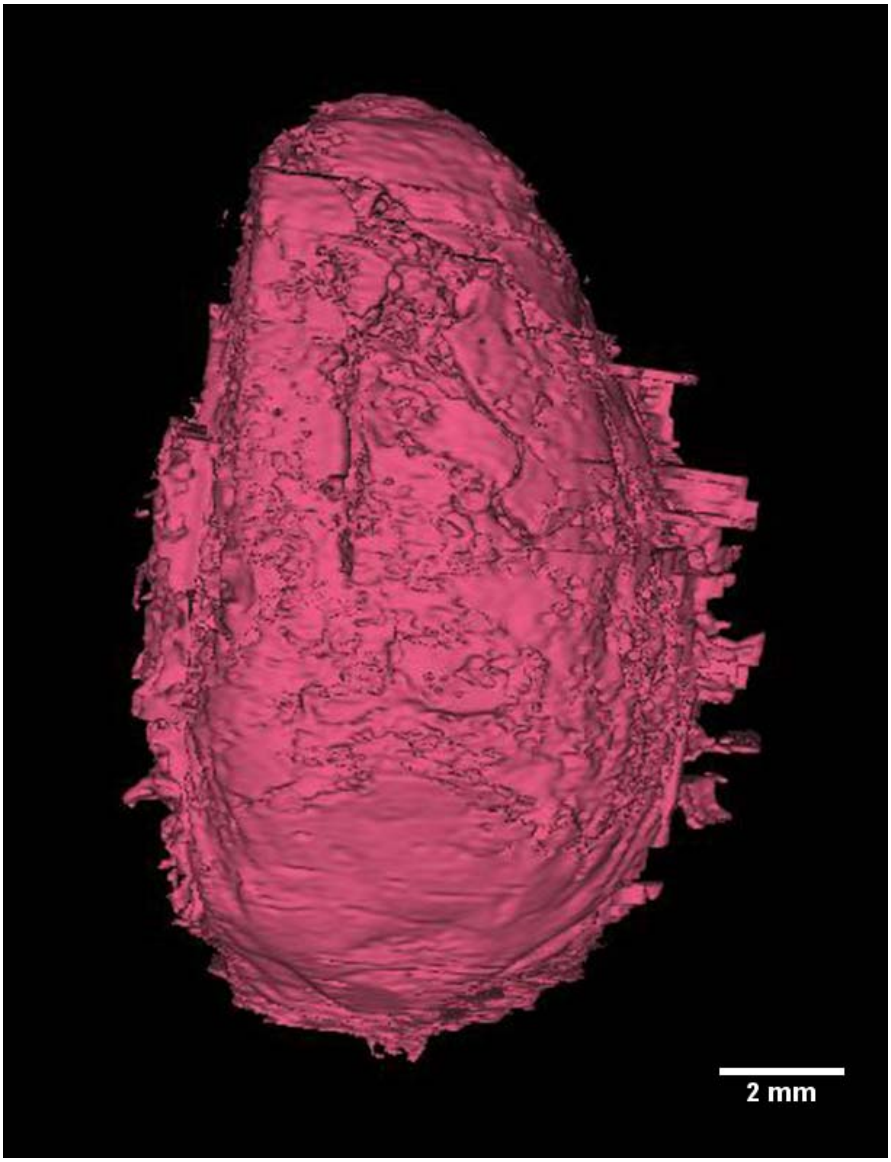

Figure 5.14. Reconstruction showing reverse of megametophyte.

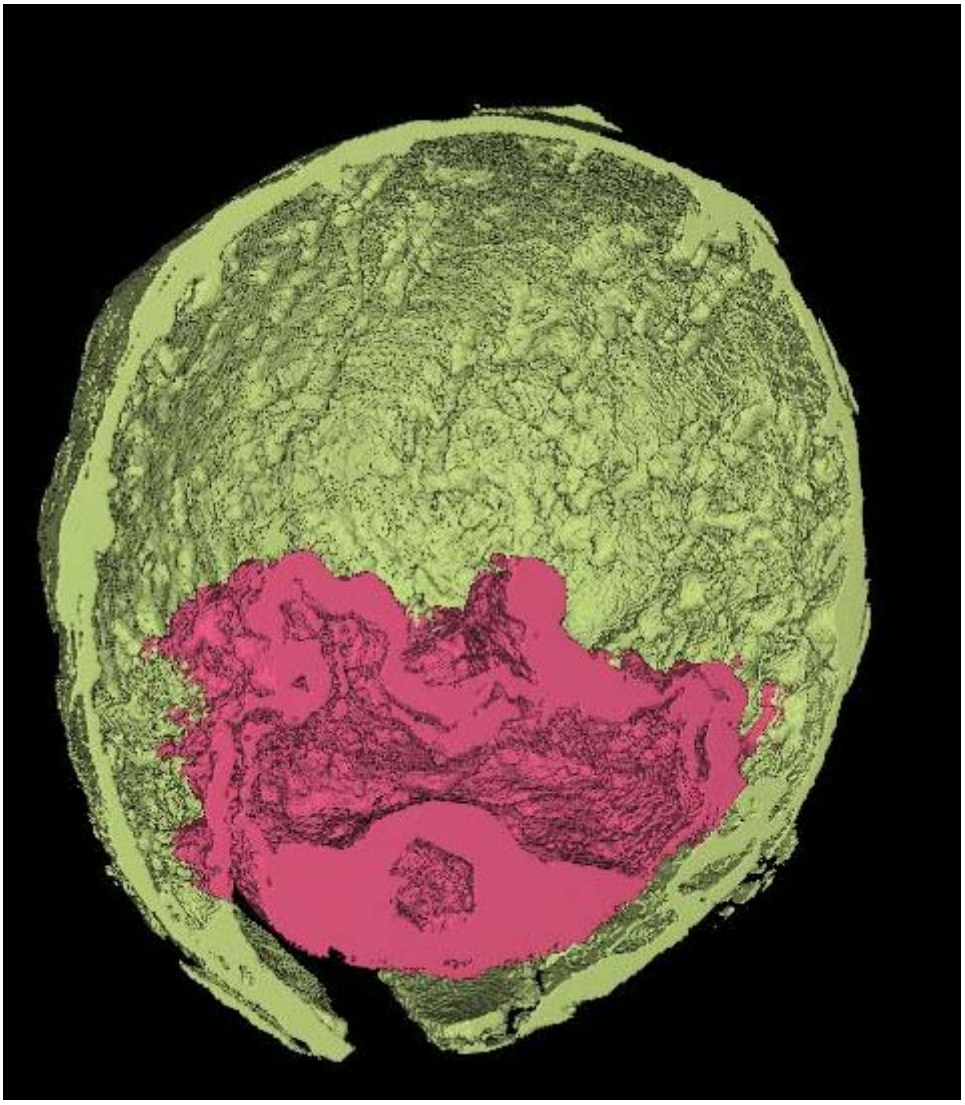

Figure 5.15. Reconstruction showing transverse cross section through fossil specimen of *Gingko* showing megagametophyte (pink) and sclerotesta (green)

It would also be possible that the corrugations provide structural support. Structures which have corrugations have a much greater amount of strength under compression in the orientation of the

corrugation than those without. It is plausible that the corrugations add to the overall structural rigidity of the megagametophyte in the earlier stage of development to stop it collapsing in on itself until the point has been reached where is has fully developed and has achieved its maximum size and tissue thickness which allows structure to be maintained. Once this point has been reached the cotyledon and hypocotyl complex would begin to provide support.

Small artefacts remain of the fleshy sarcotesta which are visible in Figures 5.13 & 5.15, which confirms link with the extant Gingkoalean taxa, small distinctions of ribs are present too, these would distinguish it from being more closely associated with Cycadophytes which do not usually possess ribs.

The internal structure of this fossil example is not as complex as the living example, probably due to taphonomic reasons. The result of this is a greatly reduced time taken to produce the reconstruction which was one month.

5.4 Discussion

The ability to visualise complex 3D structures enables a greater understanding of the morphology of *Ginkgo* and the extinct groups with which has a close affinity. When assessing fossil ovules, only a few characteristics of *Ginkgo* allow fossils to be considered as Ginkgoalean. For example, a ribbed sclerotesta is very common in *Gingko*, however, it is also common in other gymnosperms such as the Palaeozoic ovule *Pachytesta*, but in the Mesozoic only Ginkgoalean have a three ribbed structure and a fleshy sarcotesta. Where evidence is seen of a sarcotesta, then the main group of comparison is Cycadophytes which lack ribs but possess a fleshy sarcotesta.

Using the Mesozoic Ginkgoalean *Nehvizdyella* Kvacek *et al.*, 2005 (Figure 5.16 & 5.17) as an

example to determine structures in poorly preserved specimens without the aid of 3D reconstruction, as a reference and datum, it is very easy to confuse structures when boundaries are not clearly defined. *Nehvizdyella* is poorly preserved and has been interpreted as having ovules in which the sarcotesta is a non-continuous structure. In comparison with the living and extinct Ginkgoalean documented here, this structure in *Nehvizdyella* has been re-interpreted the gametophyte. There are distinct morphological similarities in transverse cross section to the gametophyte shown in Figure 5.16 & 5.17. The level of preservation is not sufficient to be able to match all of the aspects, however the gross morphology of a structure within the main body of the ovule, which in non-continuous, which has a smooth side mirroring the internal shape of the nucleus and the inner portion having a corrugated appearance.

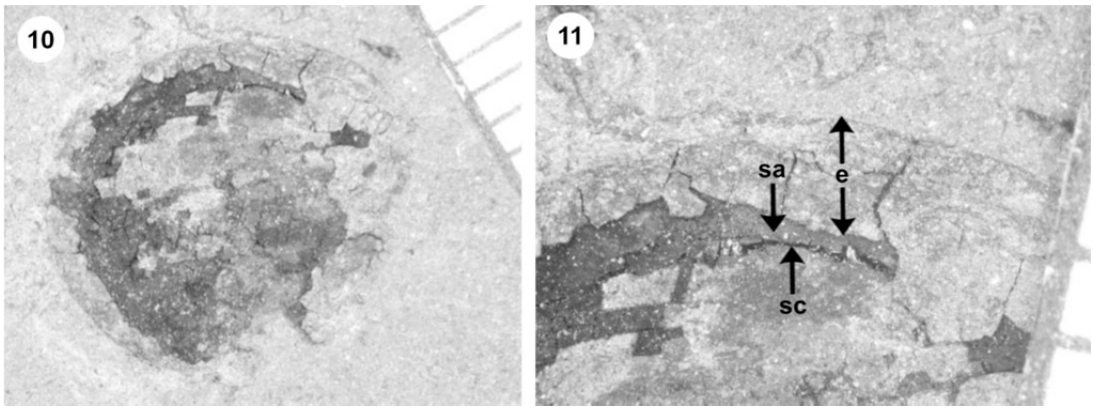

Figure 5.16 Image showing anatomy of *Nehvizdyella.* Sarcotesta (sa) endotesta (e) and sclerotesta (sc) Taken from Kvacek *et al.* (2005).

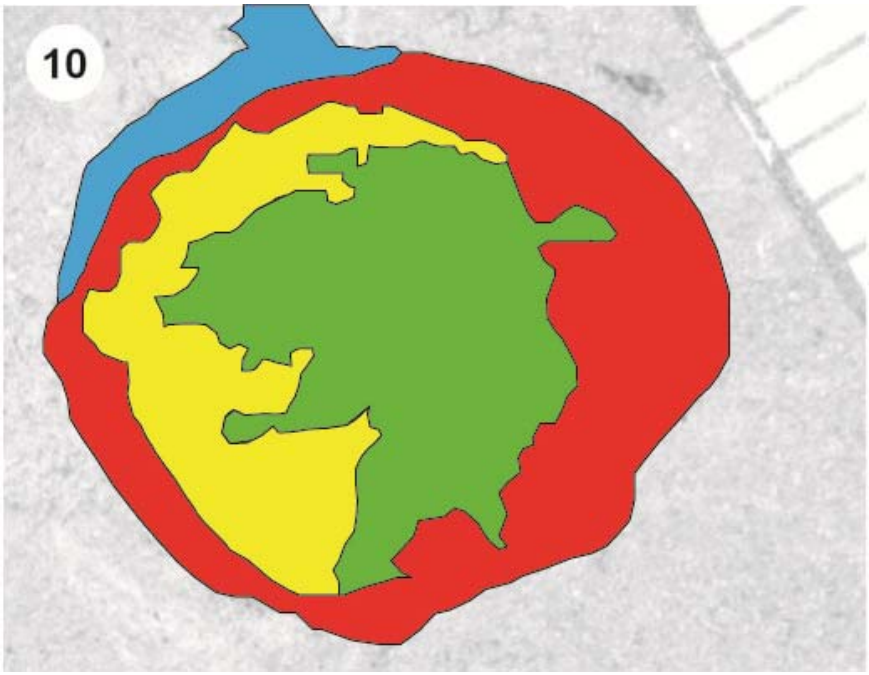

Figure 5.17 New interpretation of *Nehvizdyella,* modified from Kvacek *et al*, 2005. Blue area representing the collar, red represent the sclerotesta, yellow representing the reduced gametophyte and green representing the cavity void within the nucleus.

In *Nehvizdyella*, sclerotesta is shown to be a very thin and again non-continuous layer. As this is the hardest and structurally most rigid tissue in the ovule the current interpretation cannot be correct. Using the two previous models shown within this chapter as a basis of the new interpretation, is in keeping with both the living and fossil examples. There are many and distinct similarities between *Nehvizdyella* and the fossil specimen, including shape and position of the gametophyte, large void space and substantial sclerotesta. The only major difference is the presence of the collar in *Nehvizdyella* however, as the other specimens were not found in organic attachment to any other material, then the collar is a structure to which little emphasis should be placed up on.

From these reconstruction, of the Jurassic ovule studied here, it is clear that the fossil example

shown is indeed a member of the family Ginkgoaceae as it shows the majority of the preservable structures that is show in the living specimen, such as ribs; a nucellar beak (although reduced); remains of a sarcotesta; shape, position and size of the gametophyte and shape and size of the ovule. The only substantial difference is the lack of a cotyledon in the fossil specimen which is likely to be due to the stage of development. Being able to assign the fossil specimen a genus or indeed a species name is very difficult as a lot of ovules are assigned their species due to the information gained form either attachment to leaves and stems, or by close association to identifiable organic remains. At present no specific characters are used to define a species based only on the ovule. It is here concluded the Jurassic ovule studied is morphologically and anatomically indistinguishable from the ovule of the living species *Gingko biloba* in its pre-fertilization state, and shows a remarkable level of conservatism in the features of the ginkgoales from the Mesozoic to recent.

CHAPTER 6

DISCUSSION

Many examples of 3-D reconstructions have been shown within this thesis and during the duration of this research project 3-D reconstructions have become more widespread within paleobotany (e.g Friis *et al.*, 2007; Seyfullah, 2009; Seyfullah *et al.,* 2010, Stevens *et al.*, 2010) and also in the wider palaeontological arena (Sutton, 2008; Rahman *et al.*, 2009; Garwood & Dunlop, 2011). This rise in its utilization as a tool is somewhat similar to the development of scanning electron microscopy did in the 1960's. The methodologies set out in this thesis give a guide as to how these reconstructions can be undertaken and their limitations. However, it is also recognised that further modifications and developments are required if 3-D computer reconstructions are to become more widely used within this field. This chapter will discuss how parts of this thesis can be developed in the future and will consider possible implications that can arise.

Many of the reconstructions shown in this thesis have been produced by using previously described and prepared material, some of which represents type and figured materials. This is a

highly valuable resource which, if reconstructed properly, would allow researchers from all over the world free access to these specimens in a digital form. It is acknowledged that this would not be suitable for all specimens. However, there are a significant amount of such specimens where a part and counter-parts have been described, and a reconstruction could be easily be achieved by using scanning methods and described and shown in chapters 4 and 5.

Many details within a specimen can only really be fully understood when observed in 3D, an example being the sporangium of *Lepidocarpon* sp. A (Figure 4.13). Using traditional methods of investigation an image of this structure would only be possible from one or two angles, the structure is also too big to undergo SEM analysis which means reliance would be placed on digital photography, which as the structure is partially obscured would prove very difficult.

Serial grinding is a method which can achieve excellent results in terms of aiding the understanding of morphology and producing accurate reconstructions (Sutton *et al.*, 2006) as shown in chapter 4 with the reconstruction of *Lepidostrobus* sp A. This method is highly time consuming both in terms of specimen preparation and in image processing, especially the alignment process. Serial grinding can offer reconstructions which rival those of micro X-ray tomography. However it is unlikely that this method will be widely adopted unless the specimens simply cannot undergo scanning methods; its destructive nature is a significant drawback which means that specimens are not available in the future for subsequent analysis as and when technologies improve.

The availability of scanning equipment is increasing and at the same time the ability of such instruments to scan more difficult objects is also increasing. In addition to this, particle accelerators such as the Tomographic Microscopy and Coherent radiology experiments (TOMCAT) in Switzerland is now undertaking high resolution scans of fossil material (e.g. Friis *et al*., 2007). The increased voltages in use and speed of the X-rays allows for greater X-ray attenuation (Groso *et*

al., 2006), the result of this being that specimens in dense substrates will be able to be scanned. As such, specimens that currently do not yield dividends in existing scanning facilities may be readily examined in the future, assuming they are not subjected to destructive scanning technologies in the meantime.

When determining definitive structures to separate gymnosperms at family level purely by their female reproductive organs, many grey areas appear. The development, reduction and subsequent loss of the sclerotestal beak does raise a series of interesting questions. This is a structure which is well formed and present in many pteridosperms and is particularly pronounced in the medullosan ovule genus *Stephanospermum*. The nucellar beak is present (Figure 6.1), but slightly reduced, in *G. biloba,* but is only weakly developed in extinct *Gingko* and the same is true for modern and extinct cycads.

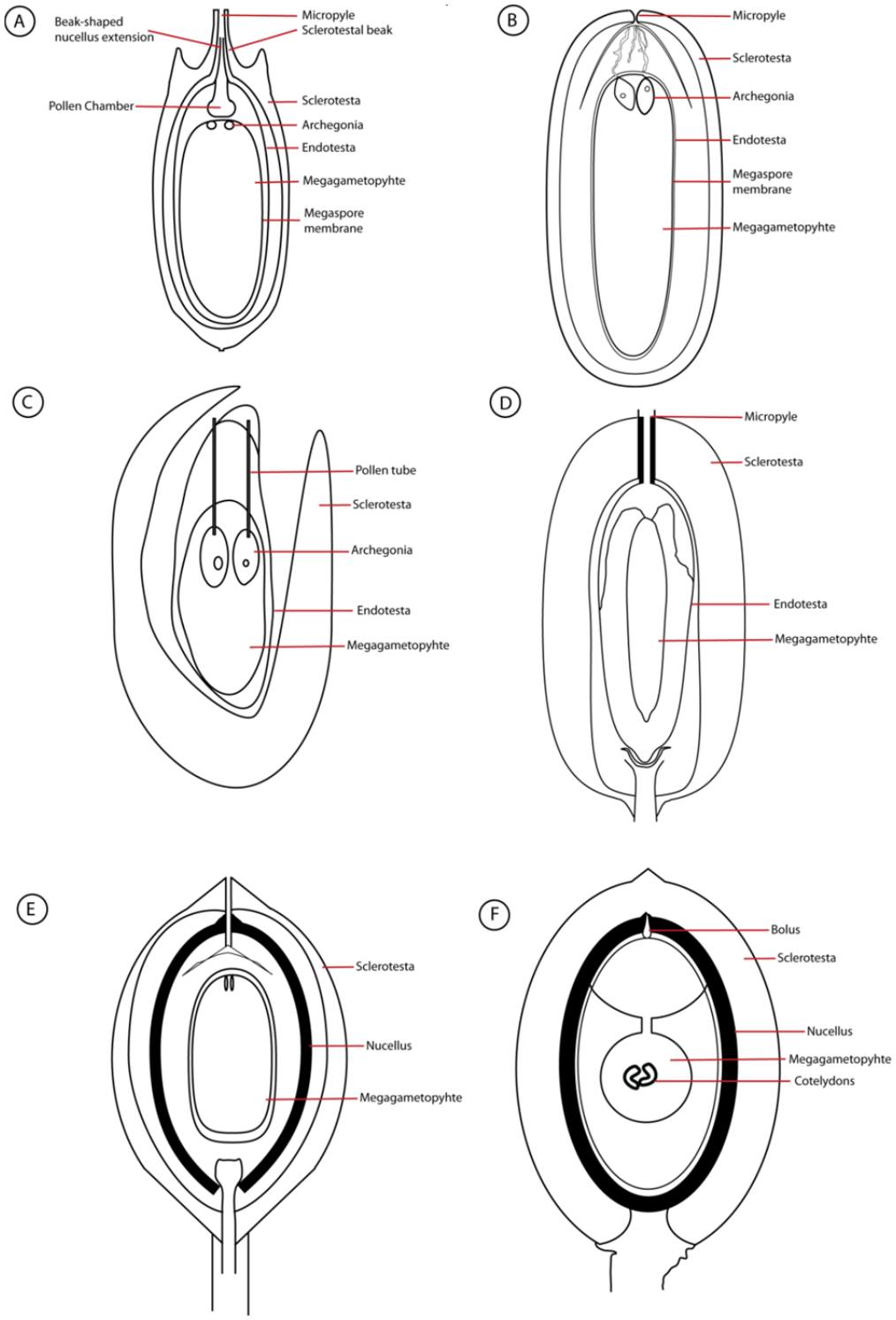

Figure 6.1 Diagram representing different genera of gymnosperm ovules, A *Stephanospernum*, redrawn from Linkies *et al.*, 2010; B, *Pinus*, redrawn from Chamberlin & Coulter, 1932; C, *Picca* redrawn from Scott, 1906; D, *Ephedra*, redrawn from redrawn from Chamberlin & Coulter, 1932; E, *Zamia*, redrawn from Chamberlin & Coulter, 1932and F, *Ginkgo biloba,* redrawn from Chamberlin & Coulter, 1932. Not to scale.

As a result, this can be ruled out as some form of evolutionary trait and is more likely to be a pollination specific structure. It is concluded most likely that highly pronounced sclerotesta beaks are present in wind pollinated species whereas species which more reduced beaks rely more heavily on insect pollination. For example *Zamia furfyracea* L. 1753 is almost exclusively pollinated by *Rhopalotria mollis* (Norstog, 1990). What does seem consistent is a thickening of the nucellus around the opening of the micropyle. It is hard to read much into this as it seems logical to be a development to support the structural integrity of the seed where there is a natural weakness at an opening point.

The sclerotestal beak, as its name suggests, is made from the hard, 'stony' cells. It is concluded that there is no obvious structural reason for this to occur, it may benefit wind pollination by making the pollen receiving tissue a stable and non-deformable opening. However, there could be a definite predation risk associated if less robust tissues formed the opening. The position and structure of the bolus is a trait which both *Gingko* and Cycads have in common, other gymnosperms do produce a small mucilage plug, commonly this is not as well defined as the bolus and seems to be more akin to a thin 'stopper' (Douglas *et al.*, 2007).

With all the variation present within gymnosperm ovules, 3-D reconstruction is an ideal tool for objective analysis between genera. Morphological analysis has to be used in datasets where fossil material is present, chapter 5 of this thesis demonstrates that the same reconstruction methodologies can be used to access both living and fossil specimens. At present, there is little agreement on the relationships between gymnosperm groups (e.g. Hilton & Bateman, 2006) (Figure 6.2). As a result of the lack of agreement in the morphological datasets and also in molecular datasets (e.g. Meltzer *et al.*, 2010) I would propose to treat more extant and extinct specimens in the same way and apply the same methodologies. Micro X-ray tomography would be the ideal solution to this as then all specimens would have the same level of

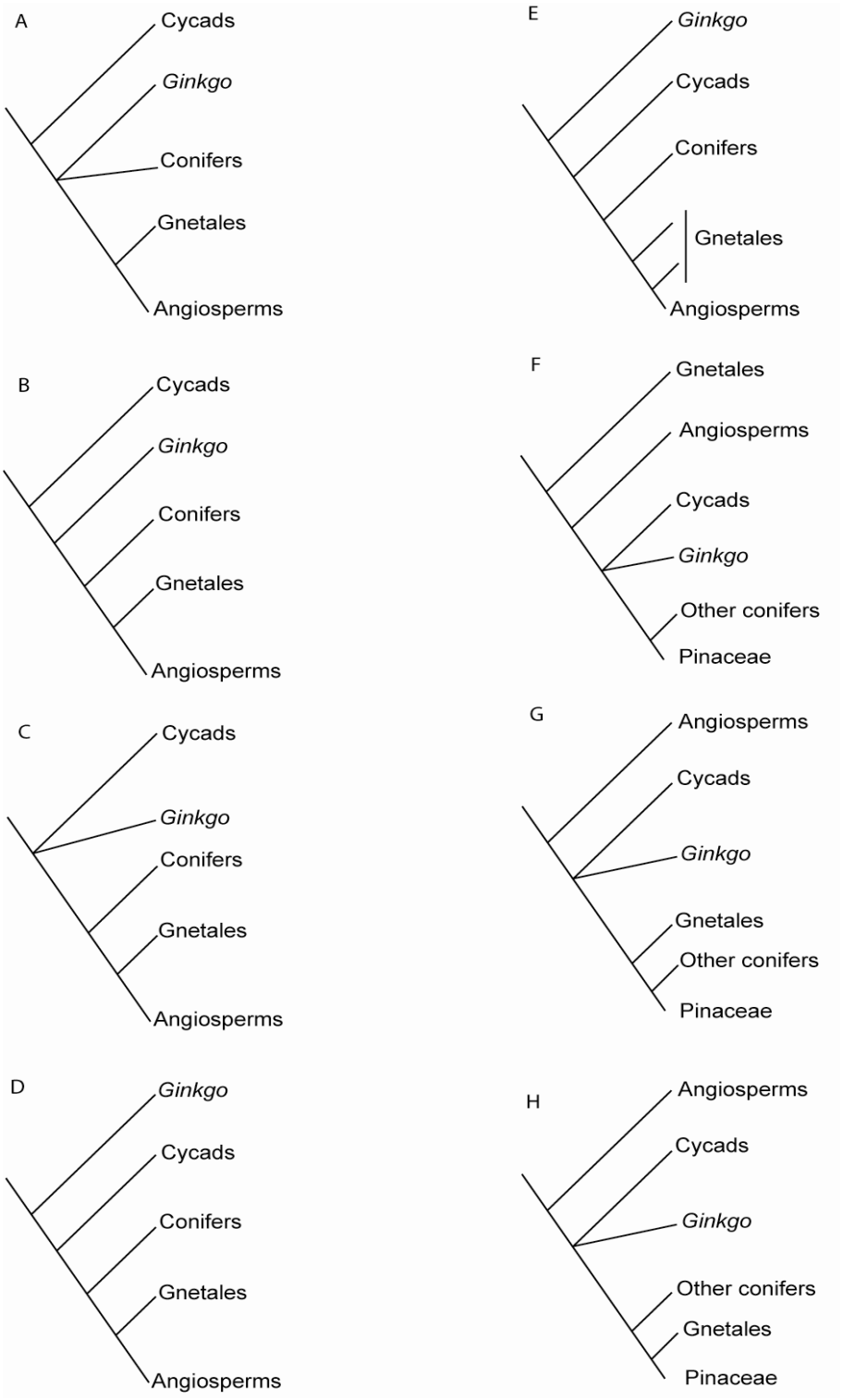

Figure 6.2 Relationships among major groups of seed plants based on previous morphological and molecular cladistic analyses. Reproduced from Hilton and Bateman 2006. A-E based on morphological cladistic analyses, F-H based on molecular cladistic analyses.

detail. At present is it rare that living plants undergo rigorous morphological assessment; for example, there is very little information available on the morphology of the ovules of *G. biloba* other than dated accounts developed in the pioneering period of descriptive plant anatomy (Chamberlain and Coulter, 1932). The description in Chapter 5 of *G. biloba* is one of the most detailed contemporary accounts. It would seem logical to apply these methods to all of the major extinct gymnosperm groups and their nearest living relatives. This would also allow for much closer comparisons to be made with the reproductive structures of angiosperms which might go some way to solve Darwin's abominable mystery.

Once 3-D models have been created there are also implications to conduct more functional studies. Finite element analysis and Computation Fluid Dynamics (CFD) could be very easily applied to these reconstructions. Finite element analysis works by parts of a structure being assigned properties and these properties then being used to calculate what forces they can withstand and how a force applied to one area of the specimen would affect other areas. CFD is used to understand how fluids (or gases) interact with structures and how the fluids are affected and then affect the structure. Once it is understood how some of these structures function and the loads that can be applies or how wind may interact, then the objective function of a structure could be used as a character along with their presence or absence. For example it may be possible to test how wind interactions on the sporophyll helps to distribute spores or even if a certain wind speed would be required remove a cone or seed from the parent plant.

Along with the methods outlined within this thesis, one other reconstruction method was attempted. Surface laser scanning (Fgure 6.3) was undertaken on the specimen *Lepidocarpon* sp. A as described in Chapter 4

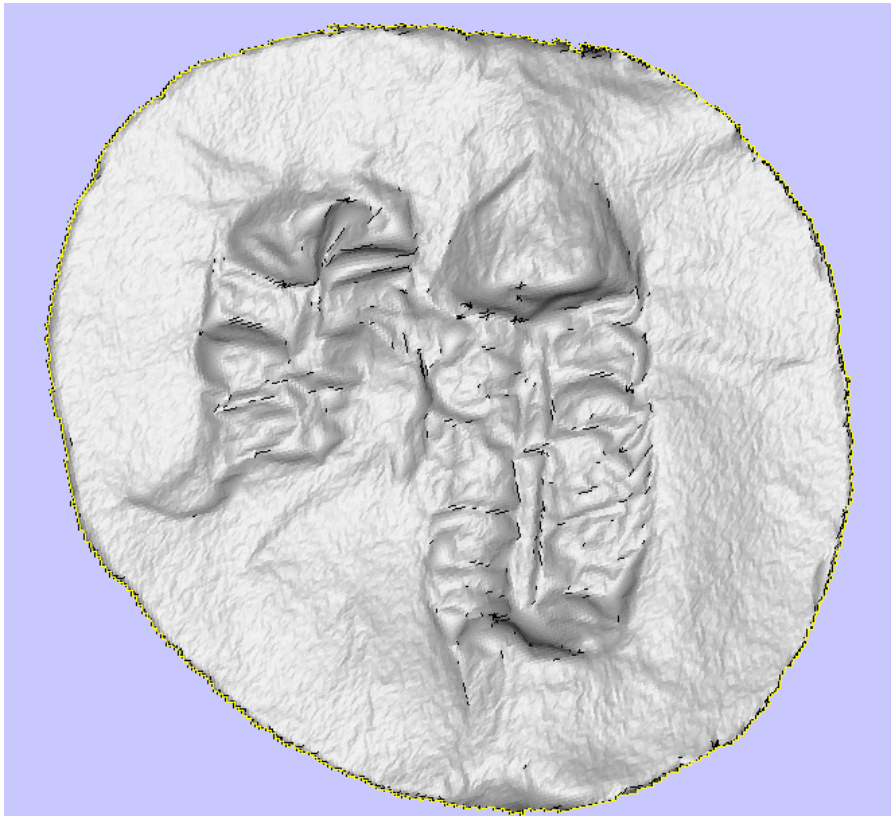

Figure 6.3 Surface scan of *Lepidocarpon* sp. A.

From the surface scan vague detail can be seen, the axis of both cones can be seen along with some of the larger and more prominent sporophylls. This method is not sufficient in quality to be deemed a viable method of reconstruction. However, higher resolution laser surface scanners are continually being developed. The advantages of these methods are that they are portable and designed for use outdoors as they are used extensively in archaeological applications. When they are able to resolve structures below 0.1mm, they will be a viable method of seeing 3-D structures based on external morphology.

Producing highly detailed 3-D reconstructions in their current form is now possible for most researchers, however the future of this aspect of palaeobiological sciences must mean collaboration with other branches of sciences. Visualising an object in true 3-D at present requires

a sterographic projector and polarising glasses. Currently true 3-D computer monitor and television sets are under development which will allow for true 3-D visualisations.

Rapid prototyping 3-D printers are also now becoming more mainstream and cost effective. The advancements now mean that several different materials can be used and at great resolutions. They allow for very complex structures to be printed. It is highly likely that with the advancement of scanning methods and them becoming more mainstream that fossil specimens will be scanned, the data transmitted electronically or stored on an open access database and a 3-D printout of the specimen can be easily produced. These can then be easily used for purposes of study and teaching.

Combining several different types of digital datasets will also be greatly beneficial. Laser scanning has been mentioned previously, currently is it not suitable for reconstructions on the scale which is shown in this thesis, however they are hugely useful when looking at the occurrence of fossil specimens and whole areas can be scanned. If a fossil forest could be found or an existing locality scanned, the precise location of each specimen could be digitally stored, added to this information could be reconstructed specimens of the same species to produce a high accurate reconstructed environment, it would then be possible to zoom in on individual facets of this environment such as any of the structures shown in this thesis, and get a wealth of information in one digital data set. Fragments of this is being undertaken, however large scale collaboration would be needed to achieve the level of detail required.

CHAPTER 7

CONCLUSIONS

The primary aim of this thesis was to show that 3-D computer reconstructions of complex paleobotanical reproductive structures could be undertaken successfully and be shown to be a valuable tool to be used alongside more traditional approaches. The reconstructions within this thesis show that this is possible and emphasise that reconstructions can be produced at various qualities and scales, with these depending on the kind of preparation previously undertaken on the specimen.

Preparation methods are critical in ensuring an accurate reconstruction is produced. In order for this to take place, the following conclusions should be adhered too. Reconstructions can be produced from previously prepared specimens as long as (1) the specimen has been accurately sectioned, (2) that each tomographic surface is parallel to adjacent surfaces, (3) that each

tomographic surface has a smooth surface, (4) that each tomographic surface is of equal or near equal spacing, (5) that only gross morphology is required from the reconstruction, and (6) and that any structure being reconstructed is larger than the spacing between tomographic surfaces. Although reconstruction from sectioned material may not hold the same aesthetic appeal or contain very finely resolved structures, they do allow for relatively fast and efficient reconstructions of a specimens gross morphology. If specimens are required to undergo traditional examination which requires serial sectioning or wafering and then be reconstructed, it is strongly recommended that alignment marks are places within the matrix surrounding the specimen but running in a parallel course through the length of the specimen to be sectioned; a minimum of three are required to provide accurate alignment.

In the case of *Flemingites arcuatus,* what would be considered crude reconstruction can provide valuable information on the arrangement of sporophyll-sporangium complexes within the cone, and from this it is shown that they are spirally arranged with six megasporophylls emerging from the axis every 360º, and that the angle at which they depart the axis ranges from 45º and 51º. This data would be very difficult to calculate without the use of a reconstruction.

The use of serial grinding is recommended where micro X-ray tomography is not available or suitable for the specimen; ideally this would be limited to specimens where there are multiple specimens as it is a destructive process that is generally not recommended for unique specimens. It is also recommended to adopted hybrid methods including take acetate peels at regular intervals through the serial ground dataset – this is important in case any digital data is lost and it also provides a permanent record of the specimen where serial grinding will totally destroy it otherwise. This type of preparation method is not viable for use on type or figured materials.

The use of X-ray tomography is recommended as the default choice for reconstructions if the equipment is available and the specimen is suitable. The lack of any invasive preparation, the fast

scan time and the pre-aligned images are ideal but the large number of images produced as a result of the close spacing of tomographic planes can result in a large amount of editing needing to be undertaken. However, a simple reconstruction to show gross morphology of the specimen can be undertaken very quickly. As much of the surrounding matrix should be removed from the specimen as possible before scanning to allow for maximum X-ray exposure.

The use of micro X-ray tomography to attain ‘surface scans’ where there is little penetration in the specimen is highly recommended. *Lepidocarpon* sp. A shows a large amount of detail including features of the large sporangium, large sporophylls with a complex compound shape and a large keel, a central axis with a thick wall and attachment scars from sporophylls. This reconstruction has also allowed highly accurate measurements of these structures to be taken which otherwise would not be possible.

Using a combination of masks and curves in the reconstruction, very complicated structures can be understood. The size, arrangement and shape of the central axis and sporophylls in *Lepidostrobus sp. A* would not be easy to understand if just one method was used. From this, it is shown that *Lepidostrobus sp. A* has a small diameter central axis with spirally arranged sporophylls which are narrow and often show a prominent keel. The sporophylls are very densely packed and overlap with each other.

By using a combination of living and fossil materials, and by using the same micro X-ray scanning techniques on both, the level of understanding of Ginkgoalean ovules from the recent to the Jurassic to the recent has been increased. Both of these specimens share very similar external morphology with the only major difference being that the living specimen displays more prominent ribs; however they are still present of the fossil examples. Both specimens are a similar size, within 10% of each other. Both of these specimens have a large internal megagametophyte which has characteristic corrugations, which allows both to inflate and to expand. There are no

distinguishable differences in morphology between the extant and extinct specimens. This shows that ovule of *Ginkgo biloba* has remained in evolutionary stasis since the Jurassic; however it remains uncertain if the Jurassic ovule belongs to the *G. biloba* as other parts of the parent plant are unknown and the ovules may have been produced by two closely related species that are differentiated on other features of the whole plant morphology (see Hilton & Bateman, 2006). Jurassic Ginkgoalean foliage from the UK is distinct from that of *G. biloba* (Harris and Millington, 1974; Taylor *et al*., 2009).

The detail in the reconstructions has also shown that other fossil ginkgoalean specimens have been structurally misinterpreted. In the case of *Nehvizdyella* (Kvacek *et al.*, 2005), a reassessment of the internal morphology should be undertaken based upon the reconstruction of the extant species of *G biloba.* and in comparison with Jurassic anatomically preserved ovules. This emphasises that 3-D reconstruction can reveal features that explain structures seen in non-reconstructed specimens and has wider impact than might otherwise be envisaged.

REFERENCES

Anderson, J. M., Anderson, H. M. 2003. Heyday of the Gymnosperms: Systematics and Biodiversity of the Late Triassic Molteno Fruitifications. Strelitzia, 15: 1-398.

Anderson, L. I., Dunlop, J. A., Eagar, R. M. C., Horrocks, C. A. and Wilson, H. M. 1999. Soft-Bodied Fossils from the Roof Shales of the Wigan Four Foot Coal Seam, Westhoughton, Lancashire, UK. Geological Magazine, 135: 321-329.

Archangelsky, S. 1965. Fossil Ginkgoales from the Tico Flora, Santa Cruz Province, Argentina. Bulletin of the British Museum Natural History Geology. 10: 121-137

Baker, P. G. 1973. A Technique for Accurate Reconstruction of Internal Structures of Micromorphic Fossils. Palaeontology, 21: 463-467.

Bek, J. S, Oplustil. 2004 Palaeoecological constraints of some Lepidostrobus cones and their parent plants from the Late Palaeozoic continental basins of the Czech Republic. Review of Palaeobotany. And Palynology 131: 49–89.

Brack-Hanes, S. D. and Thomas, B. A. 1983. A Re-Examination of *Lepidostrobus* Brongniart. Botanical Journal of the Linnean Society, 86: 125–133.

Branznal, L. 2006. Exceptional Preservation in the Upper Carboniferous Coseley Lagerstatte. PhD Thesis, University of Birmingham.

Brongniart, A.M. 1828. Prodrome d'une histoire des végétaux fossiles. 230pp

Calder. J. H., Gibling, M. R., Scott. A. C., Davies. S.J and Herbert, B. L. 2011. Pennsylvanian 'Fossil Forests' in Growth Position (T0 Assemblages): Origin, Taphonomic Bias and Palaeoecological Insights. *Journal of the Geological Society*, 168: 585-605

Chamberlin, J. M., Coulter, C. J. 1932. The Morphology of Gymnosperms. University of Chicago. 458pp

DiMichele, W. A. and Phillips, T. L. 1985. Arborescent Lycopod Reproduction and Paleoecology in a Coal-Swamp Environment of Late Middle Pennsylvanian age (Herrin Coal, Illinois,USA). Review of Palaeobotany. And Palynology. 44: 1-26.

DiMichele, W. A. and Phillips, T. L. 1994. Paleobotanical and Paleoecological Constraints on Models of Peat Formation in the Late Carboniferous of Euramerica. Palaeogeography Palaeoclimatology Palaeoecology, 106: 39–90.

DiMichele, W. A., Phillips, T. L. and Nelson. J. W. 2002 Place versus Time and Vegetational Persistence: a Comparison of Four Tropical Mires from the Illinois Basin During the Height of the Pennsylvanian Ice Age. Journal of Coal Geology, 50: 43-72.

Douglas, A. W., Stevenson. D. W., Little, D.P. 2007. Ovule Development in Ginkgo biloba L., with emphasis on the Collar and Nucellus. International Journal of Plant Sciences. 168: 1207-1236

Foley, J. D., Van Dam, A., Feiner, S K. and Hughes, J. 1995. Computer Graphics: Principles and Practice in C (2nd ed.). Addison-Wesley, 1152pp.

Friis, E .M., Crane, P. R, Pedersen, K. R., Bengtson, S., Donoghue, P. C. J., Grimm ,G. W. and Stampanoni, M. 2007. Phase-Contrast X-Ray Microtomography Links Cretaceous Seeds with Gnetales and Bennettitales. Nature, 450: 549-52.

Galtier, J. and Phillips, T. L. 1999. The Acetate Peel Technique. In: Jones, T. P. and Rowe, N. P. (eds), Fossil Plants and Spores: Modern Techniques. Geological Society, London. 67-70.

Garwood, R. J. And Dunlop, J. A. 2011. Morphology and Systematics of Anthracomartidae (Arachnida Trigonotarbida). Palaeontology, 54: 145-161.

Gastaldo R. A., Stevanovic-Walls I. M., Ware W. N. and Greb S. F. 2004. Community Heterogeneity of Early Pennsylvanian Peat Mires. Geology, 32: 693–696.

Groso, A., Stampanoni, M., Abela, R. et al 2006. Phase Contrast Tomography: An Alternative Approach. Applied Physics Letters, 88: Issue 21.

Habgood, K. S., Hemsley, A. R. and Thomas, B. A. 1998. Modelling of the Dispersal of Lepidocarpon Based on Experiments Using Reconstructions. Review of Palaeobotany and Palynology, 102: 101-114.

Hass, H. and Rowe, N. P 1999. Thin Sections and Wafering. In Jones, T. P and Rowe, N. P (eds) Fossil Plants and Spores: Modern Techniques. Geological Society London: 76-81.

Harris, T. M., Millington, W. 1974. The Yorkshire Jurassic Flora. IV. Part 1. Ginkgoales. British Museum Natural History: London. 1–78pp

Hickey, M.and King, C. 2000. Illustrated Glossary of Botanical Terms. Cambridge University Press, 208 pp.

Hilton, J., Rothwell, G. W., Cheng-Sen, L., Shi-Jun, W. and Galtier, G. 2001. Permineralized Cardiocarpalean Ovules in Wetland Vegetation from Early Permian Volcanicalistic Sediments of China. Palaeontology, 44: 811-825.

Hilton, J., Wang, S. J., and Tian, B. 2003. Reinvestigation of Cardiocarpus Minor (Wang) Li from the Early Permian Taiyuan Formation of Northern China and an Evaluation of Cardiocarpalean Ovule Taxonomy, Systematics and Phylogeny. Botanical Journal of the Linnean Society. 141: 151-175.

Hilton, J. and Bateman, R. M. 2006. Pteridosperms are the backbone of seed–plant phylogeny. Journal of the Torrey Botanical Society, 133: 119–168

Holt, B. F., Rothwell, G. W. 1997. Is *Ginkgo biloba* (Ginkgoaceae) really an Oviparous Plant? American Journal of Botany, 84: 870-872

Karnosky, D. 1981. Chamber and Field Evaluations of Air Pollution Tolerances of Urban Trees'. Journal of Arboriculture, 7: 99-105

Kirchner, M., Van Konijnenburg-van Cittert, J. H. A. 1994. *Schmeissneria microstachys* (Presl, 1833) Kirchner et Van Konijnenburg-van Cittert, gen.et sp. nov., plants with ginkgoalean affinities of Germany. Review of Palaeobotany Palynology 83: 199–215.

Krassilov, V.A. 1972. Mesozoic Flora from the Bureja River (Ginkgoales and Czekanowskiales). Nauka, Moscow, 115 pp.

Kvacek, J., Falcon-Lang, L., Dasková, J., 2005. A new Late Cretaceous Ginkgoalean Reproductive Structure *Nehvizdyella* gen. nov. from the Czech Republic and its Whole-Plant Reconstruction. American Journal of Botany. 92: 1958–1969.

Linkies. A., Graeber. K., Knight. C. and Leubner-Metzger, G. 2010. The evolution of seeds. New Phytologist, 186: 817-831.

McMullen, D. 1993. Scanning Electron Microscopy. 51st Annual Meeting of the Microscopy Society of America, Cincinnati.

Melzer R., Yong-Qiang W., Theissen G.. 2010. The naked and the dead: The ABCs of gymnosperm reproduction and the origin of the angiosperm flower. Seminars in Cell & Developmental Biology 21: 118–128

Norstog, K. J. 1990. Studies of Cycad Reproduction at Fairchild Tropical Garden, in Stevenson, D. W. (ed) Memoirs of the New York Botanical Garden, Vol. 57. The Biology, Structure and Systematics of the Cycadales, Symposium Cycad 87, Beaulieu-sur-Mer, France, April 17-22, 1987. IX+210P. New York Botanical Garden, Bronx, New York, USA. Illustrated Maps Paper Book Series: Memoirs of the New York Botanical Garden, pp 63-81. Published:1990.

Philips. T. L. 1979. Reproduction of Hetrosporous Arborescent Lycopods in the Mississippian-Pennsylvanian of Euramerica. Review of Palaeobotany and Palynology. 27: 239-289.

Rahman, I. A., Sutton, M. D. And Bell, M. A. 2009. Evaluating Phylogenetic Hypotheses of Carpoids Using Stratigraphic Congruence Indices. Lethaia, 42: 424-437.

Reed. F. D, 1941. Coal Flora Studies: Lepidodendrales. Botanical Gazette, 102: 663-683.

Samylina, V.A. 1990. *Grenana*—A New Genus of Seed Ferns from the Jurassic Deposits of Middle Asia. Botanical Zh. 75: 846–850.

Sailsbury, E. J. 1913. The Determining Factor in Petiolar Structure. New Phytologist, 12: 281-289

Scott, D. H. 1901. On the Structure and Affinities of Fossil Plants from the Palaeozoic Rocks – IV. The Seed-Like Fructifications of Lepidocarpon, a Genus of Lycopodiaceous Cone from the Carboniferous Formation. Philosophical Transactions of the Royal Society of London. Series B, 194: 291-333.

Scott, D. H 1906. Structural Botany of Flowering Plants. Adam and Charles Black, 283 pp.

Seyfullah, L. J. 2009. The Evolution and Systematics of Palaeozoic Pteridsperms. PhD thesis. University of Birmingham.

Seyfullah, L. J., Hilton, J, Liang, M. M,. 2010. Resolving the systematic and phylogenetic position of isolated ovules: a case study on a new genus from the Permian of China. Botanical Journal of the Linnean Society, 164: 84-108

Seward, A. C., Gowan. J. 1900. The Maidenhair tree. Harvard University

Sollas, I. B. J. and Sollas, W. J. 1913. A Study of the Skull Dicynodon by Means of Serial Section. Philosophical Transaction of the Royal Society London. B204: 201-225.

Sporne, K. R. 1967. The Morphology of Gymnosperms. Hutchinson Co Ltd. 216 pp

Stanislavsky, F.A. 1973. The new genus *Toretzia* from the Upper Triassic of the Donetz Basin and its Relation to the Genera of the Order Ginkgoales. Paleontology. Zh. 1, 88–96

Stevens L. G, Hilton. J, Rees. A. R., Rothwell G. W. and Bateman R. M. 2010. Systematics, Phylogenics and Reproductive Biology of Flemingites Arcuatus Sp. Nov., An Exceptionally Preserved and Partially Reconstructed Carboniferous Arborescent Lycopsid. International Journal of Plant Sciences, 171: 783-808.

Stockey, R.A. 1975. Seeds and embryos of *Araucaria mirabilis*. American Journal of Botany 62: 856-868

Sutton, M. D., Briggs, D. E. G., Siveter, David, J. and Siveter, Derek, J. 2001. Methodologies for the Visualization and Reconstruction of Three-Dimensional Fossils from the Silurian Herefordshire Laresatten. Palaeontologia Electronica. 4, Issue 2

Sutton, M. D., Briggs, D. E. G., Siveter, David, J. and Siveter, Derek, J. 2004a**.** Computer Reconstruction and Analysis of the Vermiform Mollusc *Acaenoplax Hayae* from the Herefordshire Lagerstätte (Silurian, England), and Implications for Molluscan Phylogeny. Palaeontology, 47. 293–318.

Sutton, M. D., Briggs, D. E. G., Sieveter, David J. and Sieveter, Derek J. 2004b. SPIERS A Software Package for the Analysis and Visualisation of Serial Image Data. Unplublished (SPIERS edit manual).

Sutton, M. D., Briggs, D. E. G., Siveter, David, J. and Siveter, Derek, J. 2005. Silurian Brachiopods with Soft-Tissue Preservation. Nature, 436: 1013–1015.

Sutton, M. D., Briggs, D. E. G., Siveter, David, J. and Siveter, Derek, J. 2006. Fossilized Soft Tissues in a Silurian Platyceratid Gastropod. Proceedings of the Royal Society B. 273: 1039–1044.

Sutton, M. D. 2008. Tomographic Techniques for the Study of Exceptionally Preserved Fossils. Proceedings of the Royal Society B, 275: 1587-1593.

Taylor, T. N., Taylor, E. L,. Krings. M. 2009. Paleobotany, The Biology and Evolution of |fossil Plants, Second edition. Academic press. 1252 pp

Thomas, B. A. 1981. Structural Adaptations Shown by the Lepidocarpaceae. Review of Palaeobotany and Palynology, 32: 377–388.

Thomas, B. A., Bek, J. and Oplustil, S. 2009. A New Species of Lepidostrobus from the Early Westphalian of South Joggins, Nova Scotia, Canada. Bulletin of Geosciences, 84(4): 661–666.

Zhou, Z. Y. 2009. An overview of Fossil Ginkgoales. Paleoworld, 18: 1-22

Zhou, Z. Y. 2012. Tertiary Ginkgo Ovulate Organs with Associated Leaves from North Dakota, U.S.A., and their Evolutionary Significance

Zhou, Z. Y., Zhang, B. L. 1989. A Middle Jurassic *Ginkgo* with Ovule-Bearing Organs from Henan, China. Palaeontographica B 211: 113–133.

APPENDIX 1

Int. J. Plant Sci. 171(7):783–808. 2010.

1058-5893/2010/17107-0007$15.00 DOI: 10.1086/655028

SYSTEMATICS, PHYLOGENETICS, AND REPRODUCTIVE BIOLOGY OF *FLEMINGITES ARCUATUS* SP. NOV., AN EXCEPTIONALLY PRESERVED AND PARTIALLY RECONSTRUCTED CARBONIFEROUS ARBORESCENT LYCOPSID

Liadan G. Stevens,[1,]* Jason Hilton,* Andrew R. Rees,* Gar W. Rothwell,† and Richard M. Bateman*

*School of Geography, Earth, and Environmental Sciences, University of Birmingham, Edgbaston, Birmingham B15 2TT, United Kingdom; and †Department of Environmental and Plant Biology, Ohio University, Athens, Ohio 45701, U.S.A.

Exceptionally preserved lycopsid remains from an ex situ chert–carbonate cobble found on the Yorkshire coast, United Kingdom, are here reconstructed as *Flemingites arcuatus* sp. nov. Megasporophylls are C shaped and emerge from the cone axis at a relatively acute angle. Megasporangia are adaxial on sporophylls and typically contain four megaspore tetrads. Megaspores are described as *Lagenicula wellmanii* sp. nov.; they are 1.0–1.7 mm in diameter and have a pronounced gula and numerous vermiform spines with bulbous apices. Archegonia occur in some megaspore apices, and developing oocytes are also rarely preserved. Trilete microspores found in an isolated microsporangium conform to *Lycospora orbicula*. Leaves and sporophylls are helically arranged and have stomata organized in rows along abaxial grooves. Correlation of these organs allowed the resulting partial plant to be added to an existing cladistic matrix. Analyses confirmed the provisional assignment of *F. arcuatus* to the stem genus *Paralycopodites*. Stratigraphic comparisons of the megafossils and spores restrict the likely age of the cobble from the Early Mississippian to the Middle Pennsylvanian. The plants were deposited alongside univalve crustaceans in a swamp environment where preservation was probably enhanced by local volcanic activity. The as yet unlocated lagerstätte appears comparable in quality of preservation with the Lower Devonian Rhynie Chert.

Keywords: lycopsid, Carboniferous, *Flemingites*, *Lagenicula*, *Paralycopodites*, terrestrial lägerstatten.

Introduction

Arborescent lycopsids were important components of Paleozoic wetland plant communities, dominating many peat-forming ecosystems (DiMichele and Phillips 1994; Gastaldo et al. 2004). Several extinct species of arborescent lycopsid plants that have been fully reconstructed from permineralized fossil assemblages underpin our current understanding of the morphology, anatomy, reproductive biology, growth architecture, and evolutionary history of the group (DiMichele 1985; Bateman and DiMichele 1991; Bateman et al. 1992; DiMichele and Bateman 1992, 1996; Bateman 1994, 1996). Reconstructed conceptual whole plants (sensu Bateman and Hilton 2009) also permitted phylogenetic reconstruction of the group (Bateman 1992; Bateman et al. 1992), which in turn facilitated phylogenetic classification and delimitation of monophyletic genera (Bateman and DiMichele 1991; Bateman 1992; DiMichele and Bateman 1992, 1996). However, many more taxa are known from isolated organs, including stems, roots, rootlets, leaves, cones, megasporangiate, and microsporangiate reproductive units; these organs are commonly encountered in both permineralized and compression/impression assemblages, but each presents a much narrower range of phylogenetic/taxonomic information than the reconstructions (Bateman and Simpson 1998; Bateman and Hilton 2009).

Previous studies have suggested that morphological and anatomical characters of lycopsid cones are key to delimiting family groupings (Abbott 1963; Thomas and Brack-Hanes 1984), preferably in combination with details of stem anatomy (Bateman and Simpson 1998). Many well-preserved cones of *Lepidostrobus* Brongniart and *Flemingites* Carruthers have been described from the Carboniferous compression/impression record, particularly from Euramerica. Species have been distinguished using cone architecture and arrangement, histological features, spore types, and occasionally megagametophyte structure (Chaloner 1953; Felix 1954; Balbach 1966*b*; Brack 1970).

Flemingites was established by Carruthers (1865) to describe a lycopsid cone that was mistakenly thought to bear multiple sporangia on each sporophyll. Following revision by Brack-Hanes and Thomas (1983), the cone genus now represents a demonstrably bisporangiate subset of cones previously placed within *Lepidostrobus* s.l. Brack-Hanes and Thomas (1983) listed numerous de facto synapomorphies linking the two cone genera, noting that they are separated only by the gender of their spores and the kind of spore (especially megaspores) found within their sporangia. *Flemingites* encompasses bisporangiate cones that

[1] Author for correspondence; current address: Department of Palaeontology, Natural History Museum, Cromwell Road, London SW7 5BD, United Kingdom; e-mail: l.stevens@nhm.ac.uk.

Manuscript received April 2010; revised manuscript received May 2010.

contain highly ornamented megaspores of the *Lagenicula* or *Lagenosporites* type as well as microspores assignable to a subgroup of *Lycospora* that possess a narrow equatorial flange, smooth equatorial surface, and variously ornamented distal surface. By contrast, *Lepidostrobus* cones are exclusively microsporangiate; they were produced by the same plants that bore the megasporangiate cone genera *Achlamydocarpon takhtajanii* and *Lepidocarpon* and contained less extravagantly ornamented megaspores (Bateman et al. 1992; DiMichele and Bateman 1996; Zhou et al. 2006, 2008).

Flemingites cones have been reported from the late Mississippian to the middle Pennsylvanian of Euramerica, though their vegetative correlate, the arborescent lycopsid stem genus *Paralycopodites*, has also been reported from early Mississippian strata (Morey and Morey 1977; DiMichele 1980; Meyer-Berthaud 1984; Pearson 1986; Bateman et al. 1992). The anatomically preserved genera *Anabathra* and *Paralycopodites*—and their compression equivalent, *Ulodendron* Lindley & Hutton—may be synonymous; however, DiMichele and Bateman (1996) found insufficient evidence to confidently unite the three genera. Therefore, the vegetative organs described in this study are conservatively assigned to the best-understood genus, *Paralycopodites*.

Of the 13 species of *Flemingites* recognized by Brack-Hanes and Thomas (1983), most are Pennsylvanian in age and described from compression/impression material. Because the morphology of the cone species is remarkably similar, attempts have previously been made to distinguish among them using a single putatively optimal character suite, such as sporophyll shape (Abbott 1963), megaspore type (Chaloner 1953; Felix 1954), or microspore type (Balbach 1966*a*; Courvoisier and Phillips 1975). Cladistic analysis employing the conceptual reconstructions as a framework offers the prospect of better classifying the cone species and inferring their evolutionary relationships (Bateman et al. 1992, 2007; Bateman 1994, 1996; Bateman and Simpson 1998).

This article describes and interprets lycopsid organs preserved in a recently abraded beach cobble found in Yorkshire, England. Its external surfaces displayed well-preserved stems, leaves, and cones that collectively were readily identified as an arborescent lycopsid (fig. 1). Laboratory preparation of the cobble revealed, preserved in exquisite anatomical detail, vegetative axes with attached leaves, a microsporangium containing *Lycospora*-type microspores, and, most notably, several cone fragments bearing megasporangia that contain lageniculate megaspores, often preserving cellular megagametophytes. These specimens are described using light and scanning electron microscopy, and the organization of the cone is elucidated via three-dimensional reconstruction. The article includes the description and naming of new species of the cone genus *Flemingites* and the megaspore genus *Lagenicula*. The individual plant parts are described, presented as a partial reconstruction of a new species of arborescent lycopsid, and placed successfully within the cladistic framework erected by Bateman et al. (1992). We conclude by speculating on the origin and potential significance of this enigmatic water-worn block.

Material and Methods

All specimens described in this article occurred in one ex situ beach-worn cobble (~10 × 6 cm) found on Sandsend beach on the Yorkshire Jurassic coast by amateur fossil collector D. Morgan in 2004. The cobble surface initially revealed sections through lycopsid cones, stems, and leaves, each organ evidently preserved in anatomical detail (fig. 1). Morgan then broke the cobble into 11 pieces, revealing numerous additional organs. He later deposited the material in the National Museums of Scotland (NMS G 2004.75).

Wafer sections 0.5–2 mm thick were cut on Buehler low-speed Isomet and Isomet 5000 saws with a wafering blade 10 cm in diameter and 0.3 mm thick. The sections were then polished and mounted on glass slides using Eukitt adhesive. Photographs were taken using a Canon EOS digital SLR camera alternately mounted on a Zeiss Discovery V8 stereo microscope and a Zeiss Axioscop 40 transmitted light microscope. Thin sections for chert examination were photographed using a Zeiss Axioplan 2 transmitted light microscope. Light and contrast levels were optimized using Adobe Photoshop 5.0. Pieces of the cobble were lettered A–K, and slides were numbered by NMS accession number, then original block, and finally sequence.

Samples of megaspores and microspores were extracted for scanning electron microscopy using a standard hydrofluoric acid technique (Batten 1999). Megaspores were mounted on SEM stubs, gold coated, and SEM imaged at Sheffield University, where ion microprobe analyses were also performed on the matrix of the cobble. Microspores were examined using light microscopy only.

An especially well-preserved megasporangiate section of one cone was digitally reconstructed using photographs of eight thin sections of known thickness and sequence intervals, using the software package SPIERS (Serial Palaeontological Image Editing and Rendering System; Sutton 2008). Both upper and lower surfaces of individual wafers were used for the reconstruction, together presenting 16 tomographic planes from which the organization of the cone was reconstructed.

A phylogenetic analysis was run using all available characters from the chert sections, the cone reconstruction, and associated vegetative shoots. The analysis closely followed that performed by Bateman et al. (1992), primarily using PAUP 4.0 (Swofford 2001). All most parsimonious trees were reliably found using branch and bound with amb invoked, and the result was confirmed by analyzing the same matrix in Winclada (ver. 0.9.9; Nixon 1999). Bootstrap values were obtained through 1000 heuristic replicates, and decay index values were calculated manually via sequential sets of strict consensus trees.

Results

Mode of Preservation

Ion microprobe analysis conducted during scanning electron microscopy of the plants determined that the cobble contained roughly equal amounts of silica and carbonate. Examination of thin sections under polarized light revealed that

most plant cell lumina and megaspore cavities exhibit several phases of first carbonate and then silica infilling; the carbonate occurs as micrite to microspar and the silica as both microquartz (chalcedony) and megaquartz in bands of contrasting thickness.

Surficial Features

Figure 1 shows features of the cones evident in the external surfaces of the chert block before sectioning. An oblique section of a megasporangiate cone has been revealed through natural polishing of the chert (fig. 1*A*), and a three-dimensional relief of the inside of the cone that was exposed when the cobble was deliberately fractured features internal casts of megaspores protruding from the sporangia (fig. 1*B*, 1*C*). Figure 1*D* shows an isolated and possibly dehiscent sporangium-sporophyll complex located close to the megasporangiate cone segment. Vegetative stems (fig. 1*F*, 1*G*) and isolated microphylls are exposed in longitudinal and transverse sections (fig. 1*E*) and even offer adaxial surface views (fig. 1*H*), illustrating the wide ranges of organ fragment size and orientation evident throughout the cobble.

Vegetative Shoots

The numerous vegetative shoots range from 1.2 to 6.5 mm in diameter; larger axes incorporate an exarch medulated protostele up to 0.8 mm in diameter (fig. 2*A*), whereas smaller axes possess a solid protostele (fig. 2*B*). Several subtle protoxylem strands are present around the periphery of the stele (fig. 2*B*) but are not prominent because they are quite small and expand the periphery of the xylem only slightly beyond the metaxylem. Microphyll traces diverge from the central axis in a steep spiral and can be traced through the cortex; they transgress a lacuna approximately twice the diameter of the stele before passing through the middle and outer cortex. Cells of the middle cortex are oblong and thin walled, whereas the thicker outer cortex consists of smaller, more densely packed cells (fig. 2*B*).

Leaves

Microphylls are up to 12 mm long, 4–6 mm wide, and lanceolate, with their swollen bases tapering gradually toward the apex (fig. 2*C*). They are almost terete at the point of attachment, but within 0.5 mm they have become dorsiventrally flattened into elations (fig. 2*B*). Dorsal and ventral ridges are prominent at the base but absent toward the apex. Microphylls emerge from the stem at an angle of 60°–70° relative to the apex but reflex until almost perpendicular (fig. 2*C*); the majority then curve back toward the stem apex. A single central vascular trace passes through the microphylls as a bundle of 15–20 helically thickened tracheids surrounded by parenchymatous cells and a further ring of slightly larger tracheids. Two zones of parichnos are located laterally to the vascular trace in the rhomboidal base of the microphyll (fig. 2*D*), and the ligule pit occurs on the adaxial surface of the leaf base within 0.2 mm of the point of emergence of the microphyll from the stem (fig. 2*D*). Where preserved (most commonly near the dorsal groove and toward the apex), the mesophyll consists of large (20–30 μm diameter), thin-walled parenchyma cells (fig. 2*D*). Some microphyll bases clearly show undulating zones on the abaxial surface (fig. 2*E*).

The thin-walled hypodermal cells of the microphylls are 10–45 μm long, elongated parallel to the long axis of the leaf, and arranged in a single layer. Rounded and slightly thicker-walled cells, 15–20 μm in diameter, evenly punctuate the rows of more elongate oblong cells (fig. 2*F*). Two abaxial furrows lateral to the ventral ridge contain rows of stomata (fig. 2*G*), which are orientated parallel to the long axis of the leaf and are not recessed into the epidermis. They are surrounded by six to eight irregularly shaped epidermal cells that are often shared by adjacent stoma (fig. 2*F*, 2*G*). The reniform guard cells are 30–35 μm long and produce darkened (possibly lignified) ledges surrounding the aperture.

Megasporangiate Cone Segments

Megasporangiate segments of two cones were sectioned. The first was 19 mm wide × 25 mm long and was sectioned near transversely. The second was ~20 mm wide (extrapolated from partial fragment) × 18 mm long and was sectioned longitudinally.

The cone axes resemble the smallest vegetative branches, measuring up to 3 mm in diameter and containing a solid protostele of metaxylem surrounded by smaller protoxylem cells and cortex (fig. 3*A*). Except for sporophyll traces, tissue is absent between both the stele and inner cortex and the inner and outer cortex. Radiating megasporophyll traces (~6 per 360° section) extend between the stele, inner cortex, and outer cortex. The outer cortex is two zoned; cells of the inner region are more densely packed and have slightly thinner walls than those of the outer zone (fig. 3*A*).

Megasporophylls diverge from the cone axis in a low-angle helix and are tightly packed, almost completely enclosing the megasporangia (figs. 1*A*, 1*B*, 3*B*). They form an elongated C shape rather than the near-horizontal pedicel and near-vertical distal lamina that characterize most arborescent lycopsid cones. After leaving the main axis, they project almost immediately outward at an angle of 40°–50°, curving slightly inward toward the apex. The pedicel is distinguished from the distal lamina by the "keel" (a characteristic feature of most lycopsid sporophylls), which continues throughout the megasporangium attachment zone (seen from successive slides in transverse section). The megasporophylls are 10–13 mm long and up to 6 mm in width. Megasporangia are positioned adaxially and remain attached to the megasporophylls for 3.5–4 mm when traced from the proximal end (fig. 3*C*).

Anatomically, the sporophylls broadly resemble the vegetative leaves. The epidermis consists of rounded, horizontally flattened cells, regularly punctuated with smaller round cells that have slightly thicker walls with the same dimensions as those of the vegetative hypodermal cells (fig. 2*F*). Two abaxial grooves on either side of the pedicel keel accommodate several rows of stomata. The single centrally located vascular bundle (fig. 3*C*) is surrounded by a ring of transfusion tracheids with helical thickening. Neither parichnos nor ligules were detected.

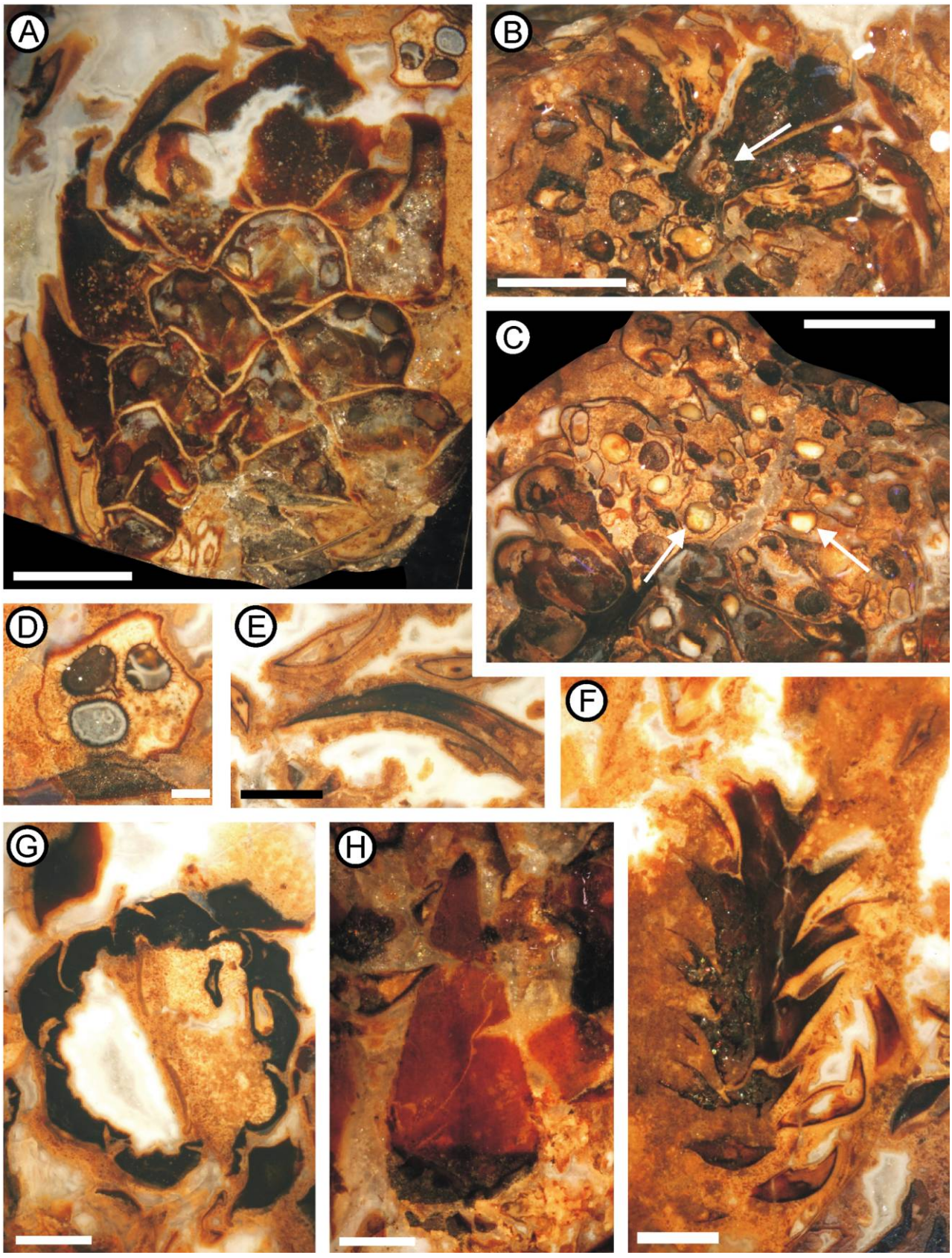
A
B
C
D
E
F
G
H

The megasporangia are 7–8 mm long × 5.5 mm in maximum diameter and elliptical in shape, tapering more gradually distally (seen from successive slides in transverse section). A subarchesporial pad is present throughout the sporangial attachment to the sporophyll and almost fills the sporangium, pressing the megaspores against its adaxial wall (fig. 3*C*, 3*D*). Two lateral grooves of the dehiscence zones along the base of the megasporangia are formed by thinning of the megasporangial wall (fig. 3*E*, arrow). The sporangial epidermis is 30 μm thick and consists of a single layer of large, radially elongate cells that are 15–20 μm × 10–15 μm and have cell walls up to 0.5 μm thick (fig. 3*F*).

Megaspores

The megaspores, typically 16 per sporangium, are roughly spherical when uncompressed (figs. 4*A*–4*C*, 5*A*). They are hologulate, with the gula being formed by the convergence of three rounded laesurae that reach 500–1000 μm in height and 300–400 μm in basal width (fig. 5*B*–5*D*), and are assignable to the megaspore genus *Lagenicula* (Bennie and Kidston 1886) Potonié and Kremp (1954) emend. Spinner (1969). The main body of the megaspore is 1300–1700 μm in diameter and covered by perpendicular spines that decrease in density from the arcuate ridge to the distal pole (figs. 4*A*–4*C*, 5*A*, 5*B*); spines are 200–300 μm long, and most are straight (fig. 5*E*). Radiating ridges increase the diameter of the hollow spine bases to 40–50 μm; the spines taper distally but terminate in a bulbous apex up to 10 μm in diameter (figs. 4*D*, 5*E*). The spine has a smooth surface that is sparsely punctuated with pores toward the base (fig. 5*F*).

The proximal pole and gula of the megaspores have baculate surface ornamentation (fig. 5*B*). Small processes up to 120 μm long are densely packed at the base of the gula but become sparse toward the apex. The inner surface of the gula is unornamented but has a rough honeycomb structure (figs. 5*D*, 6*A*).

The inner and outer surfaces of the main body of the megaspore are laevigate to minutely rugose (fig. 6*B*). The megaspore wall lacks a basal lamina, and the exine is divided into two zones. The inner zone is 7–10 μm thick and densely packed, whereas the outer zone is 15–20 μm thick and has a loose honeycomb structure, the pores rarely extending to the spore surface (fig. 6*C*, 6*D*).

Megagametophytes

Megaspores with developing archegonia and occasionally oocytic and embryonic/megagametophytic tissue were observed within several of the megaspores found in both of the megasporangiate cones sectioned. Figure 7*A* and 7*B* shows seven archegonia in several developmental stages on the proximal surface of the megaspore, surrounded by the gula. Each archegonium consists of four columns of cells that circumscribe the entrance of the archegonium and are subtended by a venter, or ventral cell. Longitudinal section shows that the archegonia consist of two layers of neck cells above the ventral cell (fig. 7*C*–7*E*). The neck cells are thin walled and up to 15 μm in diameter. The surface of the ventral cells show the remains of further cell walls, which may be surrounding tissue that has degraded during the preservation process. The structure below the archegonium in the main body of the megaspore shown in figure 7*F* may be an egg, formed as part of the developing megagametophyte. The remains of megagametophytic tissue are evident within the central body of several megaspores (fig. 4*B*). The cells are thin walled and angular, and megagametophytes are located at the proximal edges of the spores and around the interior.

Cone Reconstruction

The megasporangiate region of a *Flemingites arcuatus* cone is reconstructed diagrammatically in longitudinal section using traditional methods in figure 8. In this diagram, the positions of the megaspores are shown within individual sporangia above the subarchesporial pad. The best-preserved cone was also three-dimensionally reconstructed using SPIERS software (fig. 9). The stepped exterior margin of the specimen is the result of the relatively coarse wafer thickness and spacing. Because of the anatomy of the cone and the material available for sectioning, reconstructions of this type were necessary to trace the size and shape of the sporophyll-sporangium units, the number of megaspores in each sporangium, and the positioning of the dehiscence zone. The color-coded reconstruction (fig. 9) clearly shows the helical insertion of the sporophyll-sporangium units, the acute angle at which they leave the cone axis, and the lack of a distinct horizontal pedicel region.

Microsporangium

A single microsporangium was found in close association with a leafy branch (fig. 10*A*) that was initially assumed to be a microsporangiate fragment of an *F. arcuatus* cone. However, the supposed sporophylls contrast in shape with the megasporophylls attached to the megasporangiate cone axes and are identical to the microphylls attached to vegetative axes described above. Also, a fragment of epidermal tissue appears to have been displaced by the microsporangium

Fig. 1 Morphology of *Flemingites arcuatus* sp. nov. revealed in the external surfaces of the cobble. *A*, Oblique longitudinal section of megasporangiate cone showing spirally arranged megasporophylls subtending megasporangia enclosing megaspores. Scale bar = 5 mm (NMS G 2004.75C/K). *B*, Transverse view of megasporangiate cone base showing sporophylls arranged centrally around the cone axis (arrow). Scale bar = 5 mm (NMS G 2004.75C/K). *C*, Unpolished cone surface with megaspore casts (arrows) protruding from the sporangia. Scale bar = 5 mm (NMS G 2004.75C/K). *D*, Dissociated sporangium and sporophyll containing three megaspores. Scale bar = 1 mm (NMS G 2004.75C/K). *E*, Longitudinal section of microphyll with vascular trace visible along the central axis. Scale bar = 2.5 mm (NMS G 2004.75F). *F*, Longitudinal section of vegetative stem; microphylls are seen in longitudinal and transverse views, but the distal tips are missing. Scale bar = 2.5 mm (NMS G 2004.75J). *G*, Large decorticated stem with emergent microphylls. Scale bar = 2.5 mm (NMS G 2004.75J). *H*, Adaxial surface and cushion of a dissociated sporophyll. Scale bar = 2.5 mm (NMS G 2004.75J).

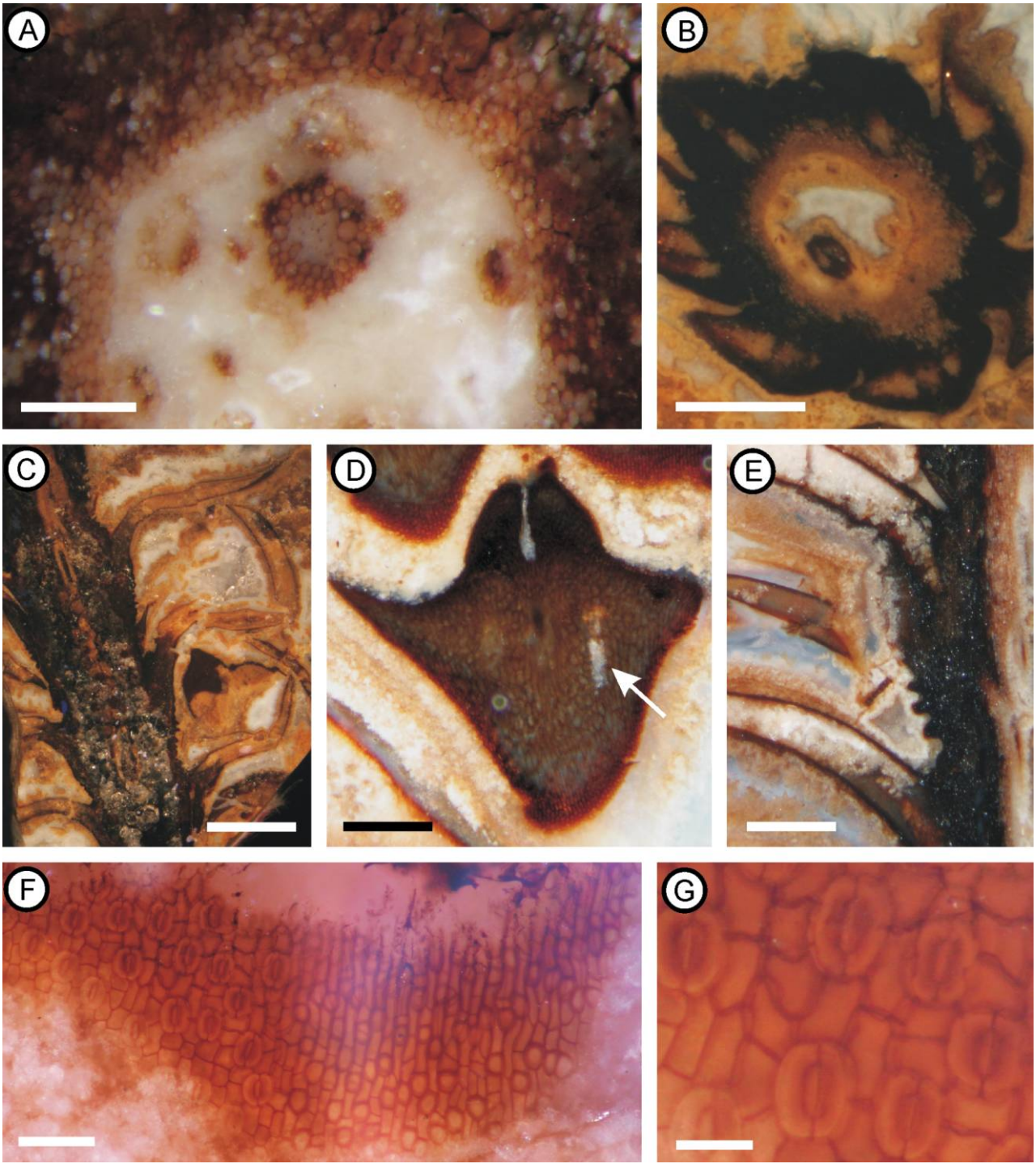

Fig. 2 Internal anatomy of vegetative structures of *Flemingites arcuatus* sp. nov. *A*, Transverse section of vegetative axis showing exarch siphonostele and microphyll traces radiating outward toward the cortex. Scale bar = 500 μm (NMS G 2004.75C). *B*, Transverse section of a smaller vegetative stem with a protostele, thick outer cortex, and microphyll bases. Scale bar = 1 mm (NMS G 2004.75C). *C*, Longitudinal section of a vegetative stem showing microphylls emerging at an acute angle before reflexing to an almost horizontal position. Scale bar = 2 mm (NMS G 2004.75E). *D*, Transverse section of microphyll with central vascular bundle, adaxial groove, and parichnos (arrow). Scale bar = 500 μm (NMS G 2004.75F1.7). *E*, Longitudinal section of a vegetative stem showing undulating cortex on the abaxial surfaces of the microphyll bases. Scale bar = 500 μm (NMS G 2004.75J2.1). *F*, Hypodermal cells and stomata on abaxial surface of microphyll. Scale bar = 100 μm (NMS G 2004.75J2.4). *G*, Enlargement of stomata from *F* showing guard cells and angular cells of surrounding hypodermis. Scale bar = 30 μm.

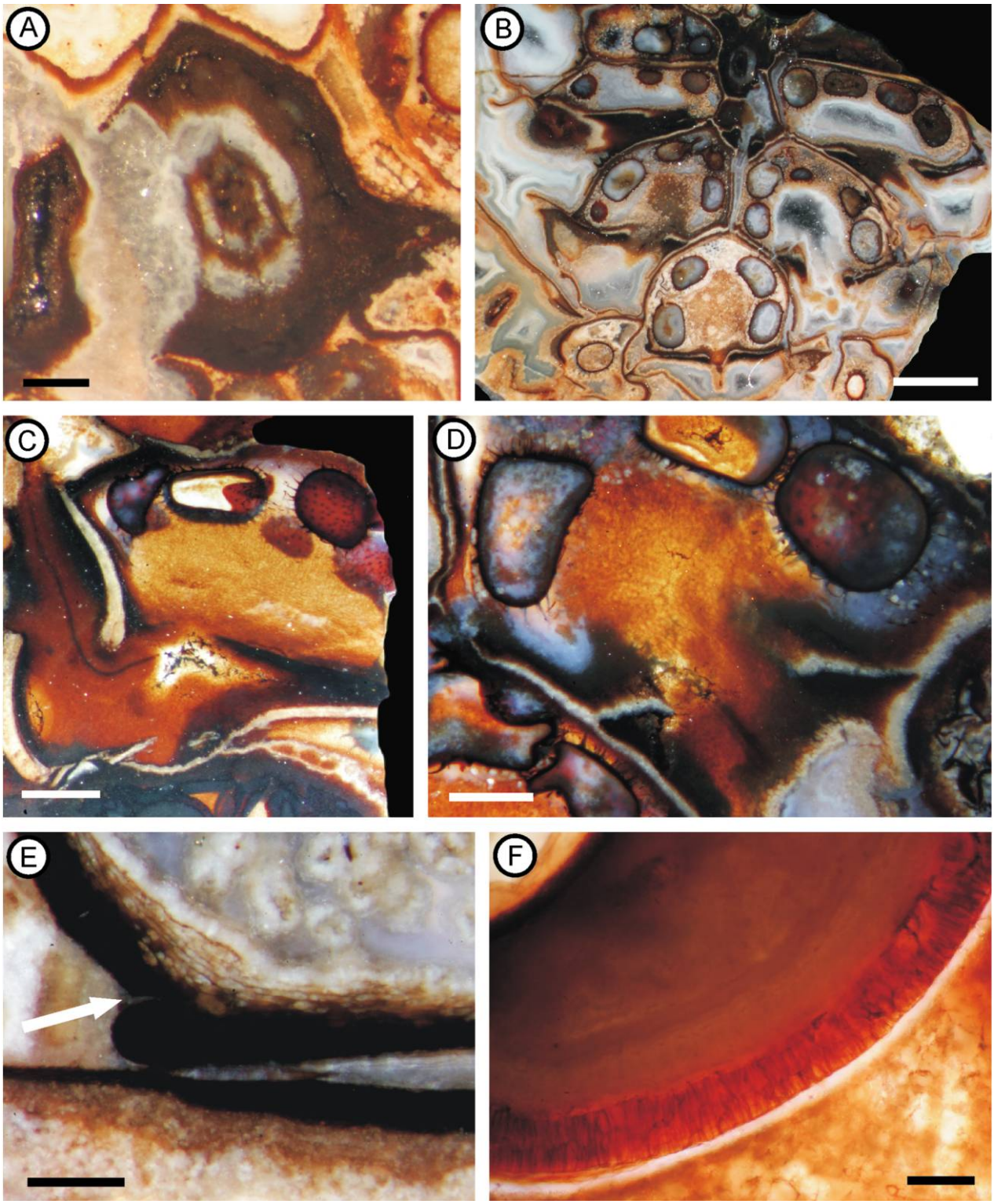

Fig. 3 Anatomy of the megasporangiate cones of *Flemingites arcuatus* sp. nov. *A*, Transverse section of a cone axis showing exarch protoxylem stele surrounded by cortex. Scale bar = 250 μm (NMS G 2004.75CK1.7). *B*, Oblique-transverse section of the cone showing megasporangia radiating from the cone axis. Scale bar = 3 mm (NMS G 2004.751.10). *C*, Oblique longitudinal section of a sporophyll-sporangium complex showing vascular trace and subarchesporial pad. Scale bar = 1 mm (NMS G 2004.75CK2.2). *D*, Transverse section of sporangium complex showing attachment to sporophyll and megaspores at the upper surface. Scale bar = 500 μm (CK2.5). *E*, Lateral groove of dehiscence zone of megasporangium (arrow). Scale bar = 200 μm (NMS G 2004.75CK1.14). *F*, Transverse section of the uniseriate megasporangium wall showing thin-walled, elongated cells. Scale bar = 30 μm (NMS G 2004.75CK1.8).

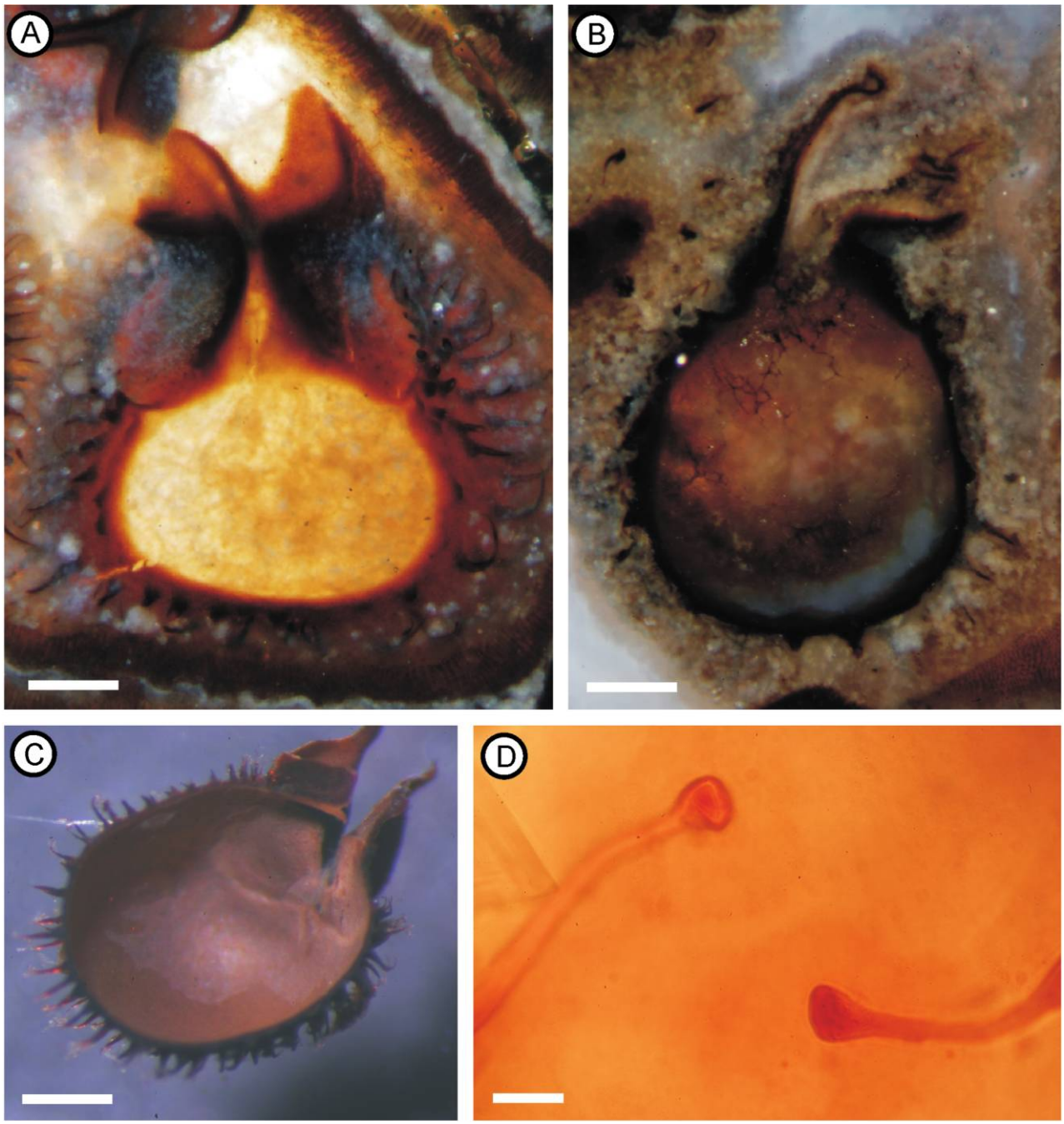

Fig. 4 Morphology of *Lagenicula wellmanii* sp. nov. *A*, *B*, Longitudinal sections of embedded megaspores showing the circular body covered in spines and triradiate gula, with possible megagametophytic tissue evident around the megaspore periphery in *B*. Scale bar = 500 μm (NMS G 2004.75CK1.9, 5). *C*, Isolated megaspore in longitudinal section showing smooth internal surface. Scale bar = 500 μm (NMS G 2004.75 isolated megaspore 1). *D*, Bulbous tip of spine from proximal face of megaspore. Scale bar = 10 μm (NMS G 2004.75CK1.9).

(fig. 10*B*), which was probably pressed into the leafy shoot during preservation. The isolated microsporangium is very similar in structure and dimensions to the megasporangium; oval in shape, 4.7 mm in length × 1.8 mm in maximum diameter (fig. 10*B*), and bounded by a single layer of elongate wall cells (fig. 10*C*). The cells measure 20–25 μm × 15–18 μm, and the cell walls are up to 0.5 μm thick. A subarchesporial pad fills approximately half of the volume, the remainder containing numerous microspores (fig. 10*D*).

Microspores

Microspores are 25–30 μm in diameter and arranged in tetrads around the microsporangium wall (fig. 11*A*, 11*B*). The distal ornamentation of the exine is granulate to mi-

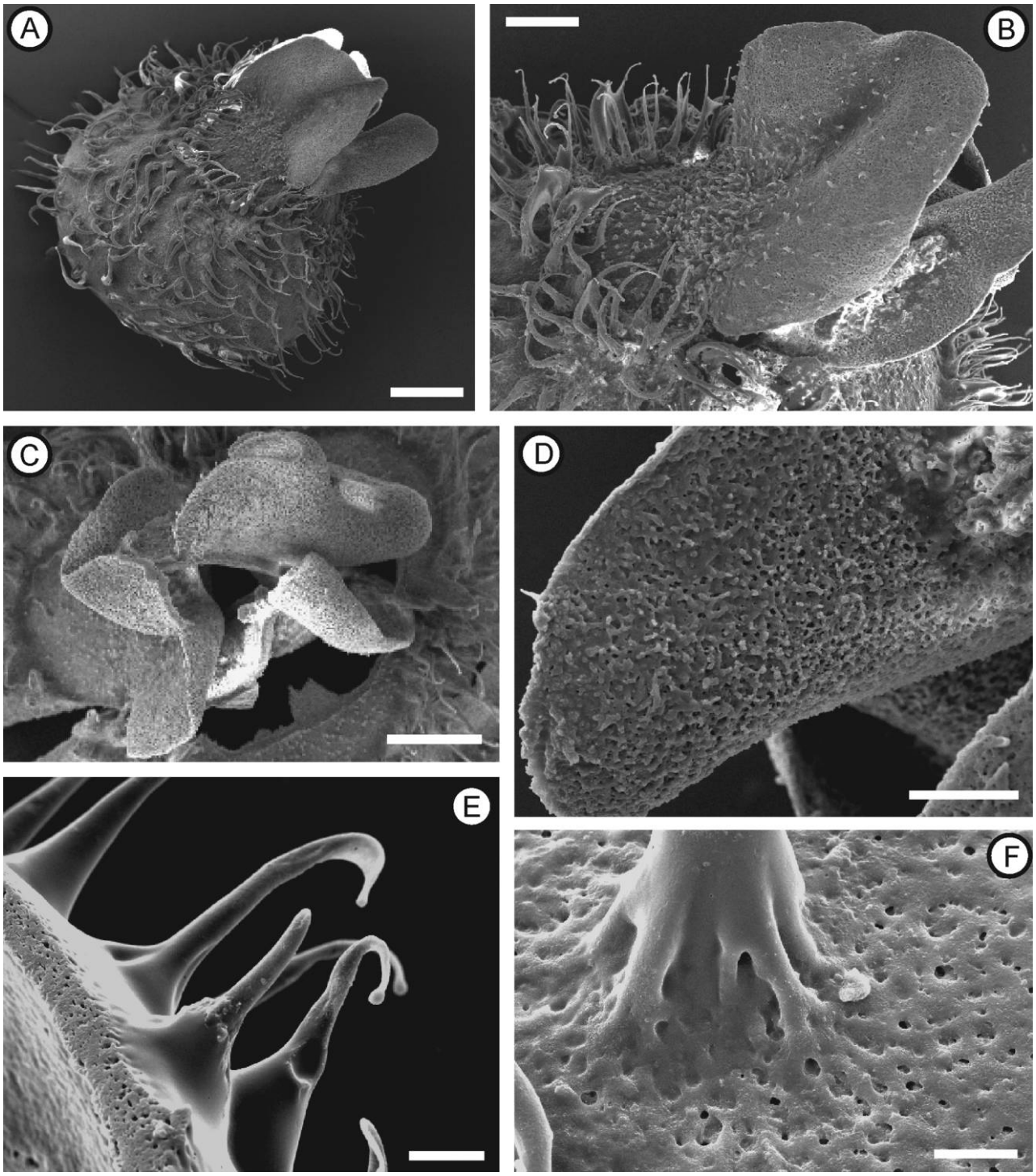

Fig. 5 SEM images of *Lagenicula wellmanii* sp. nov. megaspores. *A*, Complete megaspore showing surface spines and gula. Scale bar = 500 μm (NMS G 2004.75Meg1.02). *B*, Gula and contact face with bacculate ornamentation. Scale bar = 200 μm (NMS G 2004.75Meg1.02). *C*, Proximal view of gula with trilete lobes. Scale bar = 250 μm (NMS G 2004.75Meg1.00). *D*, Detail of gula inner surface. Scale bar = 15 μm (NMS G 2004.75Meg1.01). *E*, Spines on proximal face displaying bulbous apices (NMS G 2004.75Meg1.03). Scale bar = 50 μm. *F*, Splayed ridges and apertures of spine base. Scale bar = 25 μm (NMS G 2004.75Meg1.00).

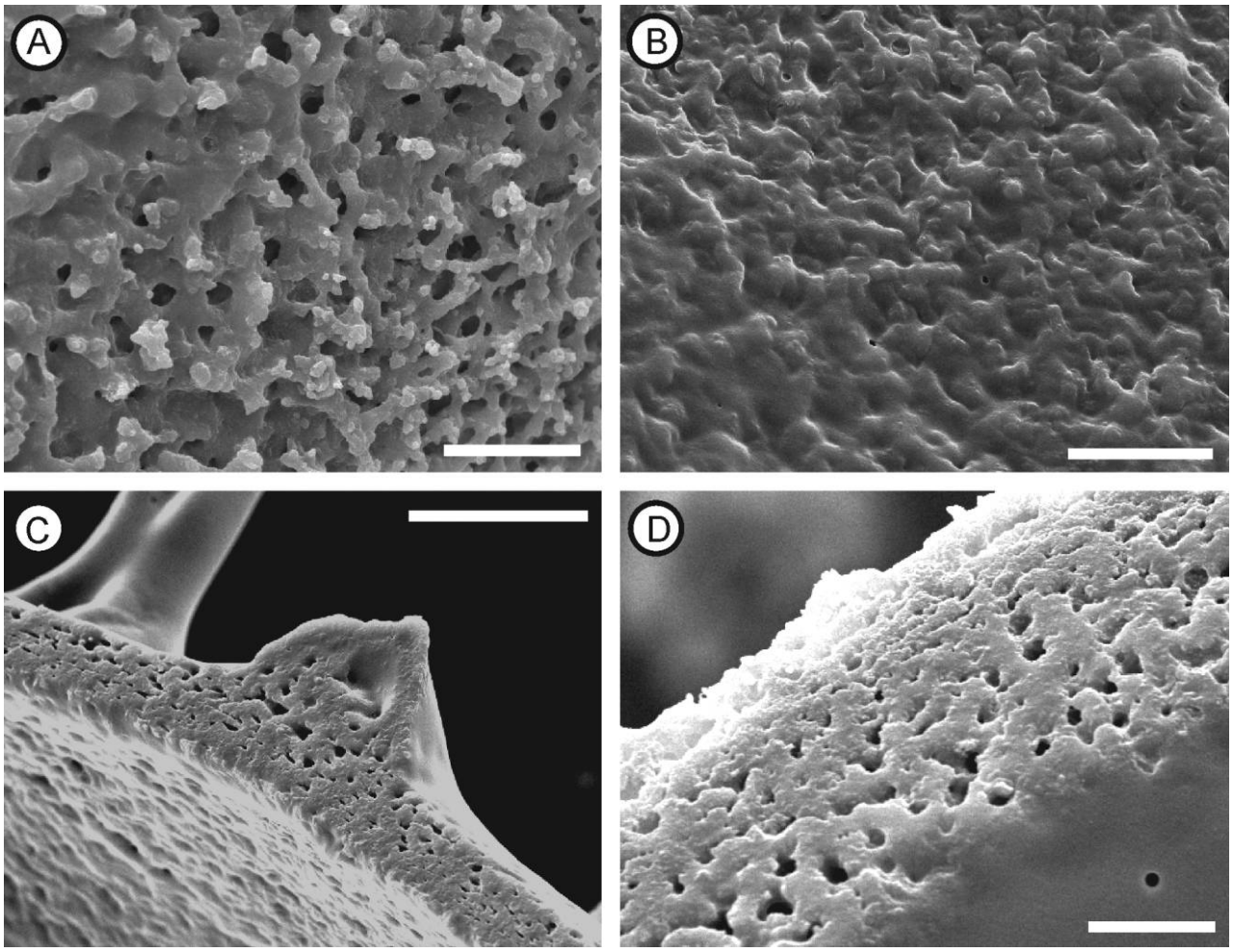

Fig. 6 Surface and exine features of *Lagenicula wellmanii* sp. nov. megaspores. *A*, Honeycomb texture of gula inner surface. Scale bar = 100 μm. *B*, Inner surface of megaspore. Scale bar = 20 μm. *C*, Transverse section of megaspore wall showing exine divided into two zones. Scale bar = 50 μm. *D*, Enlargement of megaspore wall. Scale bar = 15 μm. (All NMS G 2004.75Meg1.03.)

nutely echinate, though the proximal contact face is almost smooth. The laesurae extend almost to the equator (fig. 11C), and the cingulum is very narrow (~1 μm). The spores are elliptical in equatorial view (fig. 11*D*), and the cingulum appears as dark swellings, where it is slightly enlarged at the lateral contact surfaces. The microspores correspond to the dispersed spore species *Lycospora orbicula* (Potonié & Kremp) A.H.V. Smith and Butterworth (1967; formerly *Cyclogranisporites orbiculus* Potonié & Kremp).

Immature Cone

Figure 12*A* shows the apex of a cone that was found in close association with, but not in organic attachment to, the previously described lycopsid fragments. The cone is one-quarter the size of the co-occurring partial cones, 5 mm wide in diameter × 12 mm long. The sporophylls are 5 mm long × 2.5 mm in maximum width. The uppermost sporophylls have distinct pedicel and laminar regions and enclose upright sporangia 2 mm long × 1.5 mm wide (fig. 12*B*). Despite their smaller size, these sporophylls exhibit anatomical features very similar to those of the megasporangiate cone fragments. No spores are evident in the sporangia; most appear to lack contents, whereas the apical-most pair contains an amorphous mass of dark material (fig. 12*B*).

Systematic Paleobotany

Genus—Flemingites *(Carruthers) Brack-Hanes & B.A. Thomas*

Species—Flemingites arcuatus *L.G. Stevens & J. Hilton, sp. nov.*

Genus diagnosis. Sporophylls in spirals on the cone axis. Axis with exarch vascular bundle surrounded by cortical zones. Sporangium with narrow attachment along its length to adaxial surface of sporophyll pedicel. Ligule on adaxial surface of pedicel distal to sporangium. Lateral laminae extending beneath sporangium. Abaxial keel along length of pedicel. Pedicel extended distally to upturned lamina and

downturned heel. Cones bisporangiate with apical microsporangia and basal megasporangia. Megaspores either *Lagenicula* or *Lagenosporites* type. Microspores of *Lycospora* type with narrow equatorial flange and usually smooth proximal surface; distal surface variable in ornament.

Species diagnosis. Bisporangiate cone with C-shaped megasporophylls emerging at 40°–50° from cone axis, recurved toward its apex. Vascular bundle centrally positioned. Megasporophyll epidermis composed of elongate cells regularly punctuated with rounded cells approximately half their size. Simple stomata in rows along two abaxial furrows. Megasporangia containing ~16 megaspores and large subarchesporial pad. Megaspores assignable to *Lagenicula wellmanii* L.G. Stevens and J. Hilton sp. nov.; microspores assignable to *Lycospora orbicula* (Potonié & Kremp) A.H.V. Smith & Butterworth.

Holotype. NMS G 2004.75. C/K1.03, in figure 3*B*.

Paratypes. NMS G 2004.75. C/K1.0–1.02, 1.04–1.18, and E 1.0–1.05, in figures 1*A*–1*C*, 3*A*, and 3*C*–3*F*.

Derivation of name. The Latin *arcuatus* translates as the curve of a bow, describing the characteristic appearance of the sporophylls when viewed laterally.

Genus—Lagenicula *(Bennie & Kidston 1886) Potonié & Kremp, 1956 emend. Spinner (1969)*

Species—Lagenicula wellmanii *L.G. Stevens & R.M. Bateman, sp. nov.*

Genus diagnosis. Trilete megaspores with an apical prominence formed by the progressive expansion of the laesurae along most of their length, from the junction with the curvature of the proximal pole and the thickening of the exine of the greater part of the contact areas.

Species diagnosis. Hologulate spherical megaspore with gula one-third to one-half the diameter of the main spore body. Spines on proximal face taper from wide-ridged base to bulbous, trumpet-shaped apex. Contact face and outer surface of gula bear baculate ornamentation, dense at gula base, becoming sparse toward apex. Two-zoned exine showing honeycomb texture; inner zone more dense than outer zone, and pores rarely extending to outer surface. Inner and outer surfaces of megaspore laevigate to minutely rugose.

Holotype. NMS G 2004.75; meg-1.02 in figure 5*A*.

Derivation of name. The specific epithet *wellmanii* honors Charles Wellman (Sheffield University), who generously gave his time and expertise in the preparation and identification of the in situ megaspores and microspores of *Flemingites arcuatus*.

Locality. Sandsend beach, Whitby, North Yorkshire, United Kingdom; loose block subjected to long-distance transport.

Repository. Department of Natural Sciences, National Museums of Scotland, Chambers Street, Edinburgh, United Kingdom.

Discussion

Ontogenetic Status of Flemingites arcuatus

Before comparing *Flemingites arcuatus* with other members of the cone genus, it is important to establish that most of the current cones came at least close to attaining maturity before fossilization. Maturity is indicated by the stage of development attained by the in situ megaspores; the tetrads have separated into individual spores, and deposition of the spore walls and associated ornamentation appears complete (fig. 3*B*–3*D*). Moreover, megagametophytes with archegonia have formed within many of the megaspores (fig. 7). Yet we believe that we have identified an immature cone fragment in the Sandsend cobble; it is one-quarter the dimensions of all other co-occurring cone fragments but anatomically similar (fig. 12*A*). This suggests that ontogenetic expansion of the cone was approximately isometric. Also, the amorphous mass of dark material observed in the apical-most pair of sporangia (fig. 12*B*) presumably represents the precursors of spores and subarchesporial pad cells that had not yet formed at the time of preservation.

Comparison of the Cones with Other Species of Flemingites

The close morphological similarity evident among *Flemingites* cone species (summarized in table 1) means that credible delimitation and subsequent identification require a combination of characters. Nonetheless, several authors have attempted to pinpoint the most useful features for identification. For example, Abbott (1963) advocated sporophyll shape, and both Chaloner (1953) and Felix (1954) argued that megaspore type was most informative, whereas Balbach (1966*a*) and Courvoisier and Phillips (1975) reasoned that microspore type not only usefully delineated cone species but also provided valuable information on distribution and temporal range from the dispersed spore record. This logic is particularly apt for *F. arcuatus*, given the additional need to infer the age of the loose cobble that contains the type material.

The current cones are easily distinguished from *Flemingites noei* (Mathews) Brack-Hanes & B.A. Thomas, which is much larger in all its parts and produces far larger numbers of megaspores. This distinction also probably applies to the less well-known *Flemingites brownii* (Unger) Brack-Hanes & B.A. Thomas. At the other end of the spectrum, *Flemingites olryi* (Zeiller) Brack-Hanes & B.A. Thomas and the less well-known *Flemingites scottii* (Jongmans) Brack-Hanes & B.A. Thomas are much smaller than our specimens, though the possibility that they are immature cannot be wholly excluded. The seven remaining cone species listed in table 1 cannot be separated with confidence from *F. arcuatus* using cone and sporophyll dimensions. Distinctions between microspore species of *Lycospora* are notoriously problematic. Taking table 1 at face value, the inferred presence of *Lycospora orbicula* in the cones of *F. arcuatus* distinguishes it from all cone species but the aforementioned *F. olryi* and *F. russelianus*, though Bateman et al. (1992, their table 2) also ascribed to *L. orbicula* the microspores of *Flemingites diversus* and *Flemingites schopfii*. Several species of *Flemingites* bore *Lagenicula rugosa* megaspores, which are similar to but nonetheless distinct from the *Lagenicula wellmanii* megaspores borne only by *F. arcuatus*.

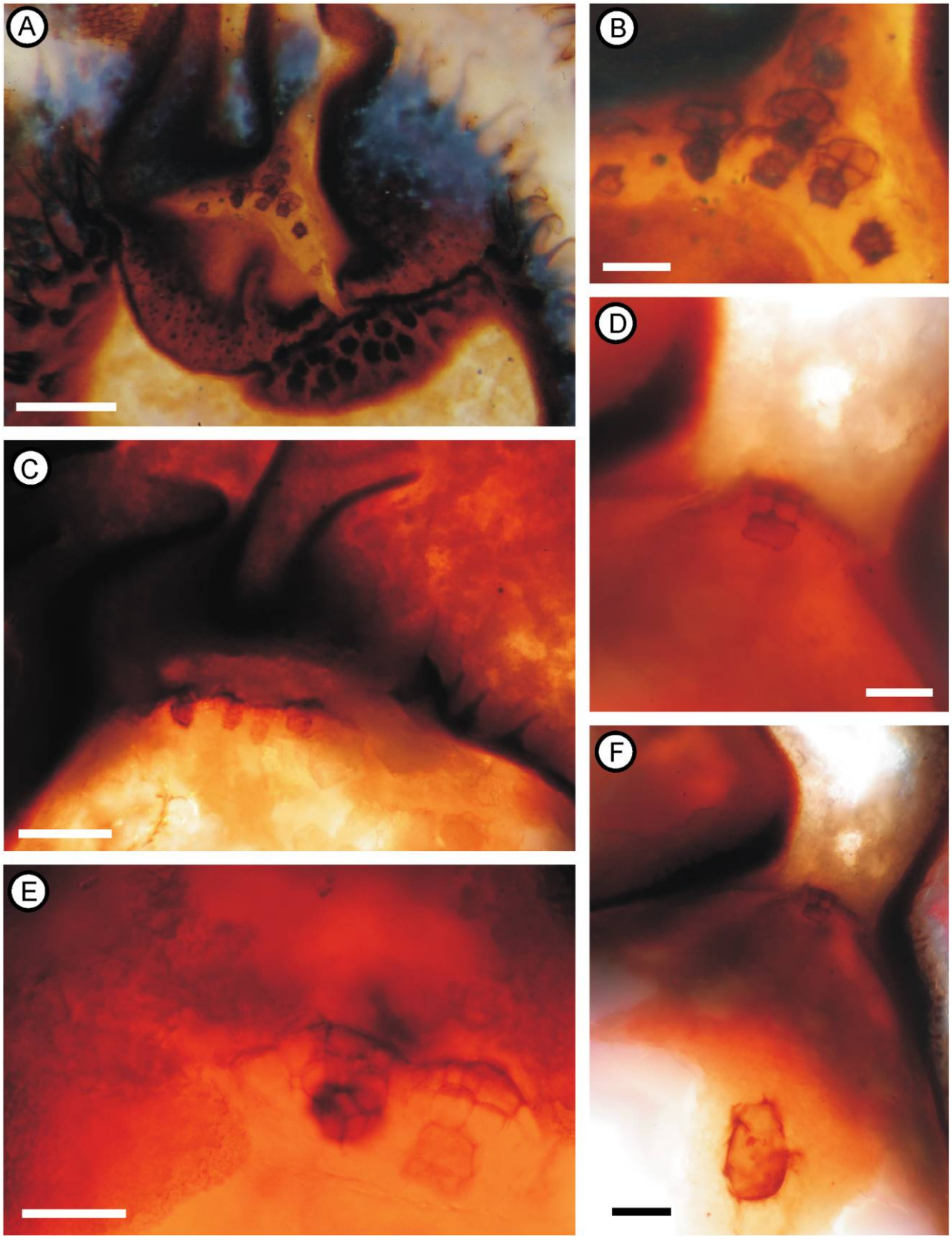
A
B
C
D
E
F

The remaining distinguishing features of *F. arcuatus* are too subtle to appear in table 1. First, the sporophylls, instead of being differentiated into distinct pedicel and lamina zones, appear to curve continually upward toward the cone apex, enclosing the sporangia at a comparatively acute angle (figs. 1*A*, 8). In transverse section, the megasporangiate segments of the cone did not show any traces of a distinct sporophyll pedicel, as would be seen if the pedicel region were (near-)horizontal. Rather, the sporophyll and sporangium complexes were seen passing through each section almost immediately after emergence from the cone axis. Both the diagrammatic reconstruction (fig. 8) and SPIERS digital reconstruction (fig. 9) clearly show the sporophylls emerging at a steep angle. By contrast, most lycopsid cone sporophylls, including other *Flemingites* species and *Lepidostrobus*, display a near-horizontal pedicel region with an upturned lamina. Second, the relatively low number of sporophyll traces per 360° spiral in the axis of *F. arcuatus* compared with *F. diversus* and especially *F. schopfii* (six, six to 10, and 10, respectively) suggests that more vertical space was needed between sporophylls in order to accommodate their comparatively vertical orientation.

Bisporangiate Nature of Flemingites arcuatus

Despite the excellent preservation of several partial cones of *F. arcuatus* at our disposal, we cannot conclusively demonstrate that any are bisporangiate—a key diagnostic character of this cone genus. However, the intimate association and similar dimensions and histology of the various organs strongly indicate that the fragments of cone and stem contained in the cobble are indeed derived from the same whole plant. Our decision to assign the megasporangiate cone fragments and isolated microsporangium to the cone genus *Flemingites* was based on several pieces of evidence. Traditional methods of characterizing lycopsid cones—for example, microspore type, megaspore type, and megaspore number—were augmented with anatomical measurements such as cell size and architectural organization. These observations were used to correlate the organs described here as well as in other *Flemingites* species. In addition, the combination of organs, coded independently in our cladistic matrix rather than defined by their inclusion in other organs, strongly supported this generic assignment.

Comparison with the best-known permineralized cone species of *Flemingites*, *F. diversus* and *F. schopfii*, shows that both are remarkably long, narrow cones exceptionally prone to fragmentation. Only one of the many cone fragments of *F. diversus* examined by Felix (1954) was arguably complete. Of the 14 most informative specimens, five contained exclusively megaspores and five exclusively microspores; only four were bisporangiate, showing a gradational transition from "female" to "male" function. Brack (1970) based her description of *F. schopfii* on 22 specimens; all were incomplete, and only five were demonstrably bisporangiate. Moreover, the type specimen at least appears to show a contrasting abrupt transition from basal megasporangia to apical microsporangia. A similar contrast pertains in the primitive bisporangiate-coned arborescent lycopsid *Oxroadia* (Bateman 1992); *Oxroadia gracilis* cones show a gradational transition zone, whereas the one complete cone of *Oxroadia conferta* reported clearly exhibits an abrupt transition. Observations by one of us (R. M. Bateman) of bisporangiate cones of extant *Selaginella* suggests that the nature of the transition may reflect a combination of the architecture and spatial orientation of the cone. Having considered this broader context, we strongly suspect that at least some cones of *F. arcuatus* were bisporangiate.

Structure of the Subarchesporial Pad

The subarchesporial pad is a "columellate dome" of parenchymatous tissue that is connected to the sporophyll and expands within the sporangium, pressing the megaspores against the adaxial and lateral regions of the sporangium wall. It is unlikely to be detectable in compression/impression specimens. The classic example of a subarchesporial pad is found in anatomically preserved specimens of *Mazocarpon oedipternum* Schopf (1941), the cone borne by *Sigillaria approximata*. Indeed, the presence of parenchyma surrounding the megaspores was scored as an autapomorphy of *S. approximata* in the cladistic analysis of Bateman et al. (1992). However, the megasporangiate cone *Caudatocarpus* was figured by Brack-Hanes (1981) as having a single functional megaspore of lageniculate type surrounded by spongy tissue that was not clearly cellularized but otherwise could be attributed to a subarchesporial pad.

On close inspection, the megasporangia of permineralized *F. schopfii* from the Pennsylvanian of North America (Brack 1970) contain tissues similar to those described here, and Felix (1954) reported that the megasporangia of *F. diversus* contain a large quantity of parenchymatous tissue, noting that it was often broken down to form trabeculae. Nonetheless, *F. arcuatus* appears to have a subarchesporial pad that is better preserved and better developed than in any other cone in the genus, rivaling that of *M. oedipternum*.

The function of the subarchesporial pad remains contentious. Brack (1970) argued that the pad offered to the developing spores either mechanical protection or nourishment. Arber (1914) observed that the pads in some *Lepidostrobus* sporangia were reduced to a thin wall of cells lining the megasporangial wall by the time that the spores were fully developed, whereas Balbach (1967) argued that there was no correlation between the level of development attained by the spores and the degree of reduction shown by the pad.

Fig. 7 Reproductive structures in *Lagenicula wellmanii* sp. nov. megaspores. *A*, Megaspore apex with archegonia neck cells visible at the gula opening. Scale bar = 300 μm (NMS G 2004.75CK1.9). *B*, Enlargement of *A* showing archegonia neck cells and developing ventral cells. Scale bar = 50 μm. *C*, Longitudinal section of a megaspore with four archegonia at the proximal surface. Scale bar = 150 μm. *D*, *E*, Developing archegonia composed of two rows of neck cells and a ventral cell at the base. Scale bars = 50 μm. *F*, Enlargement of megaspore in *D* showing archegonium and a developing oocyte in the central body of the megaspore. Scale bar = 100 μm. (*C–F*, NMS G 2004.75CK1.5.)

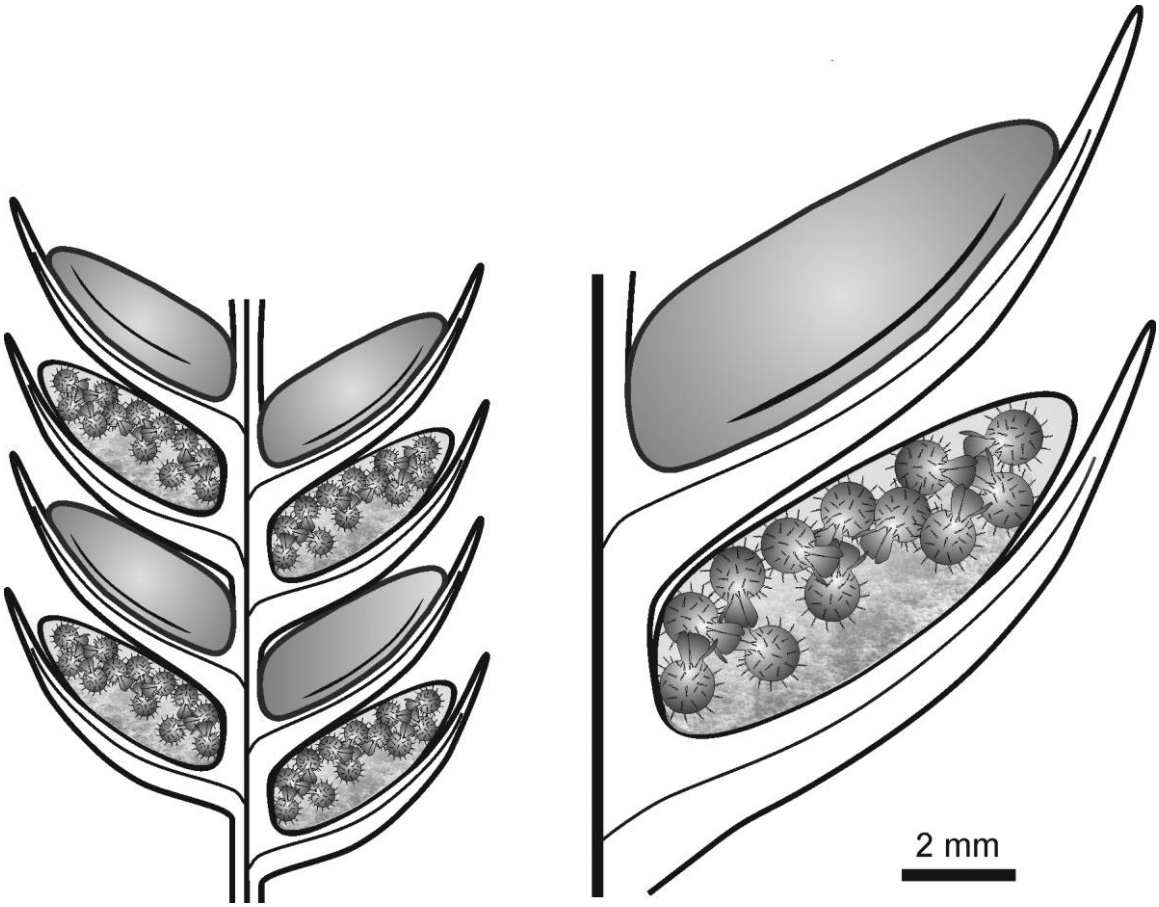

Fig. 8 Diagrammatic reconstruction of megasporangiate section of *Flemingites arcuatus* sp. nov., showing alternating internal and external anatomy of megasporangia and in situ *Lagenicula wellmanii* sp. nov. megaspores.

The sporangia described in this study appear fully mature, since the megaspores are free from their tetrads, the trilete suture is open, and megagametophytes have developed archegonia. Nonetheless, the subarchesporial pad still occupies approximately half the volume of the sporangium. Assuming that it would have degenerated once the megaspores were mature, a nutritional function is therefore unlikely.

Dehiscence Zone

The position of the dehiscence zone is likely to be dependent on the nature of the spores to be released from the sporangium and whether the sporophyll-sporangium complex is shed or remains attached to the cone during dehiscence. Paleozoic lycopsid cones are divided between polymegasporic genera and those with a single functional megaspore (DiMichele and Phillips 1994), and dehiscence mechanisms differ radically between the two groups.

In *F. arcuatus*, two lateral zones run parallel to the long axis in the distal region of the megasporangia. DiMichele and Phillips (1985) described the megaspores of *Flemingites* cones as being the primary dispersal unit, suggesting that they were shed directly from the cone. They also considered that the dispersal potential of the megaspores was limited, since the cones were frequently found in close association with fragments of the parent plant. These observations imply air dispersal from pendulous cones, with the megaspores being shed from two lateral slits, which may have been more effective for this type of dispersal than an adaxial opening on the sporangium. The limited distribution of the megaspores could be explained by a combination of their relatively large size and weight and the low height (<10 m) of the reconstructed parent tree (DiMichele 1980).

Ligules

Failure to discover a ligule in *F. arcuatus* but its recognition in the associated vegetative branches are not uncommon in studies of lycopsids and have been noted in several previous articles. Felix (1954) studied 20 *Lepidostrobus* (some now reassigned to *Flemingites*) cone species but could recognize a ligule in only one. Also, in *O. gracilis* (Alvin) R.M. Bateman and *O. conferta* R.M. Bateman (Bateman 1992) anatomically preserved lycopsids from Oxroad Bay, ligules were observed in the microphylls subtending the cones but not in the sporophylls within the cones. Ligules are far more readily detected when associated with microphylls,

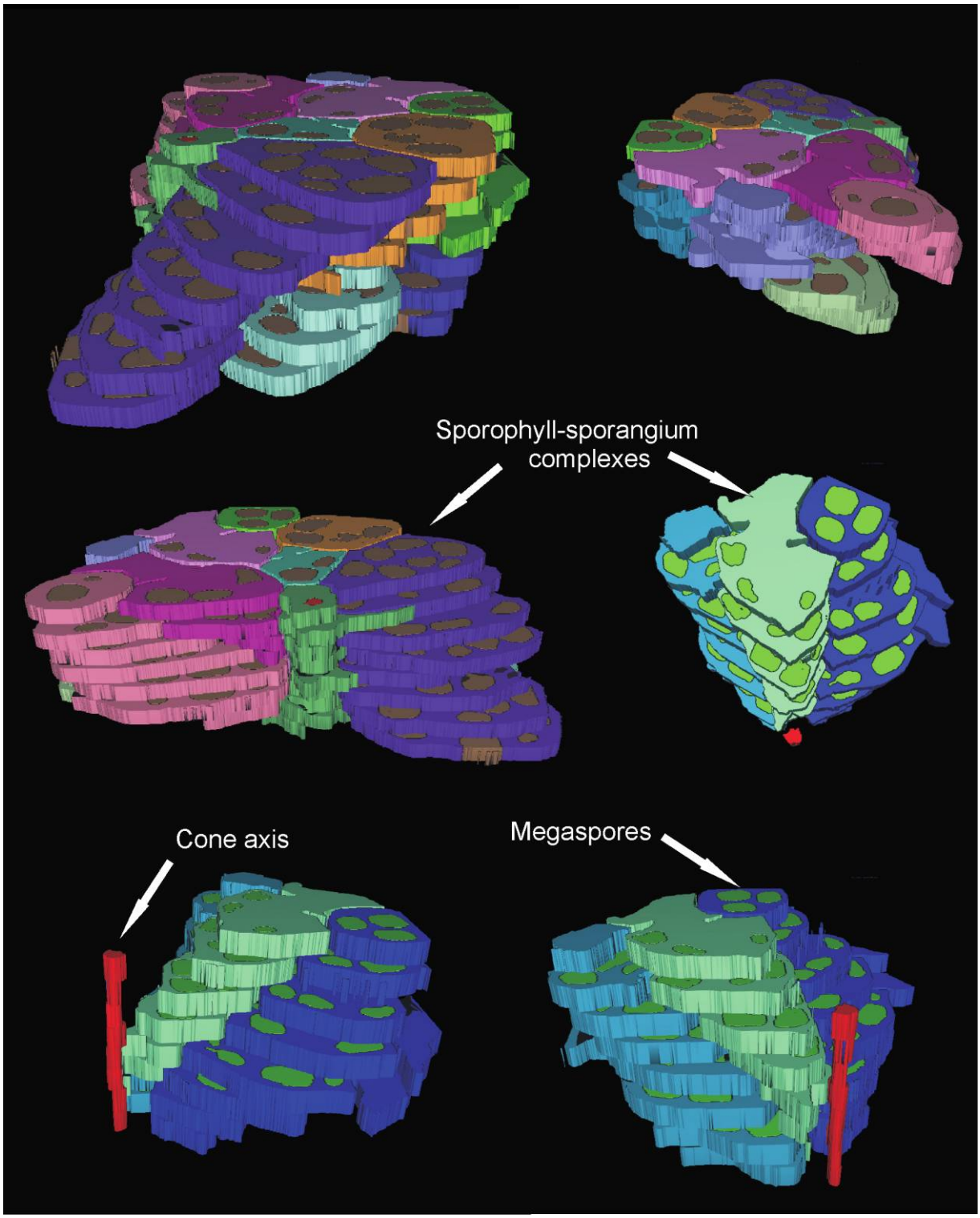

Fig. 9 SPIERS reconstruction of a megasporangiate cone section of *Flemingites arcuatus* sp. nov. based on eight wafer sections, with tomographic plates from both upper and lower surfaces of each wafer.

when they are recessed into a ligule pit, than with sporophylls, when they are located on the adaxial surface immediately distal to the sporangium. It is possible that a ligule was not detected in the megasporangia of *F. arcuatus* because it is unusually small in this species. The prominence of the ligule in *F. schopfii* (Brack 1970) suggests that the size and/or persistence of the ligule in the cone may be a taxonomically useful character, both within and beyond *Flemingites*.

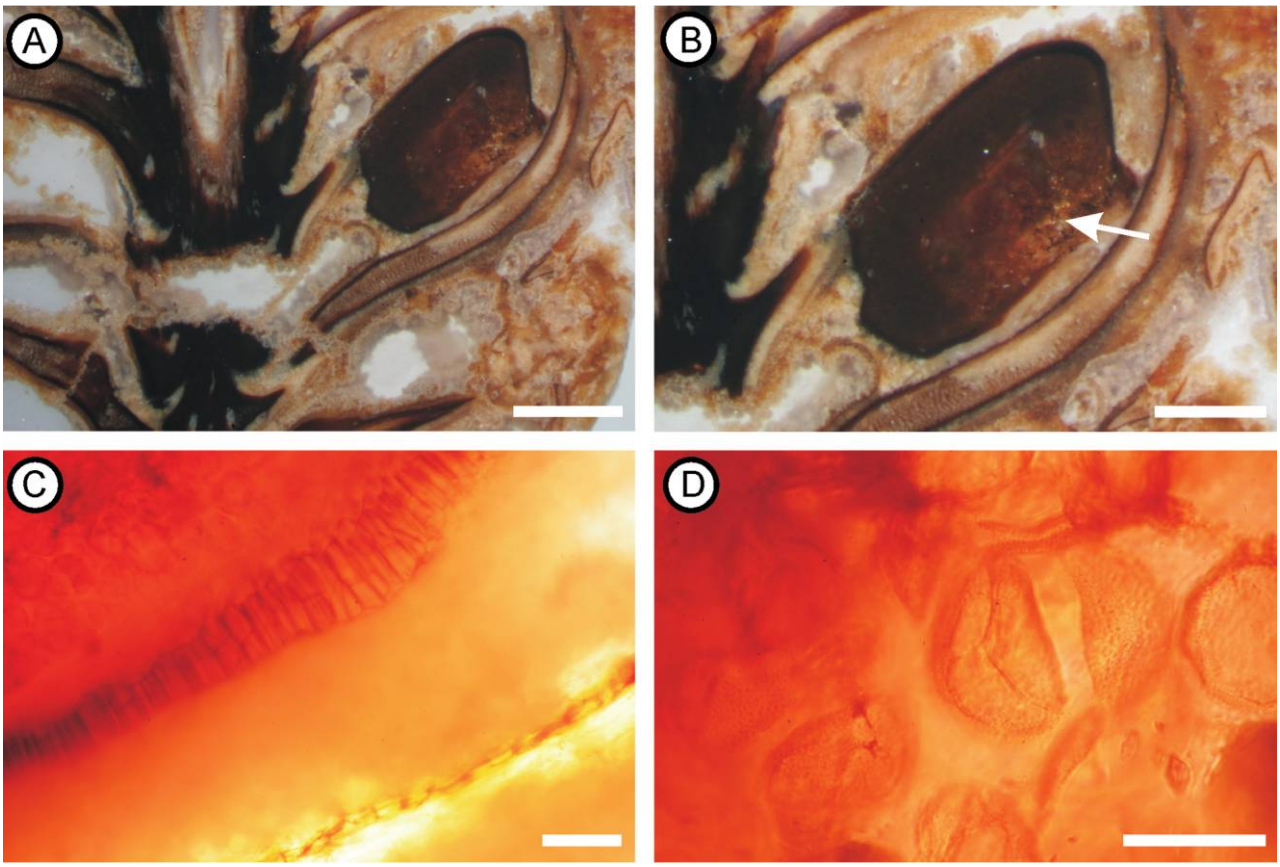

Fig. 10 Mature microsporangium of the *Flemingites arcuatus* sp. nov. plant. *A*, Microsporangium situated between microphylls of a vegetative stem fragment. Scale bar = 1 mm. *B*, Enlargement of microsporangium from fig. 8*A* with subarchesporial pad (arrow) and cluster of microspores above. Scale bar = 2 mm. *C*, Microsporangium cell wall with elongated, thin-walled cells similar to those of the megasporangia. Scale bar = 0.1 mm. *D*, Microspores in tetrads assignable to the spora dispersa *Lycospora orbicula*. Scale bar = 20 μm. (All NMS G 2004.75F1.6.)

Cuticle

Differences in preparation, as well as in mode and quality of preservation, complicate comparison of lycopsid cuticles. Descriptions of cuticle from lycopsid cones are rare, but studies of epidermal cells from leaf cushions have been used unusually extensively in the classification of the group and can be useful in correlating cone species with stem species. In a review of lepidodendrid cuticle focusing on compression specimens, Thomas (1966) stated that the epidermis in *Lepidodendron*, *Lepidophloios*, *Sigillaria*, *Bothrodendron*, and *Ulodendron* stems consists of only simple cells and stomata, with subsidiary cells surrounding the stomatal pit. By contrast, *F. arcuatus* shares with *F. schopfii* the distinction of possessing distinct bulbous cells of unknown function interspersed with the more conventional polygonal epidermal cells in both the microphylls and thee sporophylls. Both cones also organize stomata in rows parallel to the long axes of the sporophylls. Those in *F. schopfii* cover the entire abaxial surface and the distal adaxial surface, rather than being restricted to the lateral grooves, and are surrounded by four to six subsidiary cells that are indistinguishable from the epidermal cells. Stomata in *Ulodendron majus* Lindley & Hutton (the compressed stem correlates of *Flemingites* cones) are on average slightly smaller than those in *F. arcuatus* but are also simple, arranged in rows parallel to the leaf and not sunken into pits (cf. Thomas 1967, 1974).

Lagenicula *Megaspores*

Lageniculate megaspores, characterized by an unusually prominent gula, were first designated as a subdivision of *Triletes* Ibrahim by Bennie and Kidston (1886) and finally separated as the genus *Lagenicula* by Zerndt (1934). Potonié and Kremp (1956) later selected *Lagenicula horrida* Zerndt as the type species. Various authors (Piérart 1978) have attempted classifications of lageniculate megaspores, primarily by gula type, but our current understanding of the taxonomy of this spore genus is still considered unsatisfactory (Arioli et al. 2007).

The megaspore of *F. arcuatus*, *L. wellmanii* sp. nov., most closely resembles in shape and ornamentation *L. horrida*, which similarly has scarce, moderately long (72–120 μm), tapering spines with bulbous apices, though the apices of *L. horrida* are trumpet shaped rather than globose. Bulbous spine apices are relatively rare in other megaspore species.

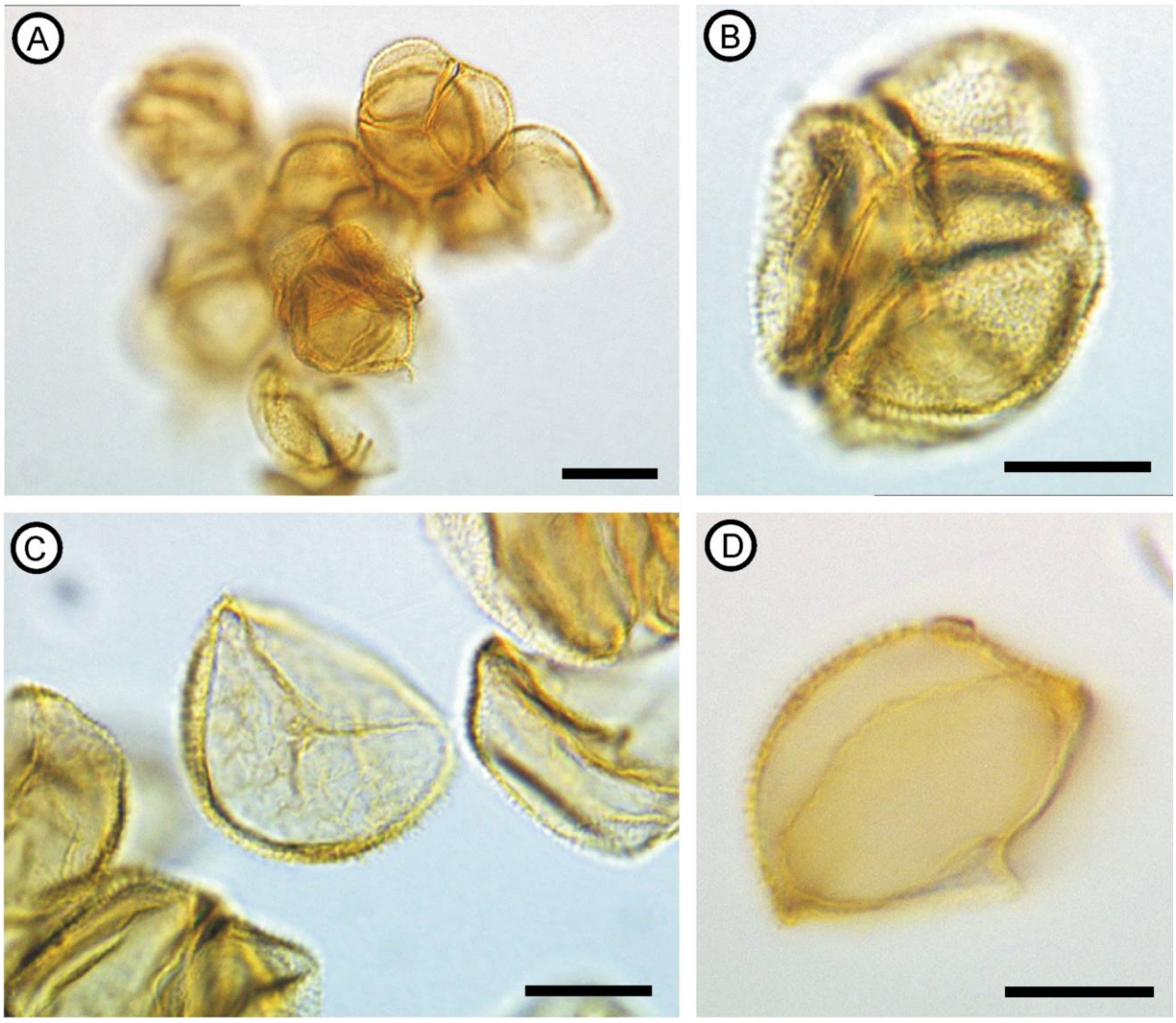

Fig. 11 Light microscopy of isolated *Lycospora orbicula* microspores. *A*, Cluster of tetrads. Scale bar = 20 μm. *B*, Single tetrad. Scale bar = 10 μm. *C*, Contact face showing trilete mark. Scale bar = 10 μm. *D*, Equatorial view showing exine thickening. Scale bar = 10 μm. (Isolated from NMS G 2004.75F1.5.)

They were observed in a "*Lepidostrobus*" (probably *Flemingites*) fructification from the Mississippian of Burntisland, Fife, by Williamson (1872), but the spores were smaller in diameter, and no gula was illustrated. The current spore is closest in size to *Lagenicula subpilosa* f. *major* (0.85–1.65 mm in diameter; Spinner 1969), but this bears much more densely packed, parallel-sided spines. *Lagenicula horrida* and *Lagenicula crassiaculeata* bear additional short spines among the longer spines, a feature absent from *L. wellmanii*. The exine of *L. wellmanii* is 20–30 μm thick and composed of two layers, broadly resembling in construction *L. horrida*, *L. crassiaculeata*, and *Lagenicula variabilis* (Winslow) Arioli et al. However, pore diameter increases more rapidly toward the outer membrane in *L. wellmanii*, more closely resembling *Lagenicula acuminata* Dijkstra & Piérart (Glasspool et al. 2000). Arioli et al. (2007) warned that the shape and orientation of the sporopollenin units may be altered through taphonomic modification. The channels that extend from the exine into the spines of *L. wellmanii* were also reported from *L. horrida* (Thomas and Blackburn 1987).

Apart from the distinct spine apices, the principal difference between *L. wellmanii* and other formally described species of *Lagenicula* is size: each feature of the megaspores found in the *F. arcuatus* cones is larger on average than in any comparable species and has a larger gula, wider laesurae, and longer spines. Although there is a risk of some taphonomic distortion in compression fossils, megaspores found in situ in coal-ball petrified cones, such as *L. subpilosa* f. *major* (Pearson 1986; Scott and Hemsley 1993), are directly comparable with *L. wellmanii*. Stratigraphically, the spinose megaspores most similar in morphology to *L. wellmanii* (*L. horrida* and *L. crassiaculeata*) range throughout much of the Carboniferous (fig. 13), though only *Lagenicula renaultii* extends beyond the Middle Pennsylvanian.

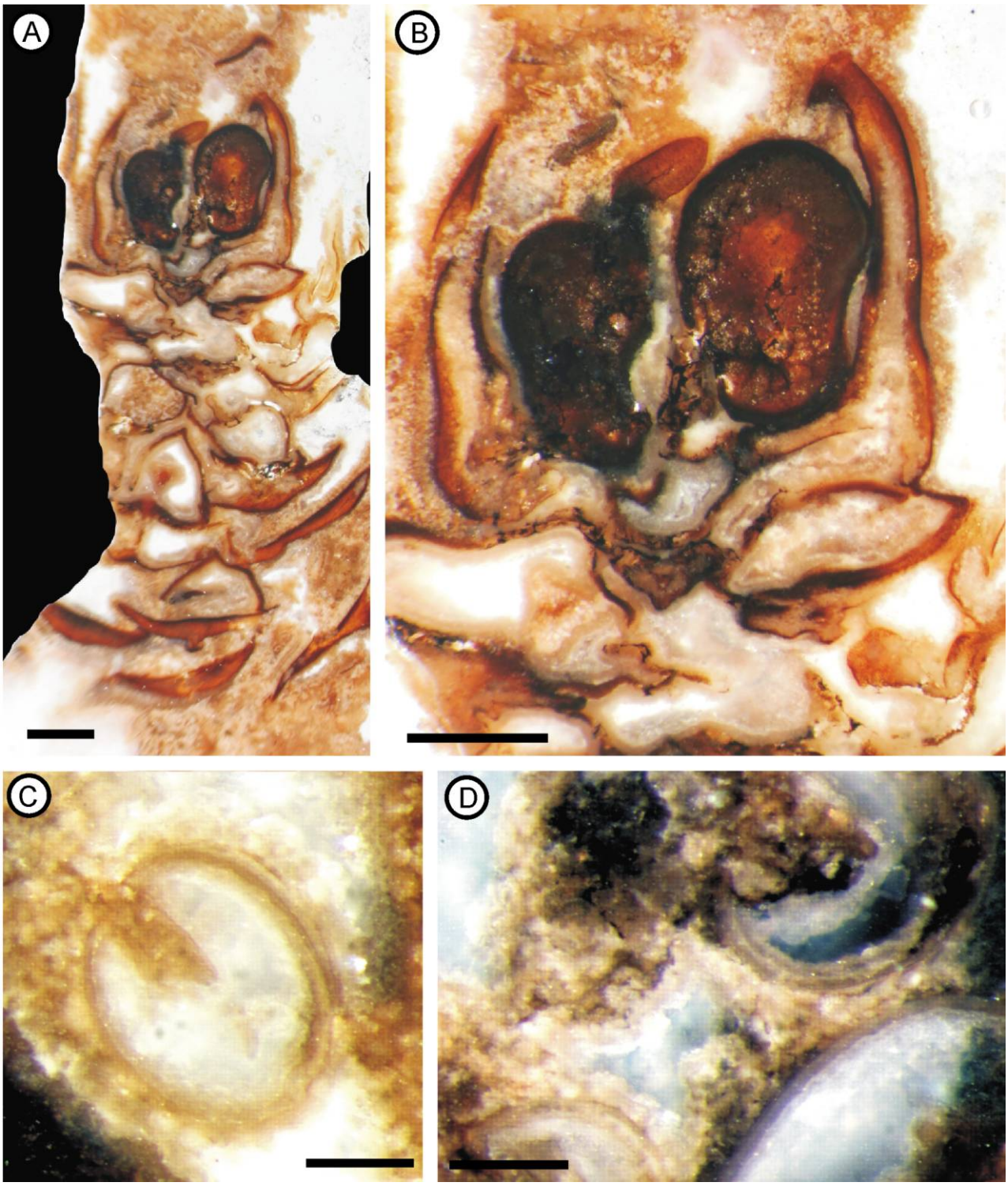

Fig. 12 Immature cone of *Flemingites* sp. nov. and associated cladoceran univalved crustaceans. *A*, Longitudinal section of immature cone displaying spirally arranged sporophylls with upright undeveloped sporangia on the adaxial surfaces. Scale bar = 1 mm (NMS G 2004.75F1.0). *B*, Enlargement of the immature sporangia at the cone apex, in vertical orientation. Scale bar = 1 mm. *C*, Univalved cladoceran crustacean found associated with the plants. Scale bar = 100 μm (NMS G 2004.75CK1.8). *D*, Cladoceran fragments with initial carbonate infilling and subsequent phases of silicification. Scale bar = 100 μm (NMS G 2004.75CK1.8).

Table 1

Comparison of Dimensions, Spore Types, and Stratigraphic Distribution of *Flemingites* Cone Species

Species	Cone width (mm)	Axis width (mm)	Sporophyll length (mm)	Sporangium length (mm)	Megaspore type	Megaspore no.	Microspore type	Age range
F. allantonensis	12–16	1.5–2.5	?	7.0	*Lagenicula* ?*crassiaculeata* (Zerndt) Potonié & Kremp	?	?	Mississippian
F. bartlettii	25	?	<20	5.0	?	?	*Planisporites* Knox	Lower Pennsylvanian
F. brownii	65	?	?	?	?	?	*Lycospora* (Schopf, Wilson & Bentall) Potonié & Kremp	Mississippian
F. diversus	<10	2.0	<10	?	*Lagenosporites rugosus* (Loose) Potonié & Kremp	16	*Lycospora* ?*subjuga* Bhardwaj	Middle Pennsylvanian
F. gallowayi	<35	?	10–15	?	?*Punctatisporites*	?	?*Planisporites*	Lower Mississippian
F. gracilis	12–18	1.5–2.5	?	5.0–8.0	*Lagenicula horrida* Zerndt	24	*Lycospora*	Middle Pennsylvanian
F. noei	55–70	7.0	7–22	20.0	*Lagenicula* spp.	>100	?	Lower Mississippian
F. olryi	6–12	1.5–2.2	?	2.5–4.0	*Lagenosporites rugosus*	?	?*Lycospora orbicula* (Potonié & Kremp) Smith & Butterworth	Middle Pennsylvanian
F. russelianus	12–20	1.5–2.5	?	5.0–8.0	*Lagenosporites rugosus*	?	*Lycospora*	Middle Pennsylvanian
F. schopfii	10–13	1.3–2.1	7.2–10.8	4.0–6.0	*Lagenosporites rugosus*	12–29	*Lycospora* ?*rugosa* Schemel	Middle Pennsylvanian
F. scottii	10	?	?	>4.0	*Lagenicula subpilosa* f. *major* Dijkstra ex Chaloner 1954	>30	*Lycospora chaloneri* Scott & Hemsley	Lower Pennsylvanian
F. arcuatus sp. nov.	10–19	<3.0	10–13	7.0–8.0	*L. wellmanii* sp. nov.	16	*Lycospora orbicula*	?

Note. *Flemingites* cone species and authorities emended by Brack-Hanes and Thomas (1983): *Flemingites allantonensis* (Chaloner) Brack-Hanes & B.A. Thomas, *F. bartlettii* (Arnold) Brack-Hanes & B.A. Thomas, *F. brownii* (Unger) Brack-Hanes & B.A. Thomas, *F. diversus* (Felix) Brack-Hanes & B.A. Thomas, *F. gallowayi* (Arnold) Brack-Hanes & B.A. Thomas, *F. gracilis* (Carruthers) Brack-Hanes & B.A. Thomas, *F. noei* (Mathews) Brack-Hanes & B.A. Thomas, *F. olryi* (Zeiller) Brack-Hanes & B.A. Thomas, *F. russelianus* (Binney) Brack-Hanes & B.A. Thomas, *F. schopfii* (Brack) Brack-Hanes & B.A. Thomas, *F. scottii* (Jongmans) Brack-Hanes & B.A. Thomas.

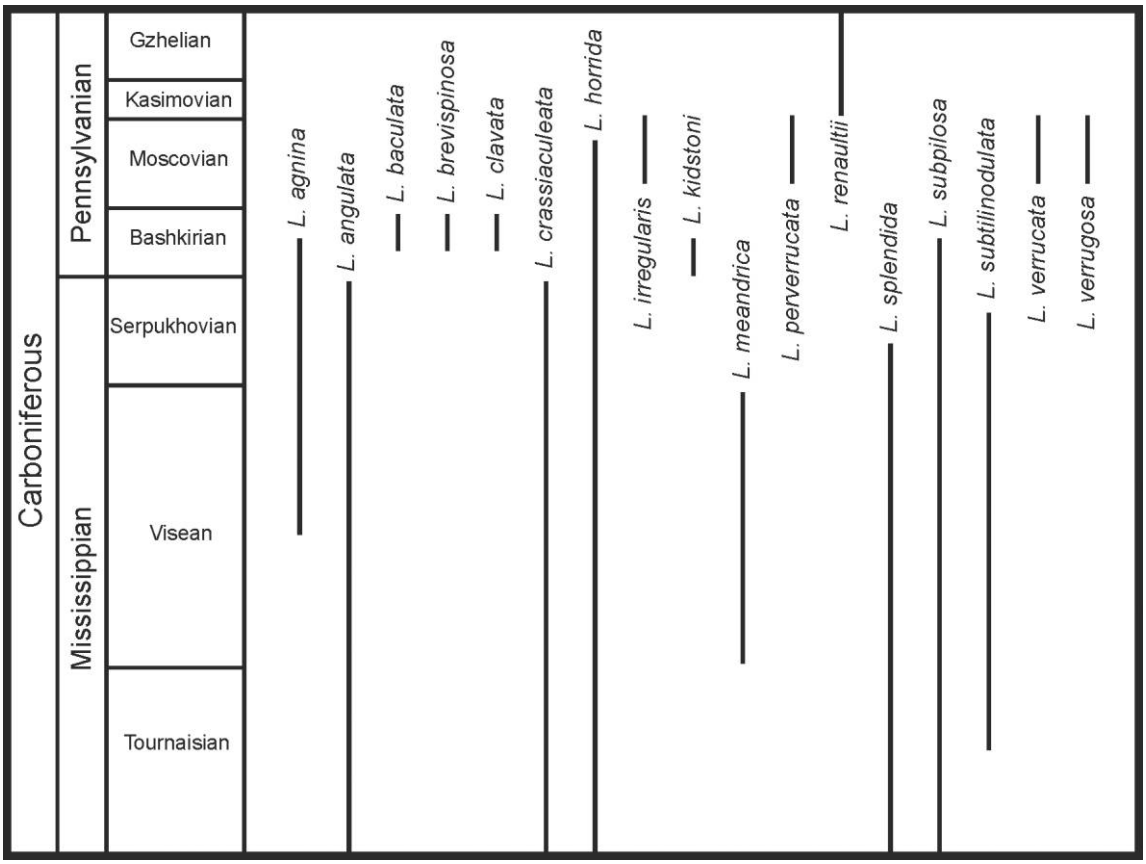

Fig. 13 Stratigraphic distribution of species of *Lagenicula* megaspores from Europe and North America (modified from Brahman and Hills 1980).

Archegonia

Spores and megagametophytes observed within the in situ megaspores of *F. arcuatus* show several ontogenetic stages, from the surficial appearance of the megaspore tetrad to the formation of cellular megagametophyte within the spore body. Archegonia and megagametophyte development have previously been reported from several genera of lycopsid cones and are broadly similar, both to each other and to their extant relatives in Selaginellales and Isoetales (cf. Bruchmann 1909, 1912; La Motte 1933; Rauh and Falk 1959; Robert 1971; Pigg and Rothwell 1983). Those studied in megaspores of *Flemingites* cones display two to three tiers of neck cells at the megaspore apex, located above a ventral cell in which the oocyte develops (Galtier 1964, 1970; Brack 1970; Brack-Hanes 1978; this study). Galtier (1964) also figured a canal between the neck cells leading inward toward the ventral cell in a *Flemingites* cone (reported as *Lepidostrobus*) found associated with *Paralycopodites brevifolius* axes (reported as *Lepidodendron veltheimianum*). This canal cannot be discerned in the archegonia of *L. wellmanii*, but its appearance (presumably a consequence of relaxation of the neck cells) may represent a later ontogenetic stage. Megaspores described from the sigillarian cone *Mazocarpon* (Pigg 1983) and from *Chaloneria* megasporophylls (Pigg and Rothwell 1983) contained archegonia exhibiting four tiers of neck cells, a number more typical of extant *Selaginella* (Bruchmann 1909, 1912; Robert 1971) and *Isoetes* (La Motte 1933; Rauh and Falk 1959).

Vascularized embryos showing bipolar growth were reported in *Setosisporites* megaspores observed in situ in *Bothrodendrostrobus* cones (McLean 1912; Stubblefield and Rothwell 1981) and in *Setispora* megaspores from *Oxroadia* cones (Bateman 1992). The archegonia in the current specimen preserve embryos in the early stages of development, but degradation of the cells makes problematic further comparison with those illustrated in previous studies. Certainly, the size and position of the embryonic tissue in the megaspores is comparable, but there is no discernible cell differentiation. The overall impression given is that there has been remarkable stasis in the reproductive biology of heterosporous lycopsids since the Carboniferous period.

Lycospora *Microspores*

Lycospora orbicula is somewhat atypical of this microspore genus in that it displays only a very narrow cingulum; the species was transferred from *Cyclogranisporites* only because of the shorter length of the laesurae (Smith and Butterworth 1967). The microspores also broadly resemble *Anaplanisporites-baccatus* (Hoffmeister, Staplin, & Malloy) Smith & Butterworth,

though this spore possesses less prominent distal ornamentation and lacks a cingulum. *Lycospora orbicula* has been recorded in the dispersed miospore record from Early to Middle Pennsylvanian coal measures, most commonly in North America (Willard et al. 1995; Calder et al. 1996; Shaver et al. 2006). The narrow cingulum found in *L. orbicula* distinguishes the species from lycospores found in *Lepidostrobus* (Balbach 1966*a*; Courvoisier and Phillips 1975; Willard 1989*a*, 1989*b*; Bateman et al. 1992; Bek and Oplustil 2004, 2006). Thomas (1970) and Brack-Hanes and Thomas (1983) recognized two groups of lycospores found in situ in lepidodendrid cone genera: narrowly cingulate lycospores with a smooth proximal surface, of the *L. orbicula* type, are reliably associated with *Flemingites* cones, whereas more broadly cingulizonate lycospores bearing proximal ornamentation are found in microsporangiate *Lepidostrobus* cones.

The in situ evidence presented here is arguably the strongest supporting the characteristic occurrence of *L. orbicula* in *Flemingites* cones. Smith and Butterworth (1967) noted the similarity between dispersed *L. orbicula* spores in British Pennsylvanian coal measures with spores found in *F. olryi* by Chaloner (1953). Microspores extracted from *F. diversus* by Felix (1954) also appeared similar to *L. orbicula* in size, ornamentation, and cingulum characters but were not formally identified in that study. More recently, in situ microspores conforming to *L. orbicula* have been identified in *Flemingites* cf. *russelianus* from the Clackmannan Coalfield in Scotland (Oplustil and Bek 2009), but the authors were unable to isolate megaspores from the cone.

Cladistic Analysis

The existence of detailed morphological cladistic matrices for land plants per se and for various groups within land plants offers an as yet underutilized opportunity to place phylogenetically additional, often less character-rich, whole-plant and partially reconstructed fossils (Bateman and Hilton 2009). For example, this approach was used by Hilton and Bateman (2006) to explore the placement of, and degree of topological instability caused by, partially reconstructed fossil species in their seed plant analysis. That same matrix was then used as a framework for more recent partial reconstructions of the pteridosperm *Eremopteris* (Cleal et al. 2009) and the putative gnetalean *Erdtmanitheca* (Friis et al. 2007), both of which occupied single, at least moderately well-supported placements within the overall topology. Similarly, Bateman et al. (2007) used the previously developed lycopsid-wide matrices of Bateman (1992) and Kenrick and Crane (1997) to place phylogenetically a single indifferently preserved organ species of a putatively early divergent homosporous lycopsid, *Hestia eremosa* R.M. Bateman, Kenrick, and G.W. Rothwell, though in this case the paucity of scorable characters led to a range of possible placements.

The morphological phylogenetic framework for arborescent lycopsids was established by Bateman et al. (1992; see also DiMichele and Bateman 1996; Bateman and Simpson 1998) via a matrix of 115 bistate characters (80 informative) scored from 16 conceptual whole plants belonging to 10 genera, all painstakingly reconstructed from anatomically preserved arborescent lycopsid fossils and rooted by a hypothetical ancestor. Their analysis included a data set for *P. brevifolius* (Morey & Morey) DiMichele that combined data from two cone species, *F. diversus* and *F. schopfii*, together with their respective in situ megaspores and microspores. The data set was complete except for seven characters describing aspects of the leaf cushions; because *Paralycopodites* retains its leaves, its leaf bases lack some of the features that characterize more derived genera. We were similarly unable to code the *F. arcuatus* plant for these seven characters. A further 41 characters could not be coded because the organs that display the characters in question have not yet been found: these included all characters of the rhizomorph, cortex, and periderm; some characters of the stele; and most characters describing the architecture of the plant and its cone (ironically, we lack the evidence needed to unequivocally score the cone as bisporangiate, despite this being a diagnostic character of the cone genus). Nonetheless, we were able to score for *F. arcuatus* 62% of the characters scored for *P. brevifolius* (fig. 15). It proved necessary to add a novel state to character 77 of Bateman et al. (1992) to accommodate the unique acutely angled sporophylls of *F. arcuatus*.

The analysis was run using PAUP 4.0 and is described in "Material and Methods." The three resulting most-parsimonious trees had topologies compatible with those obtained by Bateman et al. (1992), similarly differing only in the placement of *Chaloneria* (acting as placeholder for the lineage of unbranched isoetaleans that includes extant *Isoetes*), which alternatively placed above *Paralycopodites* (fig. 14), below *Paralycopodites*, or sister to *Paralycopodites*. Thus, the inclusion of *F. arcuatus* did not disturb the nature or the relative strengths of the relationships previously inferred. More important, the analysis placed *F. arcuatus* within *Paralycopodites* with reasonable confidence, receiving a bootstrap support of 87% and decay index of 2. A reanalysis of the matrix using only reproductive characters again paralleled that of Bateman et al. (1992), yielding broadly similar topologies but with less resolution in the lower part of the tree and weaker statistical support throughout; the sister relationship between *F. arcuatus* and *P. brevifolius* was maintained.

Focusing on *Paralycopodites* s.l., *P. brevifolius* and *F. arcuatus* differ only in reproductive characters and diverge in six states (figs. 14, 15), a number not statistically different from the average divergence of four states separating conspecific pairs elsewhere in the tree. As represented under Acctran optimization, the relationship between the two species is asymmetric, with *F. arcuatus* apparently having acquired five operationally autapomorphic states compared with only one in *P. brevifolius*.

Comparison of the two original data sets (fig. 15) readily identified five contrasting reproductive characters. The acute angle of the sporophylls (C77) is unique to *F. arcuatus*, contrasting with the obtuse insertion of *Oxroadia* sporophylls. Parenchymatous tissue enclosing the megaspores (C91) is classically considered to characterize *S. approximata*. Its recognition in *F. arcuatus* led us to reexamine other species of the cone genus and to tentatively identify similar tissue in the megasporangia of *F. schopfii* (Brack 1970). This character appears to correlate with the relative size of the subarchesporial pad and may also be subject to differential preservation; it therefore requires more careful consideration. The main characters

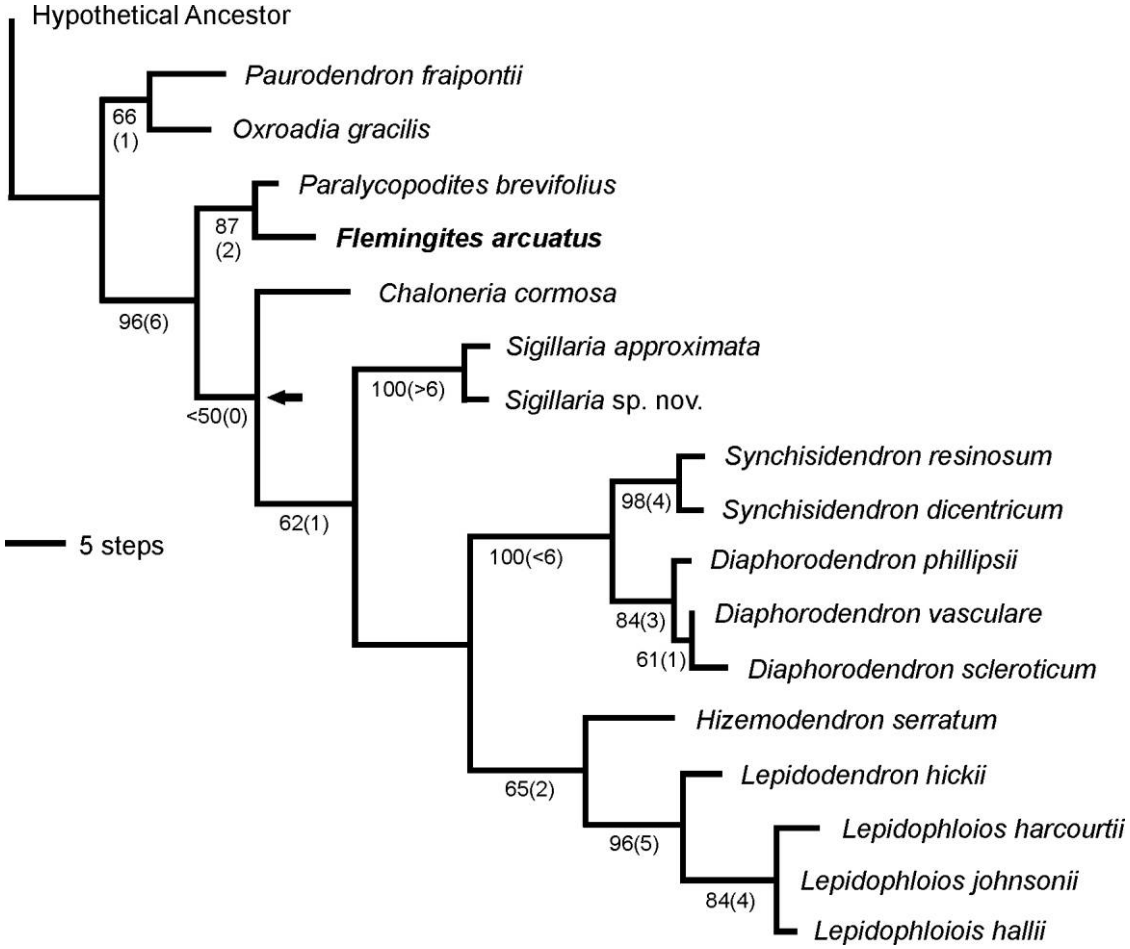

Fig. 14 Preferred of three most-parsimonious trees generated by inserting *Flemingites arcuatus* sp. nov. into the morphological cladistic matrix of Bateman et al. (1992), thus demonstrating its sister group relationship with *Paralycopodites brevifolius*. Arrow indicates the node subtending *Chaloneria* that collapses in the strict consensus tree. Branch lengths are proportional and reflect Acctran optimization. The three trees represent 83 informative characters and have a length of 168, a consistency index of 0.615 (0.691 including autapomorphies), and a retention index of 0.809. Numbers under the branches are bootstrap values based on 1000 replicates and (in parentheses) decay index values.

distinguishing *F. arcuatus* reside in its megaspore, *L. wellmanii*. The gulate laesural ornamentation (C94) is shared with *Diaphorodendron* and *Synchysidendron*, whereas the echinate ornamentation of both the distal faces (C100) is shared with *Oxroadia* and *Sigillaria* sp. nov. and the echinate ornamentation of the proximal faces (C97) with *Oxroadia* alone. The overall impression gained is that the less derived species among the arborescent lycopsids, not least *Paralycopodites*, mirror extant *Selaginella* species in showing exceptional variation in megaspore morphology; this could arguably be more finely divided in morphological cladistic analyses, though considerable homoplasy would be predicted.

Broader Taxonomic Context

As previously noted, the well-characterized stem genus *Paralycopodites* was suggested by Pearson (1986) to be a synonym of *Anabathra*, and this conclusion was initially tentatively accepted by Bateman et al. (1992). However, on closer inspection of Pearson's specimens, DiMichele and Bateman (1996) decided that there was insufficient evidence to synonymize the genera. In a further analysis of the rhizomorphic lycopsids, DiMichele and Bateman suggested that the family Ulodendraceae should accommodate the permineralized taxa *Anabathra* and *Paralycopodites*. *Ulodendron* (Thomas 1967) was also tentatively included in the group as the compression equivalent to *Paralycopodites*. An alternative system proposed by Thomas and Brack-Hanes (1984) and based on cone genera included *Flemingites* in Flemingitaceae and *Ulodendron* in the satellite taxa of Spenceritaceae. Because the material described here is permineralized, comparison of the vegetative organs is constrained to *Anabathra* and *Paralycopodites*, although the cuticle micromorphology of *Ulodendron* provides a potential means of correlation.

The vegetative organs described in this study share many features with the two published species of *Paralycopodites*: *Paralycopodites minutissimum* Morey & Morey (1977) and *P. brevifolius* (DiMichele 1980), both from the Middle Pennsylvanian of Europe and America. The smaller axes of *P. min-*

	Habit	Root	Stele	Cortex	Periderm	Leaf B.
PSBR	1110011	100110	010000001100100100	10000	10000000000010	0#######
FLAR	----0--	?-----	0??000??1100100???	?????	??????????????	0#######

	Leaf B.	Leaves	Cones	Sporophyll	Megaspores	Microspores
PSBR	1010000	1000000	0010	**0**00000000000000	00**0**00**0**100	00101000001000
FLAR	1010000	1000000	-?1?	**2**00000000000001	00**1**00**1**0**0**10	00101000001000

Symbols: – = not known whether taxon possesses relevant feature; ? = taxon possesses relevant feature but character state unknown; # = taxon known to lack relevant feature.

Fig. 15 Comparison of partial plant *Flemingites arcuatus* (FLAR) with whole plant *Paralycopodites brevifolius* (PSBR) based on 115 bistate characters detailed by Bateman et al. (1992), highlighting five contrasting states.

utissimum share the same arrangement of exarch siphonostele and cortex as those described here, but the current axes exceed the width of the largest axis described in that study. The shape and structure of the microphylls of *F. arcuatus* are also similar to both published species, with a central vascular trace surrounded by parenchyma and two lateral zones of parichnos. Leaf bases in the current specimen are similar in overall shape to those seen in the smaller branches of *P. brevifolius*. The angle of leaf attachment is more acute in *P. brevifolius* than in the current specimen, but this may be an ontogenetically modifiable character seen only in more mature axes. There is no evidence of undulations in the cortex at the leaf bases in the published specimens of *Paralycopodites*, though they do characterize *Hizemodendron*, where they are considered to be diagnostic of the partially reconstructed species *Hizemodendron serratum* (Bateman and DiMichele 1991; Bateman et al. 1992). Unfortunately, small distal branches of *Paralycopodites*, *Hizemodendron*, and *Lepidodendron* s.s. are notoriously difficult to distinguish, even when anatomically preserved, thus raising the possibility that the current block contains vegetative organs of both *Paralycopodites* and *Hizemodendron*. However, in the absence of any other (even subtle) characters separating the many small branches and cone-subtending axes observed in the block, we believe it is more likely that all of the branches within the block are conspecific and that serrated leaf bases occur on occasion in *Paralycopodites–Flemingites* as well as *Hizemodendron*.

The current specimen also shares several vegetative and reproductive characters with Pearson's (1986) description of *Anabathra pulcherrima*, on the basis of permineralized material from Berwickshire. Comparison of vegetative organs is made difficult by the disparity in axis size, since Pearson's axes were unusually large. Microphyll shape in transverse section is similar, as are the shape and arrangement of leaf bases around the stems. However, these are characters that may be similar in most arborescent lycopsids. Pearson also found spiny lageniculate megaspores associated with the material, which he compared with *L. subpilosa* f. *major*, the type of which were found in *F. scottii* cones. Although comparable in size to *L. wellmanii*, the megaspores had spines with blunt apices. Mississippian (Viséan) megaspores possessing spines with bulbous apices were reported from Burntisland, Fife, by Williamson (1872), in a cone found associated with axes belonging to "*Lepidophloios brevifolium*," a synonym of *P. brevifolius* (DiMichele 1980). The axes described by Williamson share the characteristic vascular arrangement and microphyll shape of *Paralycopodites*. However, the sporophylls are more circular in transverse section than those of *F. arcuatus* and emerge from the axis at an almost horizontal angle. The vascular system also differs from *F. arcuatus* in possessing a solid protostele with prominent protoxylem bundles, surrounded by only a narrow gap and a much thicker cortex.

Preservation and Ecology

Univalved crustaceans associated with *F. arcuatus* (fig. 12*C*, 12*D*) have been infilled with fine-grained carbonate, suggesting that carbonate mud was the original substrate and that episodic silica infilling occurred subsequent to burial of the cones. In the absence of marine biogenic contributors, sources of mobile silica are usually volcanic or hydrothermal activity (Flügel 2004) or, alternatively, chemical weathering of soils (Bateman and Catt 2007). The Sandsend cobble lacks any of the features characteristic of well-developed soils, and the most credible kind, a silcrete, characterizes deserts rather than the wetlands favored by arborescent lycopsids. A purely hot spring setting is also improbable, since higher silica-to-carbonate ratios would be expected than the ~50 : 50 ratio observed in the current cobble. Thus, although there are no obvious volcanic clasts within the chert, the fine preservation of the plant cells suggests rapid solidification consistent with volcanic activity as the source of silica. Trace element and/or isotopic analysis could shed further light on the depositional environment (Bateman 1999).

The chert composition and fine preservation of the plants is similar to that found at East Kirkton in Scotland, an Upper Mississippian locality rich in ferns and pteridosperms (Scott et al. 1994). Tuffs within the East Kirkton Limestone were described as having undergone "multi-mineral permineralisation" (Brown et al. 1994, p. 269), a process in which carbonate was deposited initially, followed by phases of silica permeating the cell walls into the cell lumena. The depositional environment was interpreted as a lake that was influenced by hot spring

and/or volcanic activity, which introduced silica into the diagenetic process (Brown et al. 1994; McHill et al. 1994).

Permineralization is generally a rapid process in volcanigenic environments (Rex and Scott 1987; Bateman and Scott 1990; Brown et al. 1994); rapidity of silicification in the Sandsend cobble is indicated by both the lack of degradation of the plant tissue and the persistence of the thin-shelled crustaceans. The corresponding lack of physical degradation suffered by the lycopsid twigs and cones suggests that they were not transported over any great distance.

Paralycopodites brevifolius plants reconstructed thus far were small trees that bore bisexual *F. diversus* and *F. schopfii* cones polycarpically on deciduous lateral branches (DiMichele and Phillips 1992, 1994). This led to rapid and prolific reproduction, perhaps explaining why so few vegetative remains, in comparison with cone specimens, have been found in the British Carboniferous. DiMichele and Phillips (1985, 1994) suggested that they inhabited peat-forming environments that were exposed to periodic flooding, since the plants are usually found associated with coal seams and thin impersistent clastic sediments. DiMichele (1980) further argued that *Paralycopodites* may have been adapted to survival in frequently disturbed environments, as evidenced by its abundant production of megaspores and relative rarity in Pennsylvanian coal sediments. These interpretations are consistent with our own more tentative inferences.

Provenance

Identifying the precise source horizon of an ex situ block such as the Sandsend cobble is generally a serious challenge, even when transport has been negligible (Bateman 1999). The Sandsend chert cobble was initially thought to be Jurassic in age, but the local sedimentary sequences lack cherts, suggesting that the cobble is exotic.

DiMichele (1980) reported three "stratigraphically complementary" cone species associated with *P. brevifolius*: *F. scottii* (Upper Mississippian), *F. schopfii* (lower Middle Pennsylvanian), and *F. diversus* (Middle Pennsylvanian). When all of the available sources of paleobotanical data are considered in a biostratigraphic context, *Paralycopodites* stems, *Flemingites* cones, *Lagenicula* megaspores (fig. 13), and *Lycospora orbicula*-type microspores are all frequent in the Middle Pennsylvanian, where admittedly the likelihood of preservation is greatest. Within the Mississippian, *Flemingites* cones bearing *Lagenicula* megaspores have been reported from the Upper Viséan of Pettycur, southeastern Scotland (Williamson 1872; Rex and Scott 1987), and vegetative axes from the Middle Viséan of Glenarbuck, southwestern Scotland (Smith 1962; Bateman and Cleal 1995). The narrowest stratigraphic range appears to be provided by the microspore species *L. orbicula*, which characterizes the Middle Pennsylvanian of Euramerica (Smith and Butterworth 1967). Geographically, most British *Flemingites* specimens have originated from southern Scotland, though one cone was found in the Middle Pennsylvanian Yorkshire coalfield, southwest of Sandsend (Thomas 1970).

The cobble was most likely transported to Sandsend by glacial action during the Pleistocene and/or by longshore drift during the Holocene; both processes occur predominantly southward in northeast England. The most obvious lithological comparisons are with Mississippian calci-siliceous lagerstätten that occur ~300 km north of the Yorkshire coast in the eastern part of the Scottish Midland Valley, notably Pettycur/Kingswood (Rex and Scott 1987) and East Kirkton (Brown et al. 1994; Scott et al. 1994). However, because none of these well-known localities provides a precise match with the composition and mode of preservation of the Sandsend cobble, we infer that this enigmatic cobble represents the first evidence of a previously unknown terrestrial lagerstätte that is presumed to be of Carboniferous (most likely Early or Middle Pennsylvanian) age and be located in northeastern England or southern Scotland. It may be comparable in quality with the Lower Devonian Rhynie Chert hot spring system (cf. Trewin et al. 2003).

Acknowledgments

We thank Lyall Anderson (formerly National Museums of Scotland) for highlighting the specimen and arranging its loan, Charles Wellman (University of Sheffield) and Duncan McLean (MB Biostratigraphy, Sheffield) for their help and expertise in processing and identifying the in situ spores, Alan Channing (Cardiff University) for provenance analysis of the chert, and Bill DiMichele for comments on the manuscript. This research was part of L. G. Stevens's PhD project at the University of Birmingham, supported by a University of Birmingham studentship that is gratefully acknowledged.

Literature Cited

Abbott ML 1963 Lycopod fructifications from the Upper Freeport (no. 7) coal in southeastern Ohio. Palaeontogr Abt B 112:93–118.

Arber A 1914 An anatomical study of the cone genus *Lepidostrobus*. Trans Linn Soc Lond 8:205–238.

Arioli C, CH Wellman, B Lugardon, T Servais 2007 Morphology and wall ultrastructure of the megaspore *Lagenicula* (*Triletes*) *variabilis* (Winslow, 1962) Arioli et al. (2004) from the Lower Carboniferous of Ohio, USA. Rev Palaeobot Palynol 144:231–248.

Balbach MK 1966*a* Miospore variation in *Lepidostrobus* and comparison with other *Lycospora*. Micropaleontology 12:334–342.

——— 1966*b* Paleozoic lycopsid fructifications. II. *Lepidostrobus takhtajanii* in North America and Great Britain. Am J Bot 53:275–283.

——— 1967 Paleozoic lycopsid fructifications. III. Conspecificity of British and North American *Lepidostrobus* petrifactions. Am J Bot 54:867–875.

Bateman RM 1992 Morphometric reconstruction, palaeobiology and phylogeny of *Oxroadia gracilis* Alvin emend. and *O. conferta* sp. nov.: anatomically-preserved lycopsids from the Dinantian of Oxroad Bay, SE Scotland. Palaeontogr Abt B 228:29–103.

——— 1994 Evolutionary-developmental change in the growth architecture of fossil rhizomorphic lycopsids: scenarios constructed on cladistic foundations. Biol Rev 69:527–597.

——— 1996 An overview of lycophyte phylogeny. Pages 405–415 *in* JM Camus, M Gibby, RJ Johns, eds. Pteridology in perspective. Royal Botanic Gardens, Kew.

——— 1999 Bulk geochemistry as a guide to provenance and diagenesis. Pages 169–173 *in* TP Jones, NP Rowe, eds. Fossil plants and spores: modern techniques. Geological Society, London.

Bateman RM, JA Catt 1985 Modification of heavy mineral assemblages in English coversands by acid pedochemical weathering. Catena 12:1–21.

——— 2007 An absolute chronology for the raised beach and associated deposits at Sewerby, East Yorkshire, England. J Quat Sci 11:389–395.

Bateman RM, CJ Cleal 1995 Glenarbuck. Pages 164–166 *in* CJ Cleal, BA Thomas, eds. Palaeozoic palaeobotany of Great Britain. Chapman & Hall/JNCC, London.

Bateman RM, WA DiMichele 1991 *Hizemodendron*, gen. nov., a pseudoherbaceous segregate of *Lepidodendron* (Pennsylvanian): phylogenetic context for evolutionary changes in lycopsid growth architecture. Syst Bot 16:195–205.

Bateman RM, WA DiMichele, DA Willard 1992 Experimental cladistic analysis of anatomically preserved arborescent lycopsids from the Carboniferous of Euramerica: an essay on paleobotanical phylogenetics. Ann Mo Bot Gard 79:500–559.

Bateman RM, J Hilton 2009 Palaeobotanical systematics for the phylogenetic age: applying organ-species, form-species and phylogenetic species concepts in a framework of reconstructed fossil and extant whole-plants. Taxon 27:1254–1280.

Bateman RM, P Kenrick, GW Rothwell 2007 Do eligulate herbaceous lycopsids occur in Carboniferous strata? *Hestia eremosa* gen. et sp. nov. from the Mississippian of Oxroad Bay, Scotland. Rev Palaeobot Palynol 144:323–335.

Bateman RM, AC Scott 1990 A reappraisal of the Dinantian floras at Oxroad Bay, East Lothian, Scotland. 2. Volcanicity, palaeoecology and palaeoenvironments. Trans R Soc Edinb Earth Sci 81:161–194.

Bateman RM, NJ Simpson 1998 Comparing phylogenetic signals from reproductive and vegetative organs. Pages 231–253 *in* SJ Owens, PJ Rudall, eds. Reproductive biology in systematic, conservation and economic botany. Royal Botanic Gardens, Kew.

Batten DJ 1999 Small palynomorphs. Pages 15–20 *in* TP Jones, NP Rowe, eds. Fossil plants and spores: modern techniques. Geological Society, London.

Bek J, S Oplustil 2004 Palaeoecological constraints of some *Lepidostrobus* cones and their parent plants from the Late Palaeozoic continental basins of the Czech Republic. Rev Palaeobot Palynol 131:49–89.

——— 2006 Six rare *Lepidostrobus* species from the Pennsylvanian of the Czech Republic and their bearing on the classification of lycospores. Rev Palaeobot Palynol 39:211–226.

Bennie J, R Kidston 1886 On the occurrence of spores in the Carboniferous Formation of Scotland. Proc R Phys Soc Edinb 9: 82–117.

Brack SD 1970 On a new structurally preserved arborescent lycopsid fructification from the lower Pennsylvanian of North America. Am J Bot 57:317–330.

Brack-Hanes SD 1978 On the megagametophytes of two lepidodendracean cones. Bot Gaz 39:140–146.

——— 1981 On a lycopsid cone with winged spores. Bot Gaz 142: 294–304.

Brack-Hanes SD, BA Thomas 1983 A re-examination of *Lepidostrobus* Brongniart. Bot J Linn Soc 86:125–133.

Brahman DR, LV Hills 1980 The stratigraphic and geographic distribution of Carboniferous megaspores. Palynology 4:23–41.

Brown RE, AC Scott, TP Jones 1994 Taphonomy of plant fossils from the Viséan of East Kirkton, West Lothian, Scotland. Trans R Soc Edinb 84:267–274.

Bruchmann H 1909 Von den Vegetationsorganen der *Selaginella Lyalii* Spring. Flora 99:436–464.

——— 1912 Zur Embryologie der Selaginellaceen. Flora 104:180–224.

Calder JH, MR Gibling, CF Eble, AC Scott, DJ MacNeil 1996 The Westphalian D fossil lepidodendrid forest at Table Head, Sydney Basin, Nova Scotia: sedimentology, palaeoecology and floral response to changing edaphic conditions. Int J Coal Geol 31:277–313.

Carruthers W 1865 On an undescribed cone from the Carboniferous beds of Airdrie, Lanarkshire. Geol Mag 2:433–440.

Chaloner WG 1953 On the megaspores of four species of *Lepidostrobus*. Ann Bot 17:264–273.

Cleal CJ, C Shute, J Hilton, J Carter 2009 A revision of the Pennsylvanian-aged Eremopteris-bearing seed-plant. Int J Plant Sci 170:666–698.

Courvoisier JM, TL Phillips 1975 Correlation of spores from Pennsylvanian coal-ball fructifications with dispersed spores. Micropaleontology 21:45–59.

DiMichele WA 1980 *Paralycopodites* Morey & Morey from the Carboniferous of Euramerica: a reassessment of generic affinities and evolution of "*Lepidodendron*" *brevifolium* Williamson. Am J Bot 67:1466–1476.

——— 1985 *Diaphorodendron*, gen. nov., a segregate from *Lepidodendron* (Pennsylvanian age). Syst Bot 10:453–458.

DiMichele WA, RM Bateman 1992 Diaphorodendraceae, fam. nov. (Lycopsida: Carboniferous): systematics and evolutionary relationships of *Diaphorodendron* and *Synchysidendron*, gen. nov. Am J Bot 79:605–617.

——— 1996 The rhizomorphic lycopsids: a case-study in paleobotanical classification. Syst Bot 21:535–552.

DiMichele WA, TL Phillips 1985 Arborescent lycopod reproduction and paleoecology in a coal-swamp environment of late Middle Pennsylvanian age (Herrin Coal, Illinois, U.S.A.). Rev Palaeobot Palynol 44:1–26.

——— 1992 Ecology and life-history biology of arborescent lycopsids in Late Carboniferous swamps of Euramerica. Ann Mo Bot Gard 79:560–588.

——— 1994 Paleobotanical and paleoecological constraints on models of peat formation in the Late Carboniferous of Euramerica. Palaeogeogr Palaeoclimatol Palaeoecol 106:39–90.

Felix CJ 1954 Some American arborescent lycopod fructifications. Ann Mo Bot Gard 41:351–394.

Flügel E 2004 Microfacies of carbonate rocks: analysis, interpretation and application. Springer, Berlin.

Friis EM, PR Crane, KR Pedersen, S Bengston, PCJ Donogghue, GW Grimm, M Stampanoni 2007 Phase-contrast x-ray microtomography links Cretaceous seeds with Gnetales and Bennettitales. Nature 450:549–553.

Galtier J 1964 Sur le gamétophyte femelle des Lépidodendracées. C R Acad Sci Paris 258:2625–2658.

——— 1970 Observations nouvelles sur la gamétophyte femelle des Lépidodendracées. C R Acad Sci Paris 271:1495–1497.

Gastaldo RA, IM Stevanovic-Walls, WN Ware, SF Greb 2004 Community heterogeneity of early Pennsylvanian peat mires. Geology 32:693–696.

Glasspool IJ, AR Hemsley, AC Scott, A Golitsyn 2000 Ultrastructure and affinity of Lower Carboniferous megaspores from the Moscow Basin, Russia. Rev Palaeobot Palynol 109:1–31.

Hilton J, RM Bateman 2006 Pteridosperms are the backbone of seed-plant phylogeny. J Torrey Bot Soc 133:119–168.

Kenrick P, PR Crane 1997 The origin and early diversification of land plants: a cladistic study. Smithsonian Institution, Washington, DC.

LaMotte C 1933 Morphology of the megagametophyte and the embryo sporophyte of *Isoetes lithophila*. Am J Bot 20:217–233.

McHill RAR, AJ Hall, AE Fallick, AJ Boyce 1994 The palaeoenvironment of East Kirkton, West Lothian, Scotland: stable isotope evidence from silicates and sulphides. Trans R Soc Edinb 84: 223–237.

McLean RC 1912 A group of rhizopods from the Carboniferous Period. Proc Camb Philos Soc 16:493–513.

Meyer-Berthaud B 1984 Les axes des lycophytes à structure conservée du Carbonifère basal (Tournasien) de la Montagne Noir: *Trebicaulis* gen. nov. et *Landeyrodendron* gen. nov. Palaeontogr Abt B 190:1–36.

Morey ED, PR Morey 1977 *Paralycopodites minutissimum* gen. et sp. nov. from the Carbondale Formation of Illinois. Palaeontogr Abt B 162:64–69.

Nixon KC 1999 Winclada (BETA), version 0.9.9. Published by the author, Ithaca, NY.

Oplustil S, J Bek 2009 Some Pennsylvanian arborescent lycopsid cones and their microspores from the British coalfields. Bull Geosci 84:203–226.

Pearson HL 1986 Structure and anatomy of the Carboniferous lycopsid *Anabathra*. Bull Brit Mus Nat Hist 40:265–292.

Piérart P 1978 Etat d'avancement de la systématique des mégaspores Lagéniculées (groupe Mégaspores C.I.M.P.). Palinol Num Extraord 1:369–373.

Pigg KR 1983 The morphology and reproductive biology of the sigillarian cone *Mazocarpon*. Bot Gaz 144:400–413.

Pigg KR, GW Rothwell 1983 Megagametophyte development in the Chaloneriaceae fam. nov., permineralized Paleozoic Isoetales (Lycopsida). Bot Gaz 144:295–302.

Potonié R, G Kremp 1954 Die Gattungen der paläozoischen Sporae dispersae und ihre Stratigraphie. Geol Jahrb 69:111–194.

——— 1956 Die Sporae dispersae des Ruhrkarbons, ihre Morphographie und Stratigraphie mit Ausblicken auf Arten anderer Gebiete und Zeitabschnitte. 2. Palaeontogr Abt B 99:85–191.

Rauh W, H Falk 1959 *Stylites* E. Amstutz, eine neue Isoetaceae aus den Hochanden Perus. Sitzungsber Heidelberger Akad Wiss Math-Natwiss Kl 5:1–160.

Rex GM, AC Scott 1987 The sedimentology, palaeoecology and preservation of the Lower Carboniferous plant deposits at Pettycur, Fife, Scotland. Geol Mag 124:43–66.

Robert D 1971 Le gamétophyte femelle de *Selaginella kraussiana* (Kunze) A. Br. Rev Cytol Biol Veg 34:93–164, 189–232.

Schopf JM 1941 Contributions to Pennsylvanian paleobotany: *Mazocarpon oepteridium* sp. nov. and sigillarian relationships. Ill State Geol Surv Rep Investig 75:1–40.

Scott AC, R Brown, J Galtier, B Meyer-Berthaud 1994 Fossil plants from the Viséan of East Kirkton, West Lothian, Scotland. Trans R Soc Edinb 84:249–260.

Scott AC, AR Hemsley 1993 The spores of the Dinantian lycopsid cone *Flemingites scottii* from Pettycur, Fife, Scotland. Spec Pap Palaeont 49:31–41.

Shaver SA, CF Eble, JC Hower, FL Saussy 2006 Petrography, palynology, and paleoecology of the Lower Pennsylvanian Bon Air coal, Franklin County, Cumberland Plateau, southeast Tennessee. Int J Coal Geol 67:17–46.

Smith AHV, MA Butterworth 1967 Miospores in the coal seams of the Carboniferous of Great Britain. Spec Pap Palaeontol 1:249–250.

Smith DL 1962 The stems of three species of lepidodendrid from the Scottish Lower Carboniferous. Ann Bot 26:533–550.

Spinner E 1969 Megaspore assemblages from Viséan deposits at Dunbar, East Lothian, Scotland. Palaeontology 12:441–458.

Stubblefield SP, GW Rothwell 1981 Embryogeny and reproductive biology of *Bothrodendrostrobus mundus* (Lycopsida). Am J Bot 68: 625–634.

Sutton MD 2008 Tomographic techniques for the study of exceptionally preserved fossils. Proc R Soc B 275:1587–1593.

Swofford DL 2001 PAUP*: phylogenetic analysis using parsimony (*and other methods), version 4.0. Sinauer, Sunderland, MA.

Thomas BA 1966 The cuticle of the lepidodendroid stem. New Phytol 65:296–303.

——— 1967 *Ulodendron* Lindley & Hutton and its cuticle. Ann Bot 31:775–782.

——— 1970 A new specimen of *Lepidostrobus binneyanus* from the Westphalian B of Yorkshire. Pollen Spores 12:217–234.

——— 1974 The lepidodendroid stoma. Palaeontology 17:78–83.

Thomas BA, V Blackburn 1987 An ultrastructural study of some Carboniferous in situ megaspores assignable to *Lagenicula horrida* and *Lagenosporites rugosus*. Pollen Spores 29:435–448.

Thomas BA, SD Brack-Hanes 1984 A new approach to family groupings in the lycophytes. Taxon 33:247–255.

Trewin NH, SR Fayers, R Kelman 2003 Subaqueous silicification of the contents of small ponds in an Early Devonian hot-spring complex, Rhynie, Scotland. Can J Earth Sci 40:1697–1712.

Willard DA 1989*a* Lycospora from Carboniferous *Lepidostrobus* compressions. Am J Bot 76:1429–1440.

——— 1989*b* Source plants for Carboniferous microspores: *Lycospora* from permineralized *Lepidostrobus*. Am J Bot 76:820–827.

Willard DA, WA DiMichele, DL Eggert, JC Hower, CB Rexroad, AC Scott 1995 Paleoecology of the Springfield Coal Member (Desmoinsian, Illinois Basin) near the Leslie Cemetery paleochannel, southwestern Indiana. Int J Coal Geol 27:59–98.

Williamson WC 1872 On the organisation of the fossil plants of the Coal Measures. III. Lycopodiaceae (continued). Philos Trans R Soc B 162:283–318.

Zerndt J 1934 Les mégaspores du bassin houllier Polonais. 1. Les couches anticlineles. Acad Pol Sci Lett 1:1–55.

Zhou YL, SJ Wang, J Hilton, GW Rothwell 2006 *Achlamydocarpon pingquanensis* sp. nov. (Lycopsida): a novel anatomically preserved lepidodendralean disseminule from the lower Permian of China. Int J Plant Sci 167:567–577.

Zhou YL, SJ Wang, J Hilton, B Tian 2008 Anatomically preserved lepidodendralean plants from the Lower Permian coal-balls of northern China: *Achlamydocarpon intermedium*, sp. nov. Plant Syst Evol 273:71–85.